



# **The Silent Canyon Caldera Complex— A Three-Dimensional Model Based on Drill- Hole Stratigraphy and Gravity Inversion**

by Edwin H. McKee<sup>1</sup>, Thomas G. Hildenbrand<sup>1</sup>, Megan L. Anderson<sup>1</sup>,  
Peter D. Rowley<sup>2</sup>, and David A. Sawyer<sup>3</sup>

Open-File Report 99-555  
Version 1.0

<http://geopubs.wr.usgs.gov/open-file/of99-555/>

Prepared in cooperation with the  
**NEVADA OPERATIONS OFFICE**  
**U.S. DEPARTMENT OF ENERGY**  
(Interagency Agreement DE-AI08-96NV11967)

1999

This report is preliminary and has not been reviewed for conformity with U.S. Geological Survey editorial standards or with the North American Stratigraphic Code. Any use of trade, firm, or product names is for descriptive purposes only and does not imply endorsement by the U.S. Government.

Manuscript approved November 23, 1999

**U.S. DEPARTMENT OF THE INTERIOR**  
**U.S. GEOLOGICAL SURVEY**

<sup>1</sup>Menlo Park, California

<sup>2</sup>Las Vegas, Nevada

<sup>3</sup>Denver, Colorado

## CONTENTS

Abstract .....	1
Introduction .....	2
Geologic Setting .....	4
Caldera Concept .....	8
Geologic and Geophysical Character of the SWNVF .....	11
Silent Canyon Caldera Complex .....	13
Volcanic Stratigraphy .....	17
Hydrostratigraphy .....	20
Timber Mountain composite unit .....	21
Topopah Spring tuff aquifer .....	22
Calico Hills composite unit .....	22
Crater Flat composite unit .....	31
Bullfrog Tuff confining unit .....	31
Belted Range aquifer .....	40
Pre-Belted Range composite unit.....	40
Basement .....	49
Structure.....	49
Basement Surface .....	56
Density-depth functions.....	58
Basin geometry .....	62
Three-Dimensional Model .....	63
Acknowledgements.....	73
References .....	73

### List of Tables

Table 1. Major stratigraphic units in the Silent Canyon complex .....	19
Table 2. Density-depth functions used to determine thickness of basin-filling deposits and calculated depths near drill hole Ue20f.....	60

### List of Figures

Figure 1. Map of the western part of the Nevada Test Site and areas to the west.

Figure 2. Diagram showing part of the three-dimensional surface of the Silent Canyon caldera fault created in “EarthVision.”

Figure 3. Diagram of collapse caldera models showing some variations observed in the field.

Figure 4. Diagrams showing isostatic residual gravity anomaly of the central part of the SW Nevada volcanic field (SWNVF) and 3D view of basement surface beneath the central part of the SWNVF.

Figure 5. Diagram showing the development of the Silent Canyon caldera complex.

Figure 6a. Distribution and thickness map of the Topopah Spring tuff aquifer.

Figure 6b. Three-dimensional view of the Topopah Spring tuff aquifer looking northeast.

Figure 6c. Three-dimensional view of the Topopah Spring tuff aquifer looking east.

Figure 6d. Three-dimensional view of the Topopah Spring tuff aquifer looking north.

Figure 7a. Distribution and thickness map of the Calico Hills composite unit.

Figure 7b. Three-dimensional view of the Calico Hills composite unit looking northeast.

Figure 7c. Three-dimensional view of the Calico Hills composite unit looking east.

Figure 7d. Three-dimensional view of the Calico Hills composite unit north.

Figure 8a. Distribution and thickness map of the Crater Flat composite unit.

Figure 8b. Three-dimensional view of the Crater Flat composite unit looking northeast.

Figure 8c. Three-dimensional view of the Crater Flat composite unit looking east.

Figure 8d. Three-dimensional view of the Crater Flat composite unit looking north.

Figure 9a. Distribution and thickness map of the BullfrogTuff confining unit.

Figure 9b. Three-dimensional view of the BullfrogTuff confining unit looking northeast.

Figure 9c. Three-dimensional view of the BullfrogTuff confining unit looking east.

Figure 9d. Three-dimensional view of the BullfrogTuff confining unit looking north.

Figure 10a. Distribution and thickness map of the Belted Range aquifer.

Figure 10b. Three-dimensional view of the Belted Range aquifer looking northeast.

Figure 10c. Three-dimensional view of the Belted Range aquifer looking east.

Figure 10d. Three-dimensional view of the Belted Range aquifer looking north.

Figure 11a. Distribution and thickness map of the Pre-Belted Range composite unit.

Figure 11b. Three-dimensional view of the Pre-Belted Range composite unit looking northeast.

Figure 11c. Three-dimensional view of the Pre-Belted Range composite unit looking east.  
Figure 11d. Three-dimensional view of the Pre-Belted Range composite unit looking north.

Figure 12a. Diagram showing the Silent Canyon caldera complex in plan view.  
Figure 12b. Three-dimensional view of Silent Canyon ring fault looking north.  
Figure 12c. Three-dimensional view of Silent Canyon ring fault looking northeast.

Figure 13. Three-dimensional diagrams showing two views of the Timber Mountain caldera margin cutting off the Silent Canyon caldera margin.

Figure 14. Map showing the major faults mapped at the surface of Pahute Mesa.

Figure 15. Diagrams showing two views of the East Boxcar, West Greeley, and Almendro faults within the Silent Canyon caldera complex.

Figure 16. Diagram showing basement surface beneath the region of the Silent Canyon caldera complex based on the inversion of gravity data.

Figure 17. Three-dimensional diagrams showing two views of the Silent Canyon caldera complex with the upper 2000 feet of rock removed down to water-table level.

Figure 18. Cross sections across the buried Silent Canyon caldera complex drawn from the “EarthVision” three-dimensional model.

Figure 19. Three-dimensional diagram of Pahute Mesa sliced along A – A’ shown in figure 18a.

Figure 20. Three-dimensional diagram of Pahute Mesa sliced along B – B’ shown in figure 18a.

Figure 21. Three-dimensional diagram of Pahute Mesa sliced along C – C’ shown in figure 18a.

# **The Silent Canyon Caldera Complex—A Three-dimensional Model Based On Drill-Hole Stratigraphy And Gravity Inversion**

E.H. McKee, T.G. Hildenbrand, M.L. Anderson,  
P.D. Rowley and David A. Sawyer

U.S. Geological Survey, Menlo Park, Calif.,  
Las Vegas, Nev., and Denver, Colo.

## **ABSTRACT**

The structural framework of Pahute Mesa, Nevada, is dominated by the Silent Canyon caldera complex, a buried, multiple collapse caldera complex. Using the boundary surface between low density Tertiary volcanogenic rocks and denser granitic and weakly metamorphosed sedimentary rocks (basement) as the outer fault surfaces for the modeled collapse caldera complex, it is postulated that the caldera complex collapsed on steeply-dipping arcuate faults two, possibly three, times following eruption of at least two major ash-flow tuffs. The caldera and most of its eruptive products are now deeply buried below the surface of Pahute Mesa. Relatively low-density rocks in the caldera complex produce one of the largest gravity lows in the western conterminous United States. Gravity modeling defines a steep sided, cup-shaped depression as much as 6,000 meters (19,800 feet) deep that is surrounded and floored by denser rocks. The steeply dipping surface located between the low-density basin fill and the higher density external rocks is considered to be the surface of the ring faults of the multiple calderas. Extrapolation of this surface upward to the outer, or topographic rim, of the Silent Canyon caldera complex defines the upper part of the caldera collapse structure. Rock units within and outside the Silent Canyon caldera complex are combined into seven hydrostratigraphic units based on their predominant hydrologic characteristics. The caldera structures and other faults on Pahute Mesa are used with the seven hydrostratigraphic units to make a three-

dimensional geologic model of Pahute Mesa using the "EarthVision" (Dynamic Graphics, Inc.) modeling computer program. This method allows graphic representation of the geometry of the rocks and produces computer generated cross sections, isopach maps, and three-dimensional oriented diagrams. These products have been created to aid in visualizing and modeling the ground-water flow system beneath Pahute Mesa.

## INTRODUCTION

The testing of underground nuclear devices at the Nevada Test Site (NTS) on Pahute Mesa (fig. 1) between 1966 and 1992 introduced radionuclides into ground-water that is flowing southwesterly beneath Pahute Mesa (Blankennagel and Weir, 1973; Winograd and Thordarson, 1975; Laczniak and others, 1996). The present water table of this ground-water system is about 600 meters (2,000 feet) below the surface of Pahute Mesa and is in the upper and middle part of a thick sequence of volcanic rocks that are the eruptive products of extinct calderas beneath, as well as outside of, Pahute Mesa. The calderas underlying Pahute Mesa on the NTS are part of what is called the Silent Canyon caldera complex (SCCC). All parts of the complex are buried beneath younger ash-flows that erupted from younger calderas outside the SCCC.

The objective of this investigation is to develop a three-dimensional geological and hydrogeological model of the SCCC that may be used for ground-water flow studies of Pahute Mesa in the northwestern part of the Nevada Test Site (NTS). The conceptual view of the buried SCCC is based, in general, on the arcuate collapse fault systems of mapped calderas, both near the SCCC and in other parts of the world. Models for such calderas derive from geologic mapping and concepts developed by Williams (1941),

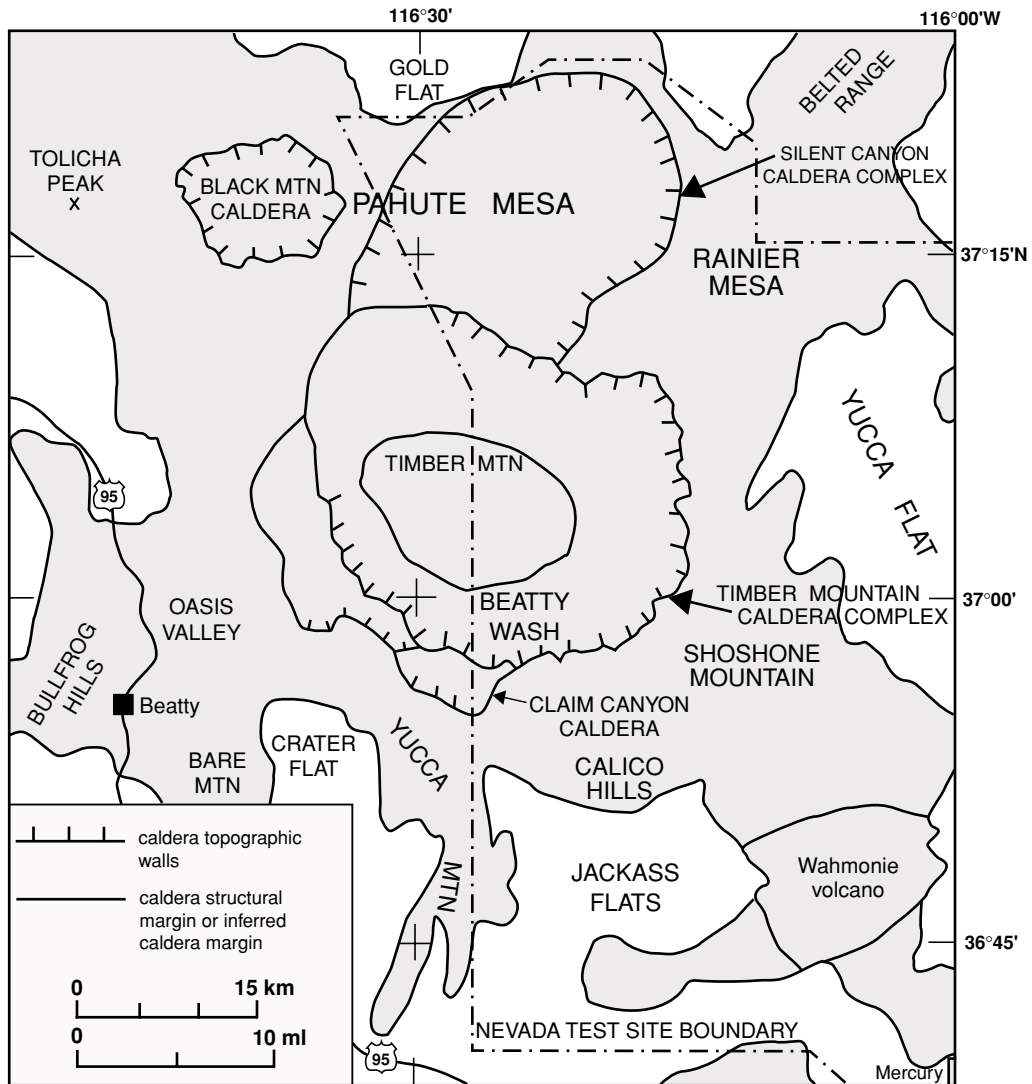


Figure 1. Map of the western part of the Nevada Test Site (NTS) and areas to the west. Shading represents mostly Miocene volcanic rocks of the southwestern Nevada volcanic field (SWNFV). The three-dimensional model developed here includes all of the Silent Canyon caldera complex.

Smith and Bailey (1968), and numerous other geologists (see the section on the caldera model). Geologic maps of Pahute Mesa give some surface control on the geology, but because the SCCC is buried by volcanic rocks from nearby younger calderas, our geologic knowledge of the subsurface is based mostly on evaluation of drill hole and geophysical information. The geologic model presented here is uses two different types of data. The caldera structure is based on the basement surface beneath Pahute Mesa as defined by gravity and projected upward to the caldera complex's topographic rim (fig. 2). The stratigraphy is based on about 52 drill sites scattered across the mesa and on geologic maps. Drill hole analysis of the petrology and petrochemistry of samples based on a compilation and rigorous review of data from numerous scientists over the past 30 years compiled by Warren and others (1999; *see* references in Warren and others, 1999 for individual contributions) was used to determine the stratigraphy in the wells.

## GEOLOGIC SETTING

The rocks that crop out on and near Pahute Mesa are mostly middle Miocene silicic volcanic rocks that are part of the southwestern Nevada volcanic field (SWNVF, fig. 1). Most of these rocks are the products of volcanoes that formed collapse calderas during and after eruption of large volume ash-flow sheets. At least six major calderas have been identified in the SWNVF (Sawyer and others, 1994; Wahl and others, 1997). The certainty of their recognition is inversely related to their relative age because the older ones were progressively collapsed into and buried by the younger calderas and related intrusions. Like calderas elsewhere in the world these calderas are the sites of thick lava accumulations, and breccias, both tectonic and volcanic, are commonly associated with such calderas. Most of the volcanic rocks are pyroclastic types (ash-flow and air-fall tuffs) that are made up of variable

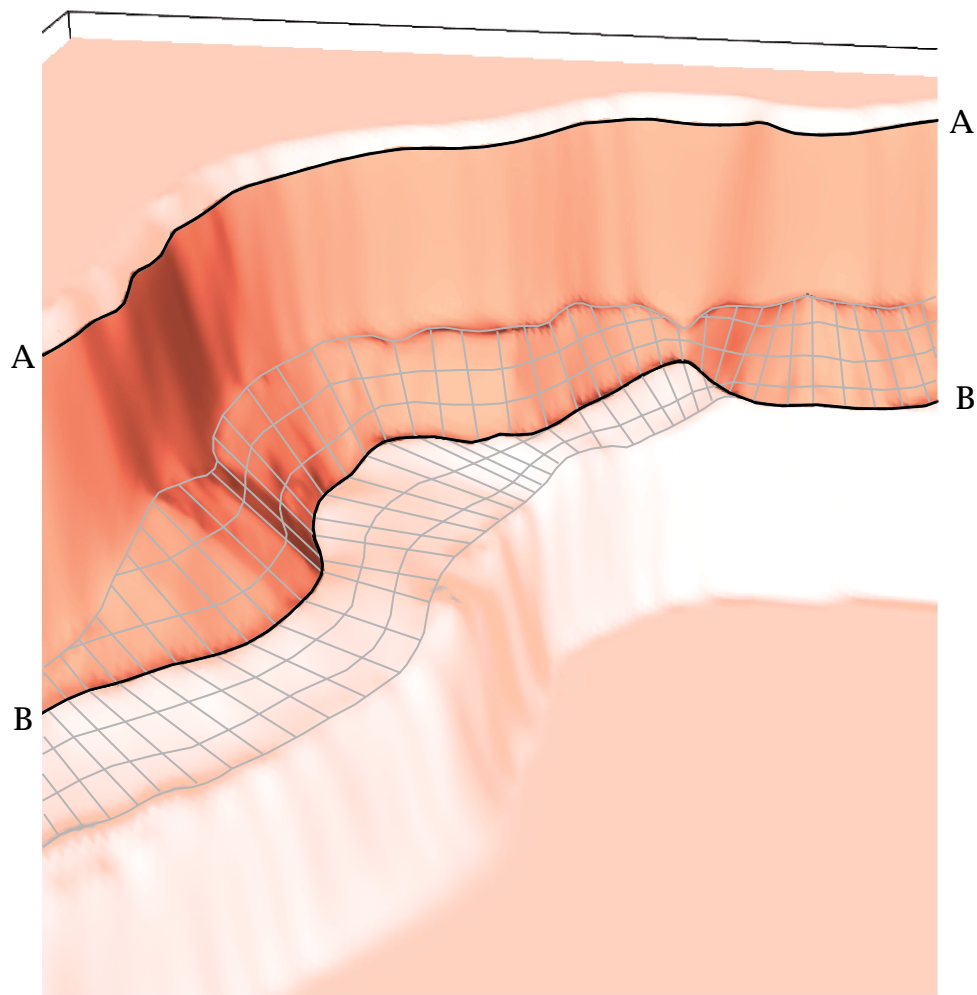


Figure 2. Part of the three-dimensional surface of the Silent Canyon caldera fault created in "EarthVision". Hatched area is the fault surface calculated from gravity. Solid lines are boundaries of the clipped polygon used to limit the upward and downward continuation of the fault surface. (A) The upper boundary is defined by the topographic rim of the SCCC taken from a geologic map (Wahl and others, 1997) and clipped at the elevation at which the Silent Canyon caldera fault dies out before reaching the land surface. (B) The lower boundary is the elevation at which the gridded fault surface (the surface between low and high density rocks defined by gravity inversion) cuts downward into the basement. The colored portion of the fault between the polygon boundaries is used in the three-dimensional model.

amounts of ash, pumice, mineral crystals, and xenolithic debris. They range from welded to nonwelded, poorly to tightly compacted, and unaltered to completely altered to a variety of secondary minerals. The lava flows form lenticular bodies with complex interfingering relationships. The ash-flow tuffs develop a sheet or layered aspect outside the calderas but are often massive where they accumulate to greater thickness inside the caldera.

The volcanic rocks known to underlie Pahute Mesa span nearly the entire period of volcanic activity of the SWNVF. Units that crop out at the surface are ash-flow sheets from the Timber Mountain caldera to the south or the Black Mountain caldera to the west (fig. 1). The youngest rocks are about 9.4 Ma (Sawyer and others, 1994). Rocks as old as about 15.0 Ma are encountered in the deepest drill holes about two-thirds of the way through the volcanic sequence based on the thickness of low density rocks determined by gravity inversion calculations. Rocks beneath the drill holes, lower in the sequence, include rocks as old as the oldest volcanic rocks in the SWNVF, about 15.5 Ma and they are most likely different units in different parts of the caldera complex. Units in the SCCC whose eruption caused caldera collapse include the 13.7 Ma Grouse Canyon Tuff and the 13.3 Ma Bullfrog Tuff (Sawyer and others, 1994). Some rocks older than the Grouse Canyon Tuff in the volcanic pile may also have erupted from the Silent Canyon complex and may have caused calderas or partial calderas that form the deepest parts of the structural basin beneath Pahute Mesa. The basement beneath the Miocene volcanic rocks is inferred to be mostly granitic rock and represents the upper part of the magma chamber within a batholithic complex from which the volcanic units of the SWNVF originated. Precambrian and Paleozoic siliceous and carbonate strata may be included as wallrock, inliers, stoped blocks, and xenoliths in this granitic basement.

All the volcanic rocks, particularly the ash-flow sheets, are types typically associated with collapse calderas. The basement configuration delineated by the gravity data is consistent with this caldera tectonic model (Healey, 1968; Healey and others, 1987; Hildenbrand and others, 1999). Although the Silent Canyon caldera complex has been recognized for several decades, the complexity of this large multi-eruptive volcanic area has led to a variety of geologic scenarios. These include: (1) a single, large, circular, collapse caldera system as shown in figure 1 (Noble and others, 1968; Orkild and others, 1969), (2) a nested, double-arcuate, caldera complex (Sawyer and Sargent, 1989; Minor and others, 1993; Sawyer and others, 1994) and (3) a group of rectilinear, fault-block basins formed by caldera collapse on preexisting linear, high-angle, normal faults (Ferguson and others, 1994). We adopt a model by which a large ellipsoid complex caldera system developed around a series of proximate, arcuate, presumed partial to whole calderas. The collapse features formed during and after eruption of some of the many voluminous ash-flow units underlying the area. Younger, high-angle faults displace rocks locally within the caldera complex. This model has aspects of all the previous models. Like Noble and others (1968) and Orkild and others (1969) most of the caldera collapse is essentially around a large circular fault zone, and like Sawyer and Sargent (1989) and Minor and others (1993) our model envisions several major periods of collapse and caldera formation. It is similar to the Ferguson and others (1994) model in that it is characterized by an exceptionally deep tectonically-formed basin (>5 km). The geologic complexities shown in the Ferguson and others (1994) model (e.g., numerous local fault-block grabens), however, do not appear in our model, because the geophysical data are insufficient to detect the high-angle fault block basins. Nor do the geologic data from drill holes in the upper 900 meters (3,000 feet) provide solid evidence for deeper rectilinear

basins. Our conceptually simple model is supported by the geological and geophysical data and provides a framework for future additional data defining caldera tectonics.

## CALDERA CONCEPT

Ash-flow tuffs, among the most voluminous of volcanic products, result from explosive eruptions that form widespread units emplaced in mere instants of geologic time. These eruptions cause virtually instantaneous evacuation of their source-underlying shallow magma chambers, causing the roof over the magma chamber to collapse. The collapse feature has been called a caldera, and this explanation became widely recognized following the landmark reviews of caldera formation by Williams (1941), ash-flow processes by Smith (1960), and resurgent calderas by Smith and Bailey (1968). Detailed mapping of many areas, especially the most widespread volcanic terranes of the U.S. such as the Great Basin, Snake River Plain, Cascades, San Juan Mountains, Rio Grande rift, as well as the Andes of Peru, disclose scores of calderas. Calderas have been found in nearly all other volcanic regions throughout the world where pyroclastic rocks occur. In particular, the study of the many larger and complex calderas in the San Juan Mountains of Colorado (Lipman, 1976 a, b, 1984; 1997; and Steven and Lipman, 1976) clarify details of caldera evolution. Work on the well-exposed Black Mountain caldera and the Timber Mountain caldera complex near Pahute Mesa by Christiansen and Noble (1965), Christiansen and others (1977), Byers and others (1968; 1976 a, b), Smith and Bailey (1968), Noble and Christiansen (1974), and Kane and others (1981) has revealed much about caldera genesis that is directly applicable to the Silent Canyon caldera complex.

Much of what is known about calderas is reviewed by Lipman (1997). He notes that although many variations exist, most well-exposed calderas are broadly similar to each other (fig. 3). Most calderas form above shallow

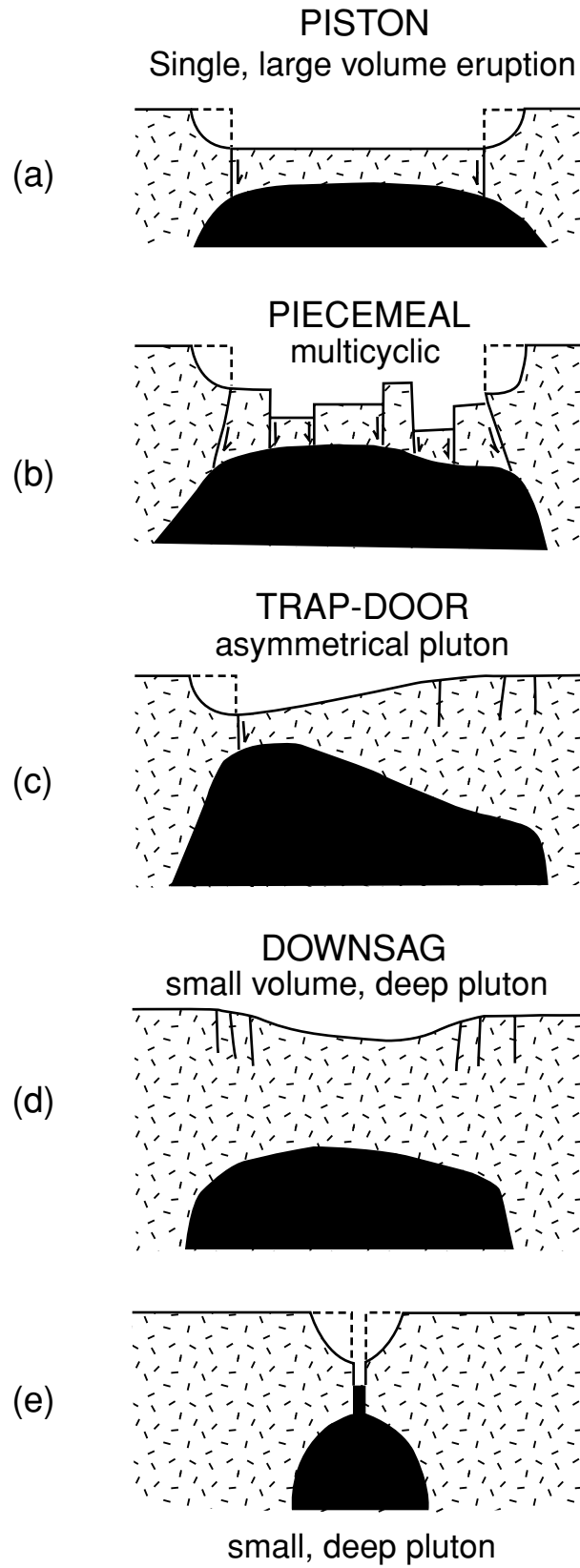


Figure 3. Collapse caldera models showing some of the variations that have been observed in the field. The Silent Canyon caldera complex is probably a combination of all of these variations. Figure is from Lipman, 1997, figure 2.

cupolas that rise (intrude) above the tops of a batholithic complex. When the cupola intrudes near the surface, a violent eruption occurs. Because most cupolas are circular in plan, most calderas are also circular. This original shape for roof failure is defined by arcuate ring faults that dip steeply into the underlying cupola. These ring faults define what is called the structural margin of the caldera. When a ring fault extends to the earth's surface, rocks inside the ring fault subside to create a basin. The basin floor generally subsides as a single piston-like plate, although piecemeal subsidence of parts of the floor has been noted in a number of calderas (fig. 3b). The scarp that results from collapse of the caldera floor has a slope above the angle of repose; therefore breccia formed by landslide debris, avalanches and rockfalls break away from the scarp, all eroding the structural margin until the scarp reaches its angle of repose and attains stability. The retreat of the caldera edge as a result of these processes makes the caldera larger. The outer edge of this zone of mass wasting is called the topographic margin of the caldera. Products of the landslides are spread into the interior of the caldera, where they intertongue with the products of continued volcanic eruption. The sum total of the deposits, known as intracaldera deposits, consists mostly of ash-flow tuff and interlayered collapse breccia. Continued eruption results in further subsidence of the caldera floor. Intracaldera deposits also include generally post-collapse subordinate volumes of lava flows that erupt from vents and small domes commonly located along the ring fracture faults. In the waning stages of caldera eruption, magma from the original magma chamber commonly rises and intrudes the intracaldera fill and may uplift by resurgence the caldera fill along the ring faults thereby destroying the caldera floor and resulting in a structural dome.

Variations in caldera geometries summarized by Lipman (1997) and shown here in figure 3 include the trap door caldera, in which only one side subsides along a partial, arc-shaped, ring fault (fig. 3c), a downsag caldera, in which the magma chamber is so deep that no through-going fault develops (fig. 3d), and a small funnel-shaped caldera, in which the floor was so disrupted that the caldera is more similar to a breccia pipe and was more likely excavated explosively rather than formed by subsidence (fig. 3e).

#### GEOLOGIC AND GEOPHYSICAL CHARACTER OF THE SWNVF

Starting in the 1950's, the Nevada Test Site (NTS) and adjacent areas of southern Nevada were geologically mapped at 1:24,000 and 1:48,000 scale. These maps were the basis for the adoption of the concept of calderas as the source for most of the volcanic rocks in the region -- rocks that comprise the SWNVF. Later updated summary maps and reports endorsed and expanded on the caldera model in the SWNVF although the location of some segments of the caldera margins and the interpretations about other aspects of the geology were modified as new information was added with each new generation of maps. The map pattern of calderas on the recent summary geologic map of the NTS (Wahl and others, 1997) evolved from maps of Minor and others (1993), Sawyer and others (1995), Carr and others (1996), and the report of Sawyer and others (1994). The most recent geologic map of the NTS (Slate and others, 1999) does not change the caldera model.

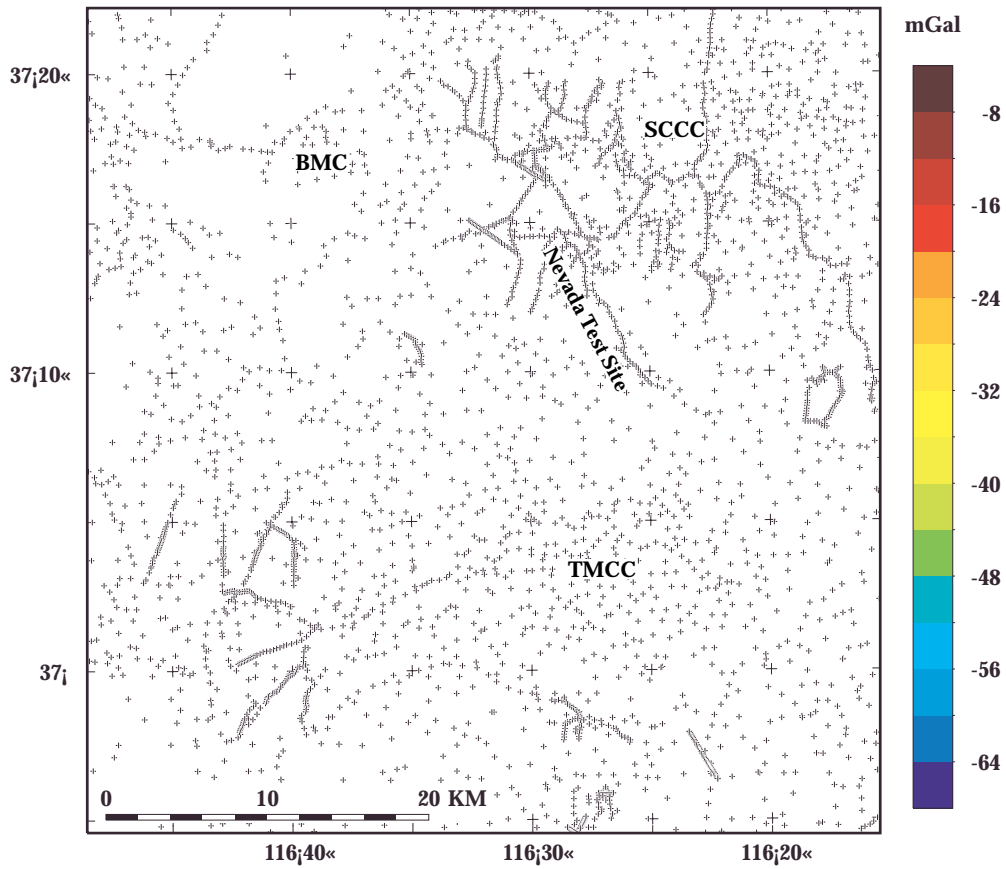
Geophysical mapping has been a major component of the geologic investigation of the NTS. The early geophysical studies (e.g., Healey, 1968; Kane and others, 1981) interpreted a caldera origin for the gravity anomaly beneath Pahute Mesa. Kane and others (1981) noted that the geophysical data near Timber Mountain suggested that some deformation caused by volcanic events has been accommodated along straight-line faults that are aligned in

such a fashion as to give a curvilinear appearance to the regional structure. He suggested that some of the curvilinear geometry was caused by erosion and landsliding of caldera walls. Recent geophysical investigations (Ferguson and others, 1994; Grauch and others, 1997; McCafferty and Grauch, 1997; Hildenbrand and others, 1999; Mankinen and others, 1999; and Schenkel and others, 1999), which synthesize much new data use more refined geophysical modeling methods of gathering and reducing data, likewise support a caldera model for the structure beneath Pahute Mesa. Where caldera outlines are well expressed by geologic parameters, gravity maps usually reveal the structural margins of the caldera as the boundary between lower density caldera fill and higher density basement or country rock. Where calderas are buried and geologic mapping cannot define them, geophysical data provide a means to define calderas.

## SILENT CANYON CALDERA COMPLEX

Pahute Mesa is underlain by a circular, cup-shaped gravity anomaly that is one of the most prominent gravity lows in the western conterminous United States. The SCCC was first recognized on the basis of this large negative gravity depression (Healey, 1968). This deep, circular basin defined by the inversion of gravity data (Hildenbrand and others, 1999 and fig. 4) is interpreted to be a volcanic basin filled with low density, locally- derived lavas and tuffs and covered by younger welded ash-flow tuffs. The Silent Canyon caldera, named after Silent Canyon in the north-central part of Pahute Mesa, was applied to this buried volcano-tectonic feature by Healey (1968), Noble and others (1968) and Orkild and others (1968, 1969). These geologists recognized that some of the regional ash-flow sheets originated at Pahute Mesa and they postulated that these ash-flow eruptions caused subsidence that created the depression. The main collapse of the Silent Canyon caldera was attributed to eruption of the Tub Spring and Grouse Canyon Members of the Belted Range Tuff (Noble and others, 1968). The Tub Spring Tuff is now separated from the Belted Range Group and its source is uncertain. These tuffs are encountered at depths of 1,200 m (4,000 ft) or more below the surface in drill holes on Pahute Mesa. A second collapse of the SCCC, named the Area 20 caldera, was equated with eruption of the Bullfrog Tuff (Sawyer and Sargent, 1989). This caldera is shown diagrammatically in maps by Sawyer and others (1994, 1995), Ferguson and others (1994) and Wahl and others (1997). We, however, do not model the Area 20 caldera because the gravity surface beneath the SCCC defines a ridge across the trace of the projected down-dropped Area 20 caldera fault indicating that a caldera subsidence related to the Area 20 caldera displacing the basement cannot be distinguished in this area. Both caldera forming tuffs, the Grouse Canyon and

### (a) Isostatic Residual Gravity Anomaly



### (b) Basement surface

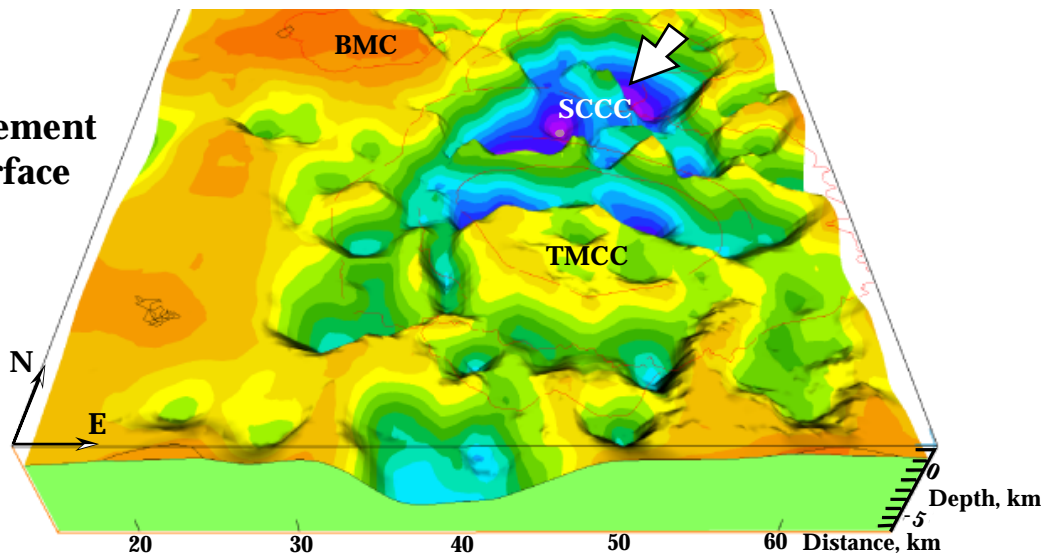


Figure 4. (a) Isostatic residual gravity anomaly of the central part of the SW Nevada volcanic field (SWNVF) from Hildenbrand and others (1999). Anomalies express to first order the average density of the middle and upper crust. Small crosses represent locations of gravity stations. Letters denote: TMCC—Timber Mountain caldera complex, SCCC—Silent Canyon caldera complex, and the BMC—Black Mountain caldera. (b) 3D view of the basement surface beneath the central part of the SNVF (from Hildenbrand and others, 1999). Note the deep ovoid basin beneath the Silent Canyon caldera complex (highlighted by the white arrow). No vertical exaggeration.

the Bullfrog, are thicker within the SCCC than in regions surrounding the complex, have substantial amounts of related post-caldera lavas, and both are comprised of facies that reflect near-source, intracaldera accumulation. In addition, roughly the upper one-third of the SCCC is comprised of younger, regional ash-flow sheets whose sources are from the south or west of Pahute Mesa. These sheets become progressively thinner and constant in thickness as they successively fill, and ultimately blanket, the depression produced by the earlier caldera collapses. The combined maximum thickness of all the units, including the caldera-forming Grouse Canyon and Bullfrog tuffs, related lavas and overlying basin-filling tuffs, however, accounts for only about one-half of the total volcanic fill in many parts the volcanic depression (see figs.19, 20, and 21). Below the Grouse Canyon Tuff there is estimated to be as much as 3,000 m (9,900 ft) of rock in the deepest parts of the depression. Because only the upper part of this basal 3,000 m (9,900 ft) of rock has been penetrated by drilling, little is known about it except from regional gravity measurements. Gravity analysis indicates that the basin fill is less dense than the basement. It is most likely silicic volcanic rock similar to the known lavas and tuffs in the upper part of the depression and in surrounding regions. The fact that these presumed volcanic rocks fill a circular deep, depression in the lower part of the SCCC suggests that they are also caldera-related eruptive rocks. We envision, therefore, that there was significant caldera collapse prior to those reasonably established Grouse Canyon caldera-forming eruptions that occur about midway in the stratigraphic sequence. The only evidence of this old caldera system is the deep circular basin defined by inversion of the gravity data (Healey, 1968; Ferguson and others, 1994; Hildenbrand and others, 1999) which makes up the deepest part of the regional gravity low. It is deeply buried and, except for its shape, mostly obscured by later collapse

calderas. It is analogous in many respects to the large tuff-filled hole or depression in pre-Tertiary rocks beneath Crater Flat about 20 miles south of Pahute Mesa (Snyder and Carr, 1984). This feature, postulated to be a caldera complex by Snyder and Carr (1984) was outlined by gravity inversion modeling in the same manner as the SCCC is modeled here.

In summary, the SCCC is a multiple collapse system that developed by a combination of piston-like, trap door, and downsag calderas (fig. 3) formed repeatedly during eruption of large volume ash-flow tuffs from beneath what is now the central part of Pahute Mesa. Collapse was essentially along various parts of this ring fracture system. The caldera forming phases of this volcanic center lasted a little more than 2 million years, from at least 15.5 to 13.3 Ma. The remnants of these caldera basins filled with volcanic rocks during the following 4 million years from volcanoes south and west of the SCCC. The oldest of these caldera-burying tuffs show considerable thickening at Pahute Mesa, but successively younger tuffs are more uniform in thickness (sheet-like), reflecting the gradual filling of the depression. As much as 6,000 m (19,800 ft) of low density volcanic or sedimentary rocks fill the SCCC at some places. Beneath the two major caldera-forming eruptive tuffs (Grouse Canyon and Bullfrog Tuffs), the sequence probably contains at least one caldera forming tuff and a variable thickness of Miocene lava flows and intrusive rocks that were the first volcanic rocks of the SWNVF. These volcanic rocks were deposited on weakly metamorphosed Precambrian and Paleozoic sandstone, shale, and limestone intruded by a granitic batholithic complex that was the magma source of the subsequent volcanic eruptions. Development of the SCCC is shown schematically in figure 5.

## VOLCANIC STRATIGRAPHY

As much as 6,000 m (19,800 ft) of Tertiary rocks underlie Pahute Mesa in the SCCC based on gravity inversion data. The deepest drill hole on Pahute Mesa (UE 20f, fig.18) penetrates 4,147 m (13,686 ft) of Tertiary rock in a location above the basement near the western margin of the caldera complex. Other deep drill holes bottom in volcanic rocks at other places in the caldera; most are about one-half way down in the sequence of moderately low-density rocks that fill the depression. The rocks encountered in the more than 85 drill-holes on Pahute Mesa are mostly silicic volcanic types including ash-flow and air-fall tuffs, lava flows, and other types of pyroclastic rocks. This sequence contains units named and mapped in areas surrounding Pahute Mesa, and serves as a guide to the stratigraphy of the buried section at Pahute Mesa. The ash-flow tuffs are especially useful in identifying the units of the SCCC because each is unique in its phenocryst content and whole rock and mineral chemistry. Relative thickness, degree of welding, number and type of xenolithic inclusions, and amount of alteration are an indication of proximity to the source but are much less important in correlating units.

The names of the rock units used here (Table 1) follow the terminology of Sawyer and others (1994), Warren and others (1999), and Drellack and Prothro (1997) and the hydrostratigraphic units are a modification of the classification devised by Drellack and Prothro, (1997) and the hydrogeologic units outlined by Warren (1994). The unit identification from the drill holes is based on petrology and rock chemistry compiled by Warren and others (1999). The units vary significantly in thickness and geometry in this volcano-caldera setting. The lava flows tend to be tabular, steep sided bodies that have complex interfingering relationships. The pyroclastic rocks, which reflect more closely the surface on which they were deposited, show pronounced

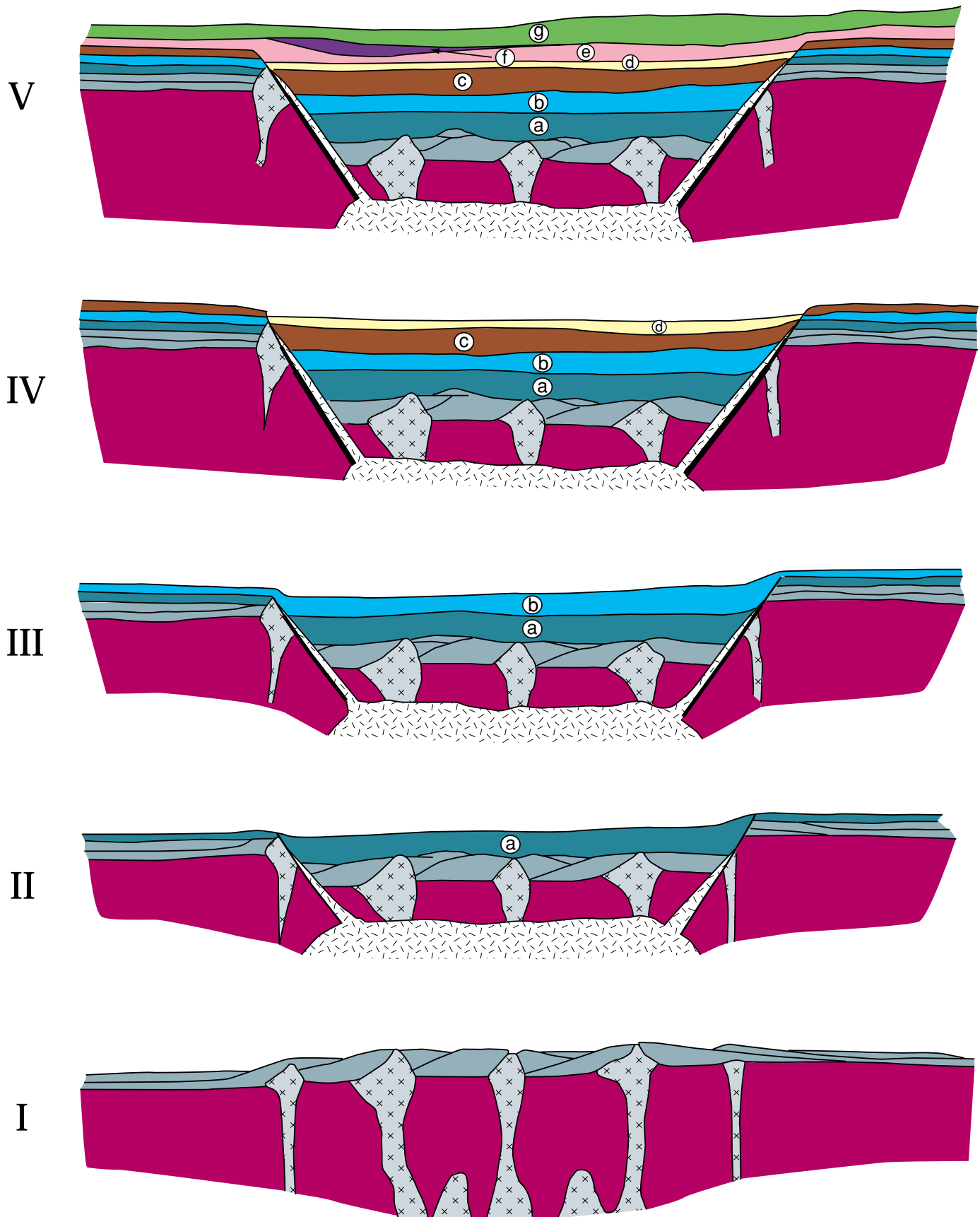


Figure 5. Development of the Silent Canyon caldera complex. Hydrostratigraphic units outlined omn table 1. The sequence of events, from bottom to top, includes three caldera forming ash-flow eruptions (a, b, c) and four caldera filling and overlapping units (d, e, f, g). (a) Pre- Belted Range composite unit, (b) Belted Range aquifer, (c) Bullfrog Tuff confining unit, (d) Crater Flat composite unit, (e) Calico Hills composite unit, (f) Topopah Spring tuff aquifer, (g) Timber Mountain aquifer.

thickening in depressions and are laterally more continuous. The major ash-flow tuffs outlined in table 1 have a layered, sheet-like aspect in many localities.

Table 1. Summary of major stratigraphic units in the Silent Canyon complex, volcanic source and hydrostratigraphic unit. The classification is based on data from Warren and others (1999) and is a modification of the classification of Drellack and Prothro (1997).

Name	Volcanic source	Hydrostratigraphic unit
Thirsty Canyon Group Gold Flat Tuff Trail Ridge Tuff Pahute Mesa Tuff Rocket Wash Tuff	Black Mountain caldera	
volcanics of Fortymile Canyon Beatty Wash Formation		
Timber Mountain Group Ammonia Tanks Tuff Rainier Mesa Tuff rhyolite of Fluorspar Canyon tuff of Holmes Road rhyolite of Windy Wash	Timber Mountain caldera complex	Timber Mountain composite unit (mostly above water table)
Paintbrush Group rhyolite of Benham rhyolite of Scrugham Peak Tiva Canyon Tuff rhyolite of Delirium Canyon rhyolite of Echo Peak rhyolite of Silent Canyon Topopah Spring Tuff	Claim Canyon caldera	Tiva Canyon Tuff is locally saturated
	Claim Canyon caldera ?	Topopah Spring tuff aquifer
Calico Hills Formation		Calico Hills composite unit
Crater Flat Group tuff of Pool rhyolite of Inlet Prow Pass Tuff tuff of Jorum rhyolite of Sled rhyolite of Kearsarge andesite of Grimy Gulch Bullfrog Tuff	Silent Canyon caldera complex ? (filling)	Crater Flat composite unit
	Silent Canyon caldera complex	Bullfrog Tuff confining unit
Tram Tuff Belted Range Group Dead Horse Flat Formation	Silent Canyon caldera complex (filling)	Belted Range aquifer
Grouse Canyon Tuff	Silent Canyon caldera complex	

comendite of Split Ridge	
comendite of Quartet Dome	
Tram Ridge Group	Pre Belted Range composite unit
Lithic Ridge Tuff	
rhyolite of Picture Rock	
Tunnel Formation	
volcanics of Quartz Mountain	
rhyolite of Quartz Mountain	
tuff of Tolicha Peak	
dacite of Mount Helen	
volcanics of Big Dome	
Tub Spring Tuff	Silent Canyon caldera complex ?
volcanics of Oak Spring Butte	Pre-Belted Range composite unit
tuff of Yucca Flat	
Redrock Valley Tuff	Silent Canyon caldera complex ?
Tuff of Twin Peaks	
tuff of Argillite Wash	
older Tertiary volcanic rocks	

## HYDROSTRATIGRAPHY

The hydrogeology of Pahute Mesa was summarized by Blankennagel and Weir (1973). Later evaluation of the ground-water flow in a much larger region that includes Pahute Mesa was made by Winograd and Thordarson (1975), Borg and others (1976) and Laczniaik and others (1996). These studies show the general direction and depth of the ground-water flow and indicate the principal factors that influence it. In order to understand the details of the flow, it is especially important to understand the structures of the SCCC, not only as they relate to the thickness and lithologic character of the stratigraphic units, but as permeable or impermeable channels.

The rocks in and near Pahute Mesa are classified hydrologically on the basis of their lithologic properties. These properties include the amount of compaction and welding, amount of alteration, and the type of secondary mineralization. Compaction and welding influence the amount of fracturing which, in turn, have a strong control on permeability. A comprehensive evaluation of the hydrogeologic characteristics of the volcanic units in the SCCC and a hydrostratigraphic classification of these rocks is in Laczniaik and others (1996) and Drellack and Prothro (1997). For this study, the 41 stratigraphic units (Table 1) are combined or split according to their

hydrologic properties into three categories-- aquifers, confining units, and composite units. The composite unit, a name first used by Drellack and Prothro, (1997), contains both aquifers and confining units. The composite units defined here are similar but are not the same as those used by Drellack and Prothro, (1997). In this investigation some units are classified as composite units because they change from aquifer to confining unit by compaction, welding, alteration or other hydrologic altering process across relatively short distances.

Table 1 lists the seven hydrostratigraphic units used in the model developed here and the stratigraphic units from which they are derived. These groups are comprised mostly of rocks with similar hydrologic characteristics and are typically a certain lithologic type such as welded tuff or altered non-welded tuff. The thickness and distribution of a rock unit was also a factor in developing the hydrostratigraphic groups. Thin or local units are difficult to show at the scale of 1:48,000 used for this three-dimensional model. At this scale, in an area the size of Pahute Mesa, stratigraphic units of about 400 ft (120 m) thick are the minimum that can be shown in cross section (less than 0.1 in or about 2 mm thick). Because the hydrostratigraphic units in this study and the hydrostratigraphic units developed for western and central Pahute Mesa by Drellack and Prothro (1997) are both based on drill-hole petrology of Warren and others (1999) there is a strong similarity between the two hydrostratigraphic classifications. The Drellack and Prothro (1997) model recognizes 21 hydrostratigraphic units, we have combined many of these into seven units.

Timber Mountain composite unit Because most of the Timber Mountain composite unit lies above the water table at Pahute Mesa, only the lower part is hydrologically significant in this area. The upper part, which includes tuffs of the Thirsty Canyon Group and the Ammonia Tanks Tuff of the Timber Mountain Group, is everywhere above the water table at Pahute Mesa. These welded tuffs are readily fractured and have the hydrologic properties of an aquifer. The Rainier Mesa Tuff underlies the Ammonia Tanks Tuff and, in the

southwest part of Pahute Mesa (south-central part of Area 20), is below the water table and is an aquifer. Beneath the Rainier Mesa Tuff, and locally beneath the water table, is a sequence of relatively thin lava flows and nonwelded tuff. This sequence includes the rhyolite of Flourspar Canyon, the tuff of Holmes Road, the rhyolite of Windy Wash, the rhyolite of Benham, the rhyolite of Scrugham Peak, the Tiva Canyon Tuff (a significant aquifer in the southwestern part of Pahute Mesa), the rhyolite of Delirium Canyon, the rhyolite of Echo Peak, and the rhyolite of Silent Canyon (Table 1). Where these units lie below the water table, the lava flows and welded tuffs are aquifers, whereas the nonwelded tuffs and areas of alteration and secondary mineralization in the lavas and welded tuffs are mostly confining units. Because neither aquifer nor confining unit is the dominant hydrologic type, this interval of rocks is classified as a composite unit and is part of the Timber Mountain composite unit.

#### Topopah Spring Tuff aquifer

The Topopah Spring Tuff, mostly a thin unit in the Pahute Mesa area, thickens in the southwestern part of the SCCC (fig. 6) where it lies mostly below the water table. It is a fractured, moderately welded tuff that acts as an aquifer.

#### Calico Hills composite unit

The Calico Hills Formation is a caldera-filling group of lava flows and tuffs. It is found across most of the SCCC (fig. 7), with the thickest deposits in western Area 20. The upper units of the Calico Hills composite unit, found in the eastern part of the SCCC, are vitric, weakly-to non-welded tuffs that act as an aquifer. Where these tuffs are altered (mostly to zeolites), they restrict the flow of water. The formation contains lenticular lava flows that are interlayered with tuffaceous rocks that are locally altered to clay minerals and zeolites. The lava flows and unaltered tuffs tend to be permeable, whereas the altered tuffs are impermeable. This thick and complex group of intertonguing aquifers and confining units is important in the western part of the SCCC; it

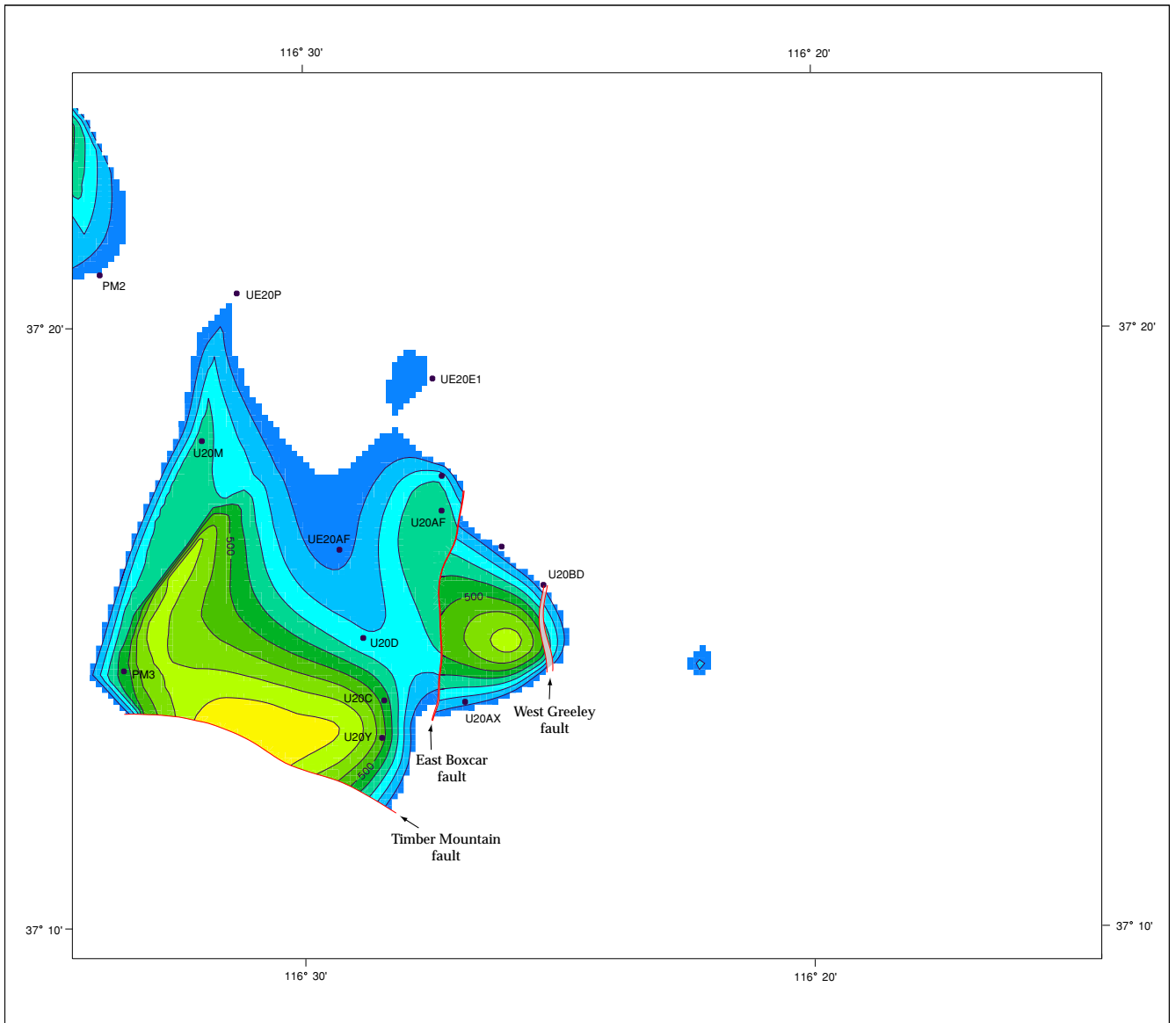


Figure 6a. Topopah Spring tuff aquifer. Distribution and thickness map (thickness in feet). Fault traces are grey where the orientation of the fault is not vertical and a thickness calculation is not possible. Drill holes that penetrate this unit or units stratigraphically beneath it are labelled by number; control points used to constrain the surface in EarthVision are dots. No thickness is shown south of the Timber Mountain caldera fault because of lack of drill hole control.

[Link to oversize version](#)

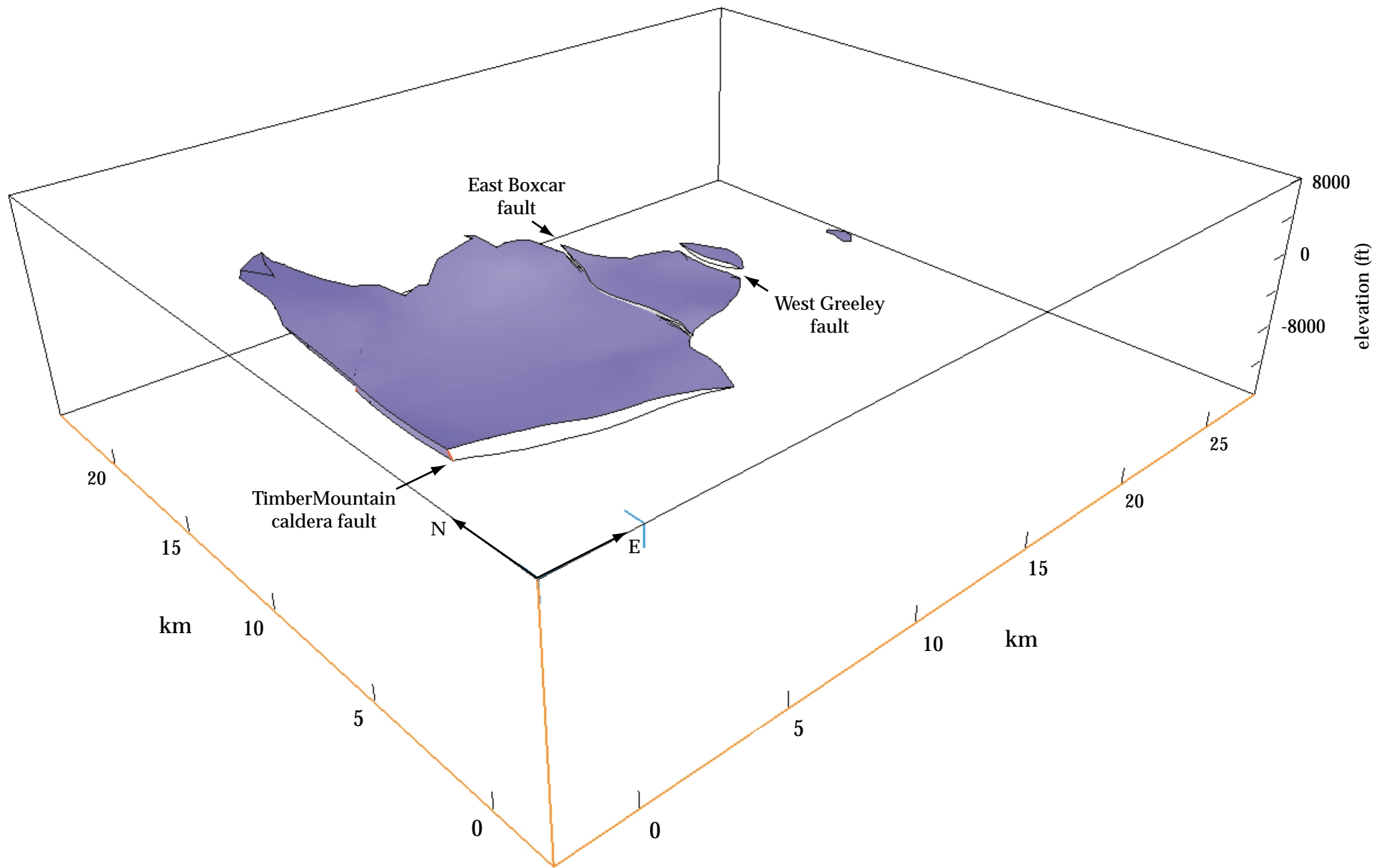


Figure 6b. Topopah Spring tuff aquifer. No vertical exaggeration. Three-dimensional view looking NE. Note the trace and offset on the East Boxcar and West Greeley north-south faults. Timber Mountain fault block is omitted because of lack of drill hole control.

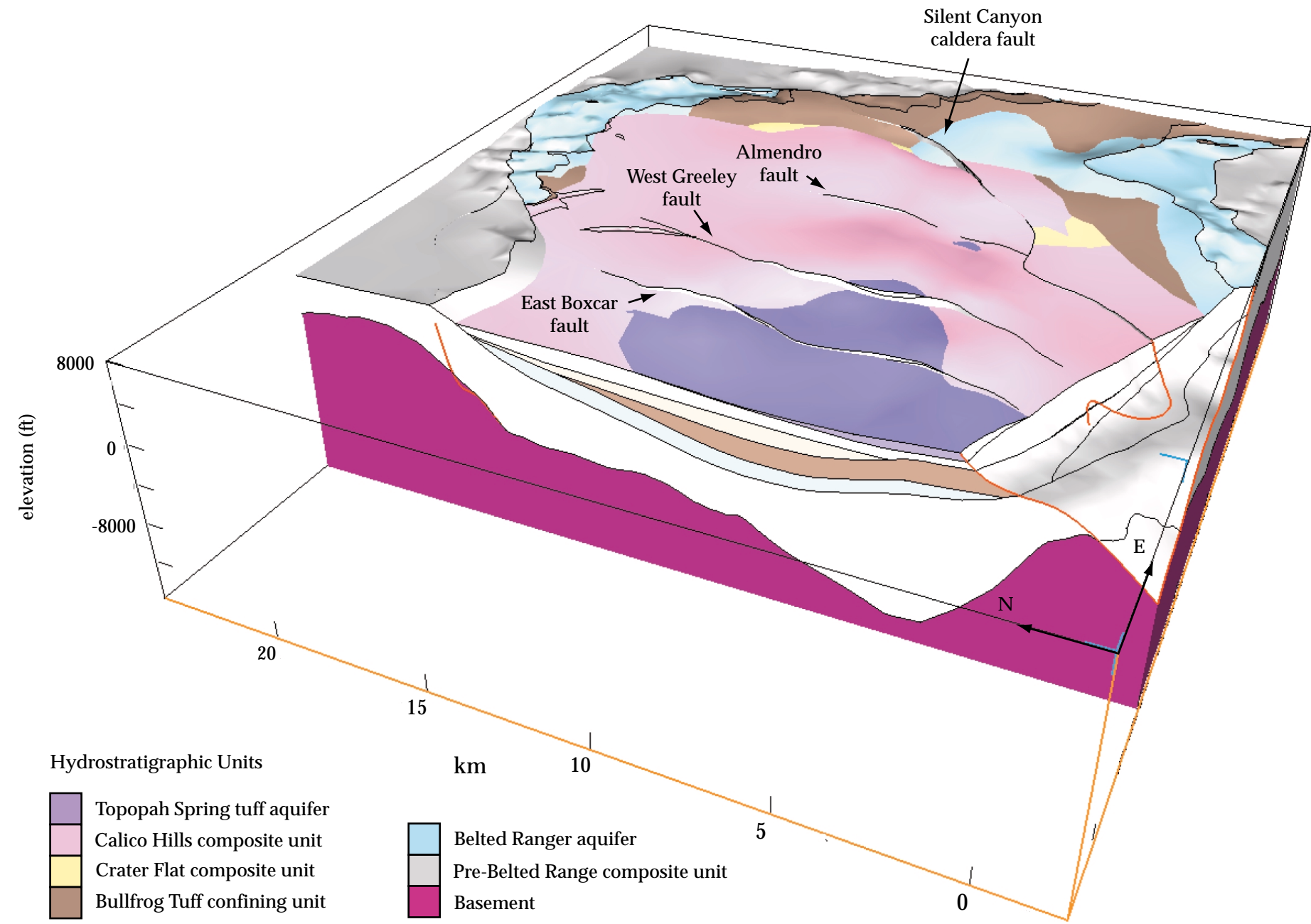
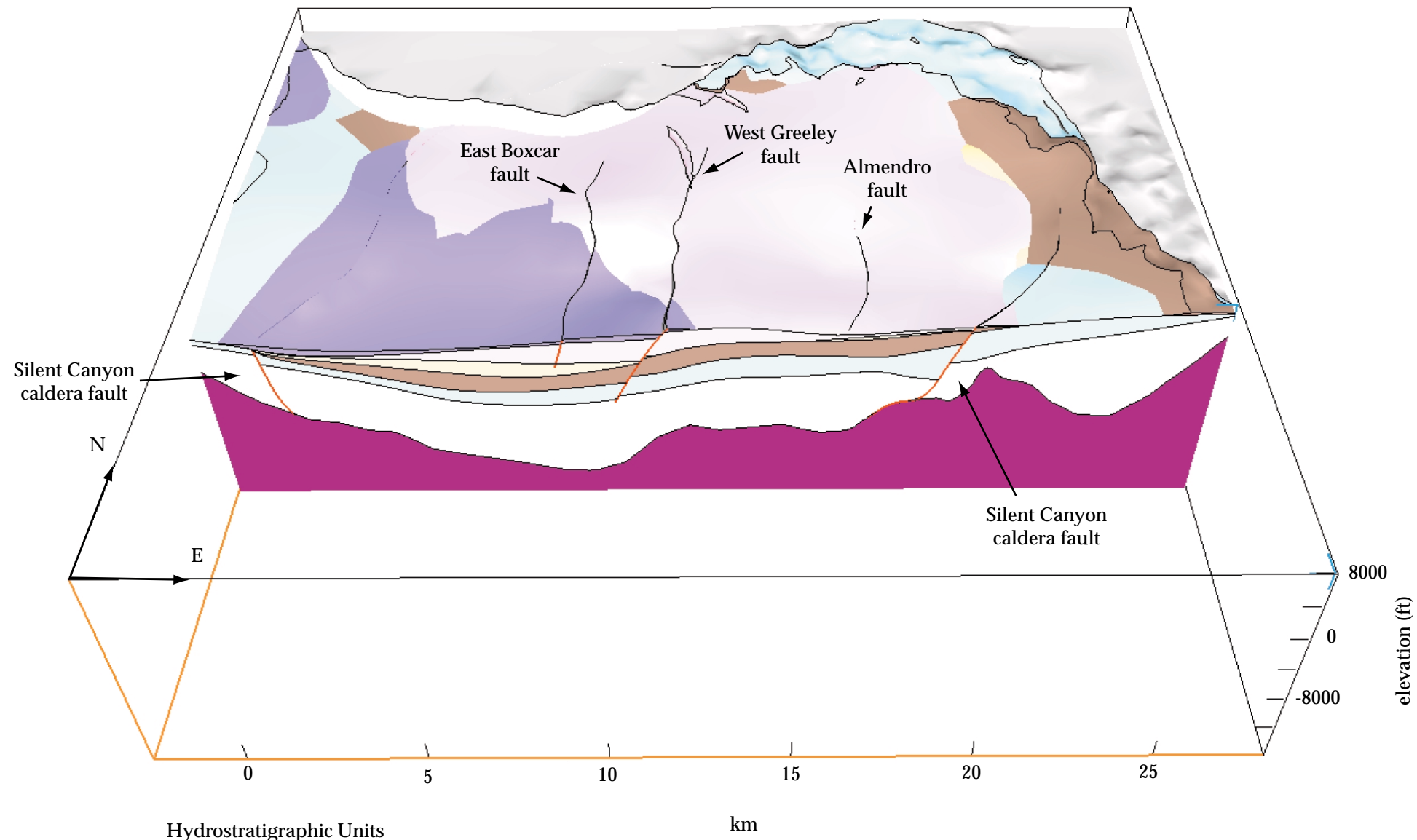


Figure 6c. Topopah Spring tuff aquifer. No vertical exaggeration. Three-dimensional view looking east, shown in place over lower units. Timber Mountain fault block is omitted because of lack of drill hole control.



Hydrostratigraphic Units

- |  |   |
|--|---|
| <ul style="list-style-type: none"> <li><span style="display: inline-block; width: 15px; height: 15px; background-color: #800080; border: 1px solid black; margin-right: 5px;"></span> Topopah Spring tuff aquifer</li> <li><span style="display: inline-block; width: 15px; height: 15px; background-color: #FF69B4; border: 1px solid black; margin-right: 5px;"></span> Calico Hills composite unit</li> <li><span style="display: inline-block; width: 15px; height: 15px; background-color: #FFFF00; border: 1px solid black; margin-right: 5px;"></span> Crater Flat composite unit</li> <li><span style="display: inline-block; width: 15px; height: 15px; background-color: #8B4513; border: 1px solid black; margin-right: 5px;"></span> Bullfrog Tuff confining unit</li> </ul> | <ul style="list-style-type: none"> <li><span style="display: inline-block; width: 15px; height: 15px; background-color: #ADD8E6; border: 1px solid black; margin-right: 5px;"></span> Belted Ranger aquifer</li> <li><span style="display: inline-block; width: 15px; height: 15px; background-color: #A9A9A9; border: 1px solid black; margin-right: 5px;"></span> Pre-Belted Range composite unit</li> <li><span style="display: inline-block; width: 15px; height: 15px; background-color: #800080; border: 1px solid black; margin-right: 5px;"></span> Basement</li> </ul> |
|--|---|

Figure 6d. Topopah Spring tuff aquifer. No vertical exaggeration. Three-dimensional view looking north, shown in place over lower units.

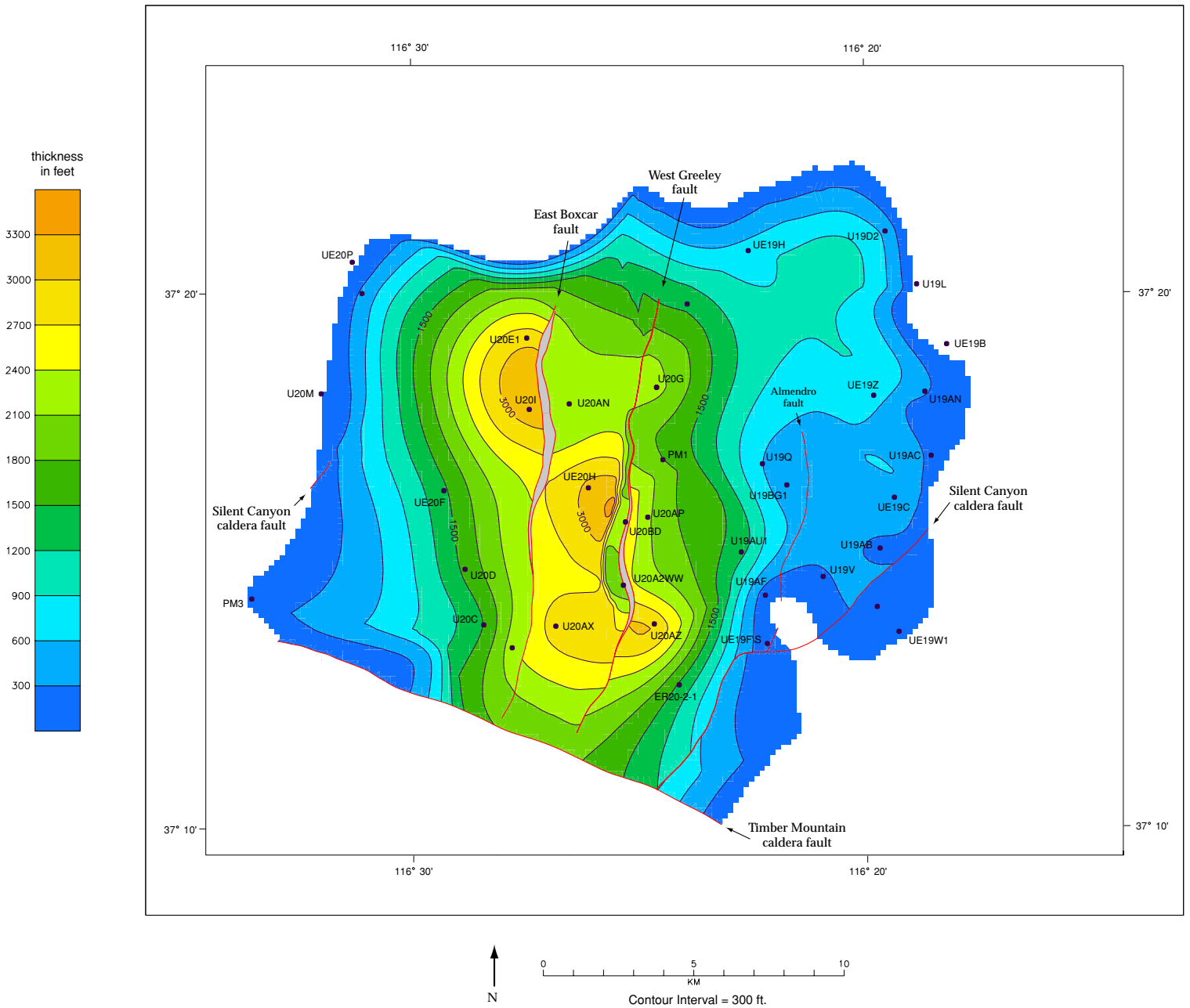


Figure 7a. Calico Hills composite unit. Distribution and thickness map (thickness in feet). Fault traces are grey where the orientation of the fault is not vertical and a thickness calculation is not possible. Drill holes that penetrate this unit or units stratigraphically beneath it are labelled by number; control points used to constrain the surface in EarthVision are dots. No thickness is shown south of the Timber Mountain caldera fault because of lack of drill hole control.

[Link to oversize version](#)

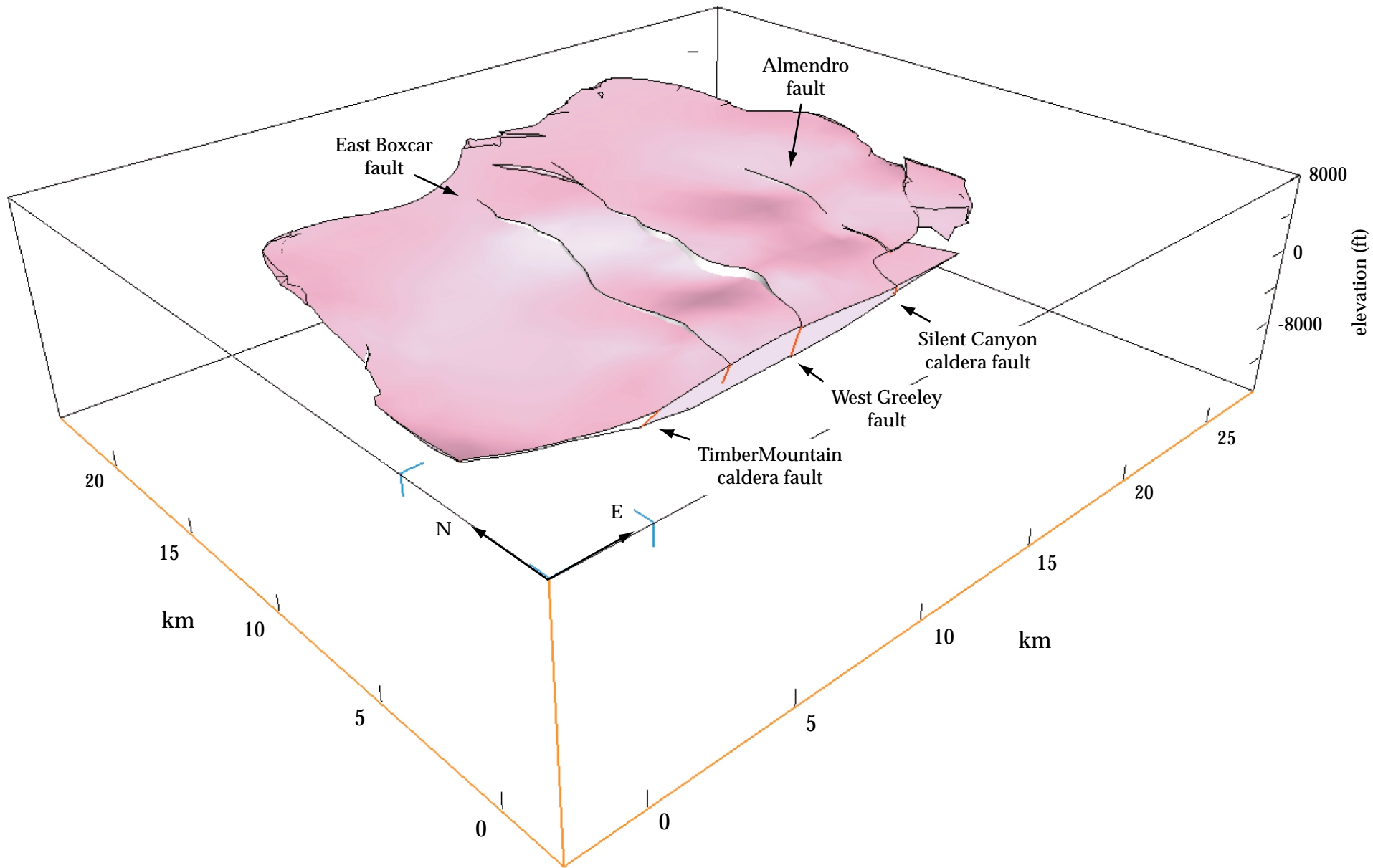


Figure 7b. Calico Hills composite unit. No vertical exaggeration. Three-dimensional view looking NE. Note the trace and offset of the north edge of the Timber Mountain caldera margin, and the East Boxcar, West Greeley, and Almendro north-south faults. Timber Mountain fault block is omitted because of lack of drill hole control.

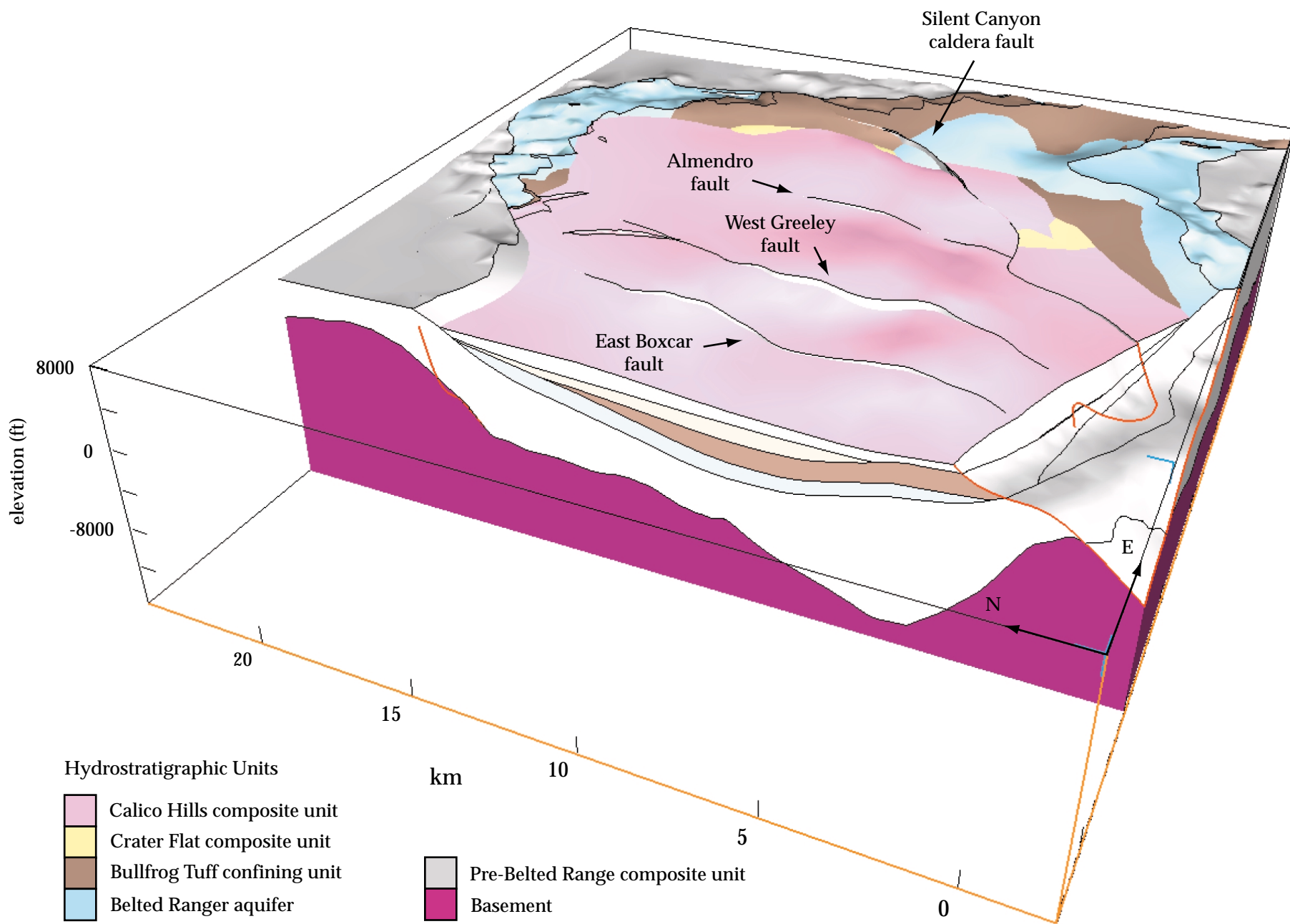
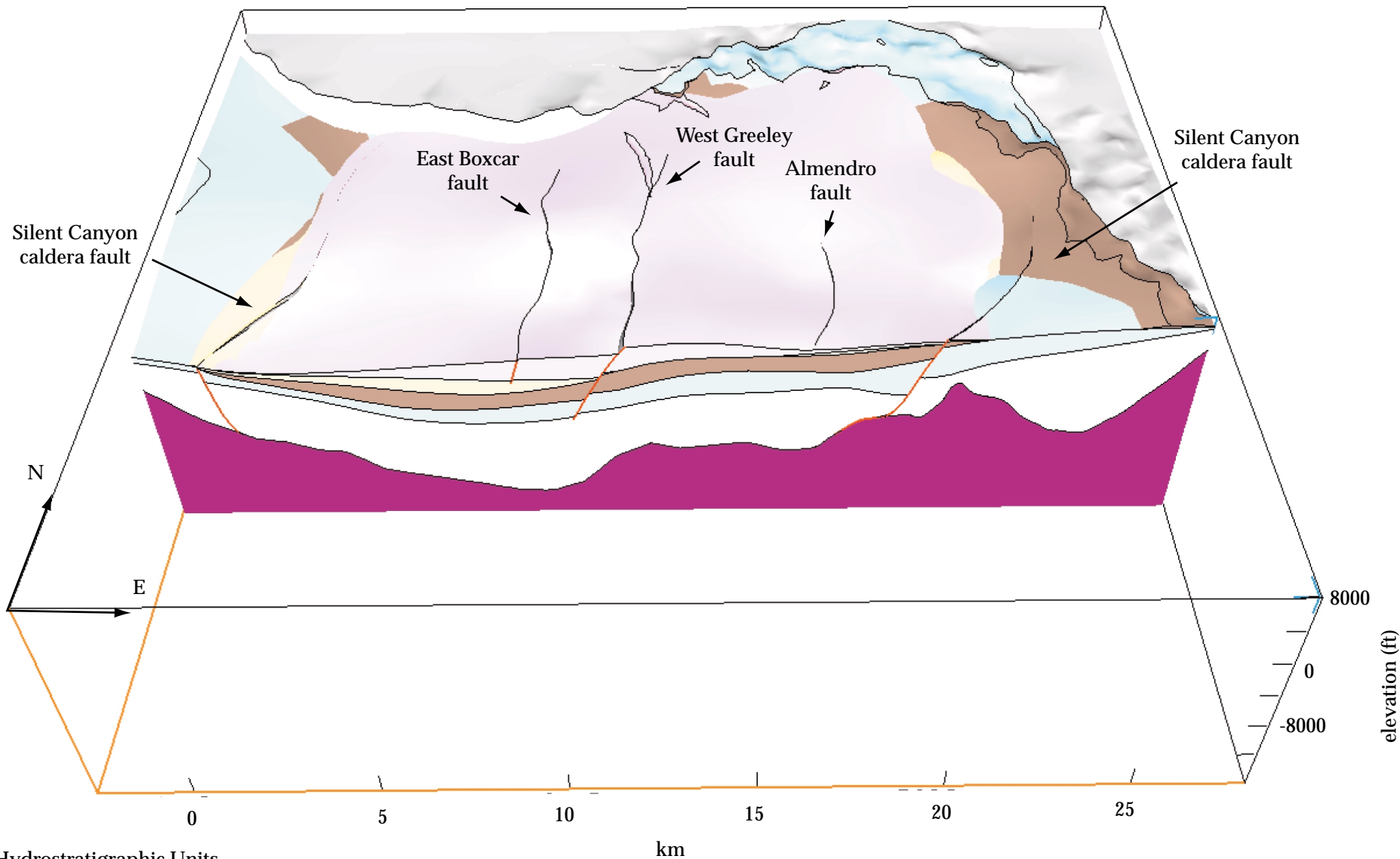


Figure 7c. Calico Hills composite unit. No vertical exaggeration. Three-dimensional view looking east, shown in place over lower units. Timber Mountain fault block is omitted because of lack of drill hole control.



Hydrostratigraphic Units

- Calico Hills composite unit
  - Crater Flat composite unit
  - Bullfrog Tuff confining unit
  - Belted Ranger aquifer
- Pre-Belted Range composite unit
  - Basement

Figure 7d. Calico Hills composite unit. No vertical exaggeration. Three-dimensional view looking north, shown in place over lower units.

thins abruptly north, west and south of the caldera margin. Most of the Calico Hills composite unit is saturated.

#### Crater Flat composite unit

Stratigraphic units above the Bullfrog Tuff in the Crater Flat Group are caldera-filling lava flows and tuffs of various types that make up the Crater Flat composite hydrostratigraphic unit. Most of these rocks are found in the western part of the SCCC (Area 20, fig. 8), where collapse associated with Bullfrog tuff eruption was apparently greatest. Distinctive lava or tuff units from the upper part of the Crater Flat Group include, in descending order, the tuff of Pool, the rhyolite of Inlet, the tuff of Jorum, the rhyolite of Sled, and the rhyolite of Kearsarge. These units are only locally present and are mostly aquifers except for zeolitized parts of the tuff of Jorum and the rhyolite of Sled. Intertonguing, non-welded tuffs, which are zeolitized in many places, are impermeable and form lenticular flow barriers. The three-dimensional distribution of the permeable and impermeable zones in the Crater Flat composite unit and the Calico Hills composite unit above it create a complicated ground-water flowpath in the western part of the SCCC. In the eastern part of the SCCC, in Area 19, the Crater Flat composite unit is comprised of the rhyolite of Kearsarge, a lava aquifer and a thin sequence of non-welded devitrified and altered tuffs that may act as flow barriers.

#### Bullfrog Tuff confining unit

The Bullfrog Tuff is considered to be a major caldera-forming, eruptive unit of the SCCC (Sawyer and Sargent, 1989; Ferguson and others, 1994; Sawyer and others, 1994). Its eruption is cited as the cause of a nested caldera within the SCCC, called the Area 20 caldera by these authors. The tuff occurs across the entire caldera complex but is especially thick in the west central part of the structure (fig. 9). Outside and east of the buried caldera complex rim the Bullfrog Tuff is relatively thin. Within the SCCC, where the Bullfrog Tuff is thickest, it is non-welded and lithic-rich and has been extensively zeolitized, making it a confining unit. The Bullfrog Tuff confining unit is the most significant confining unit in the SCCC. It is widespread and relatively

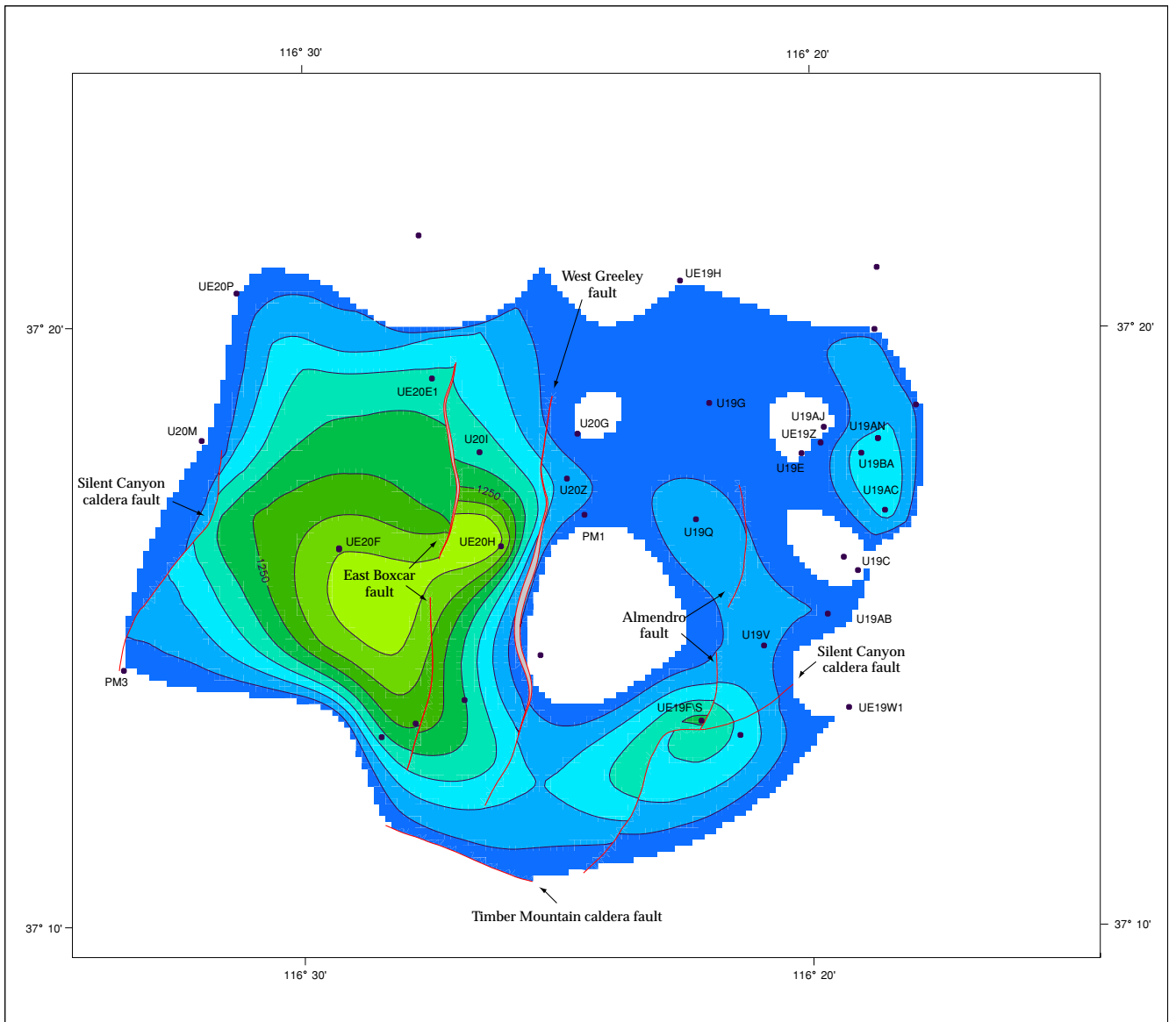


Figure 8a. Crater flat composite unit. Distribution and thickness map (thickness in feet). Fault traces are grey where the orientation of the fault is not vertical and a thickness calculation is not possible. Drill holes that penetrate this unit or units stratigraphically beneath it are labelled by number; control points used to constrain the surface in EarthVision are dots. No thickness is shown south of the Timber Mountain caldera fault because of lack of drill hole control.

[Link to oversize version](#)

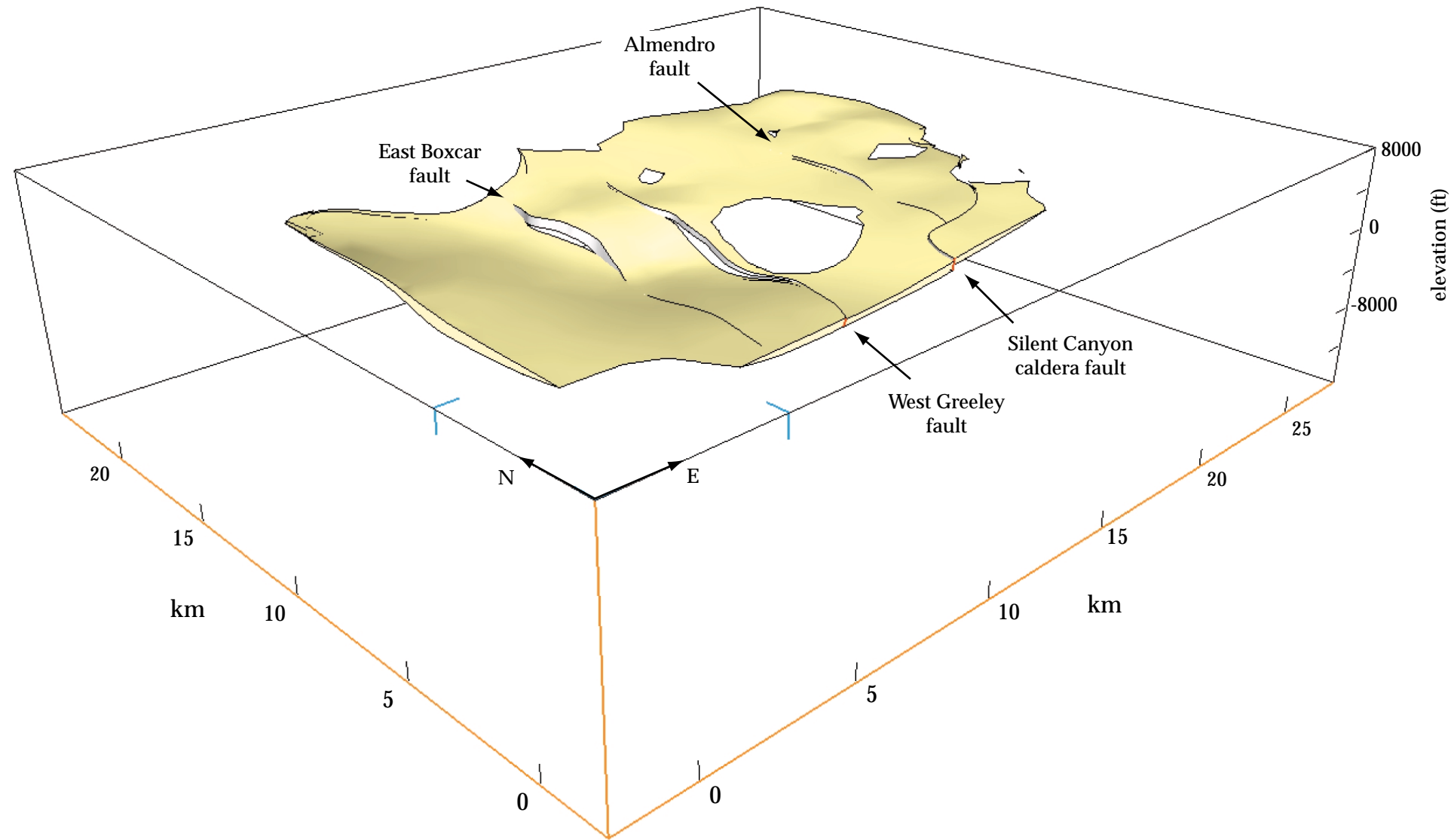


Figure 8b. Crater Flat composite unit. No vertical exaggeration. Three-dimensional view looking NE. Note the trace and offset on the north edge of the Timber Mountain caldera margin, and the East Boxcar, West Greeley and Almendo north-south faults.

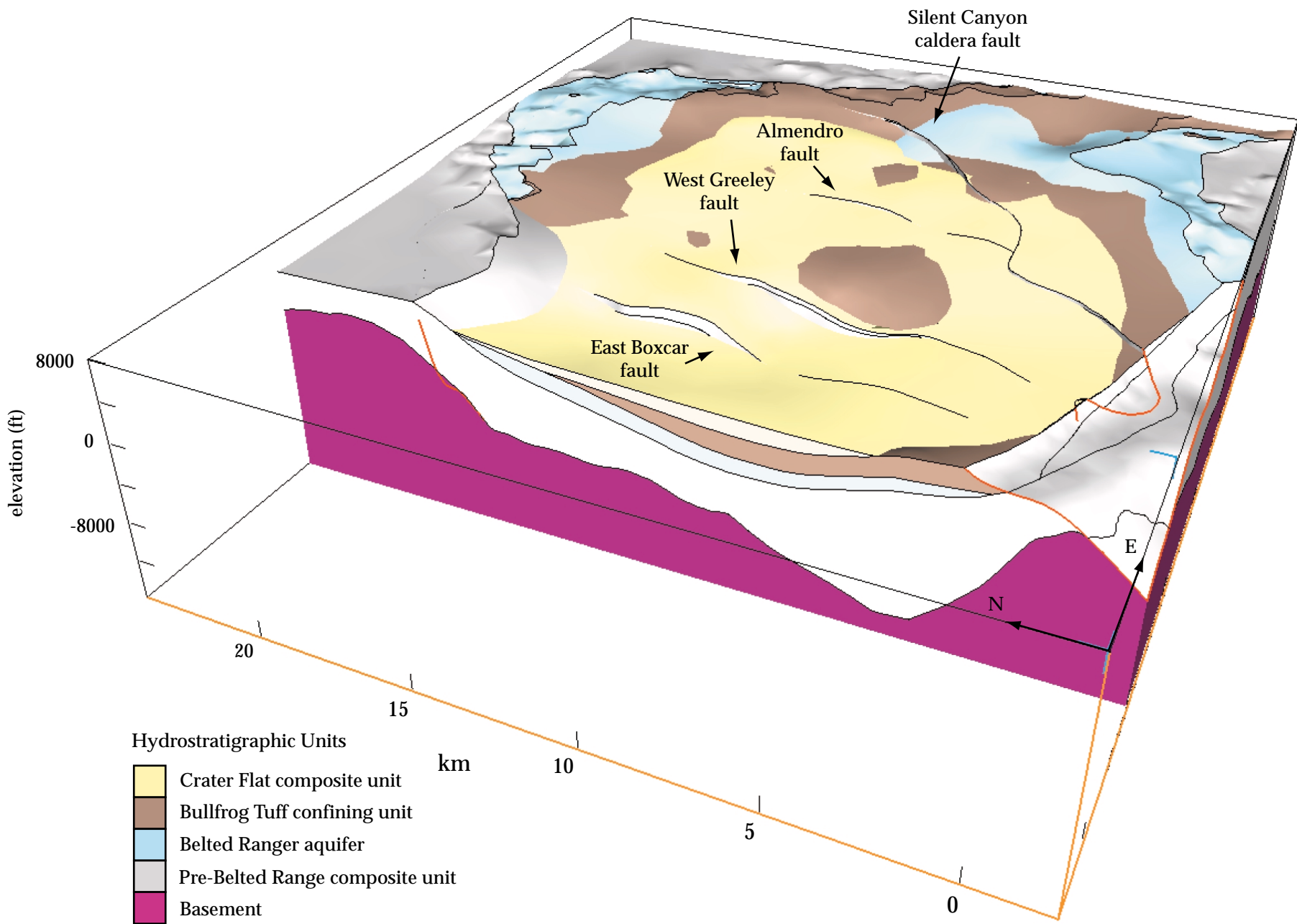


Figure 8c. Crater Flat composite unit. No vertical exaggeration. Three-dimensional view looking east, shown in place over lower units. Timber Mountain fault block is omitted because of lack of drill hole control.

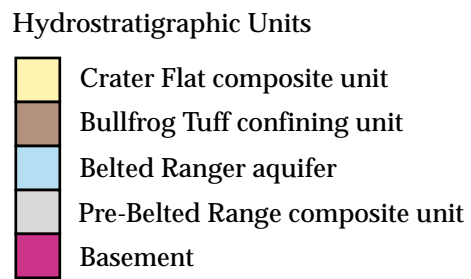
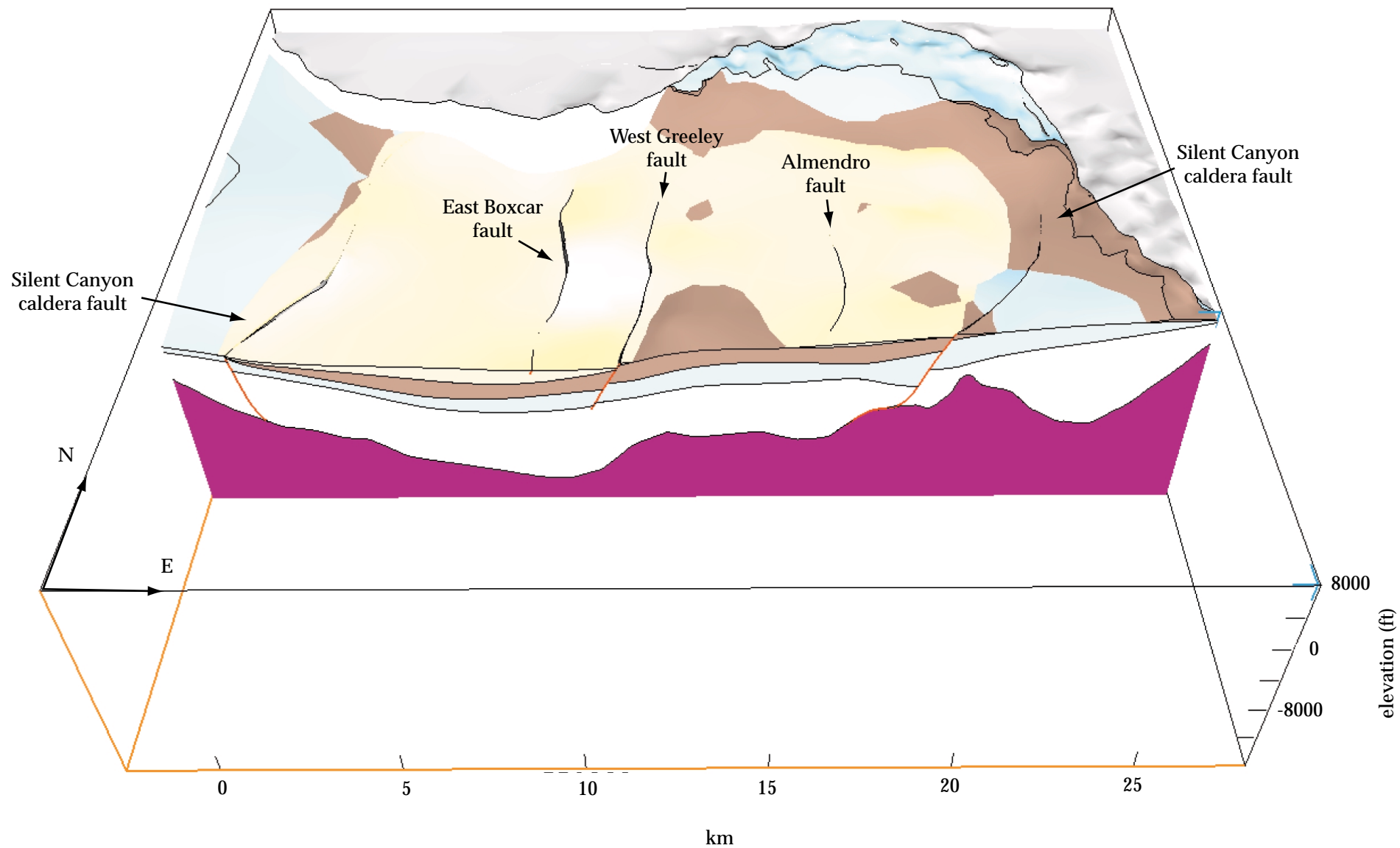


Figure 8d. Crater Flat composite unit. No vertical exaggeration. Three-dimensional view looking north, shown in place over lower units.

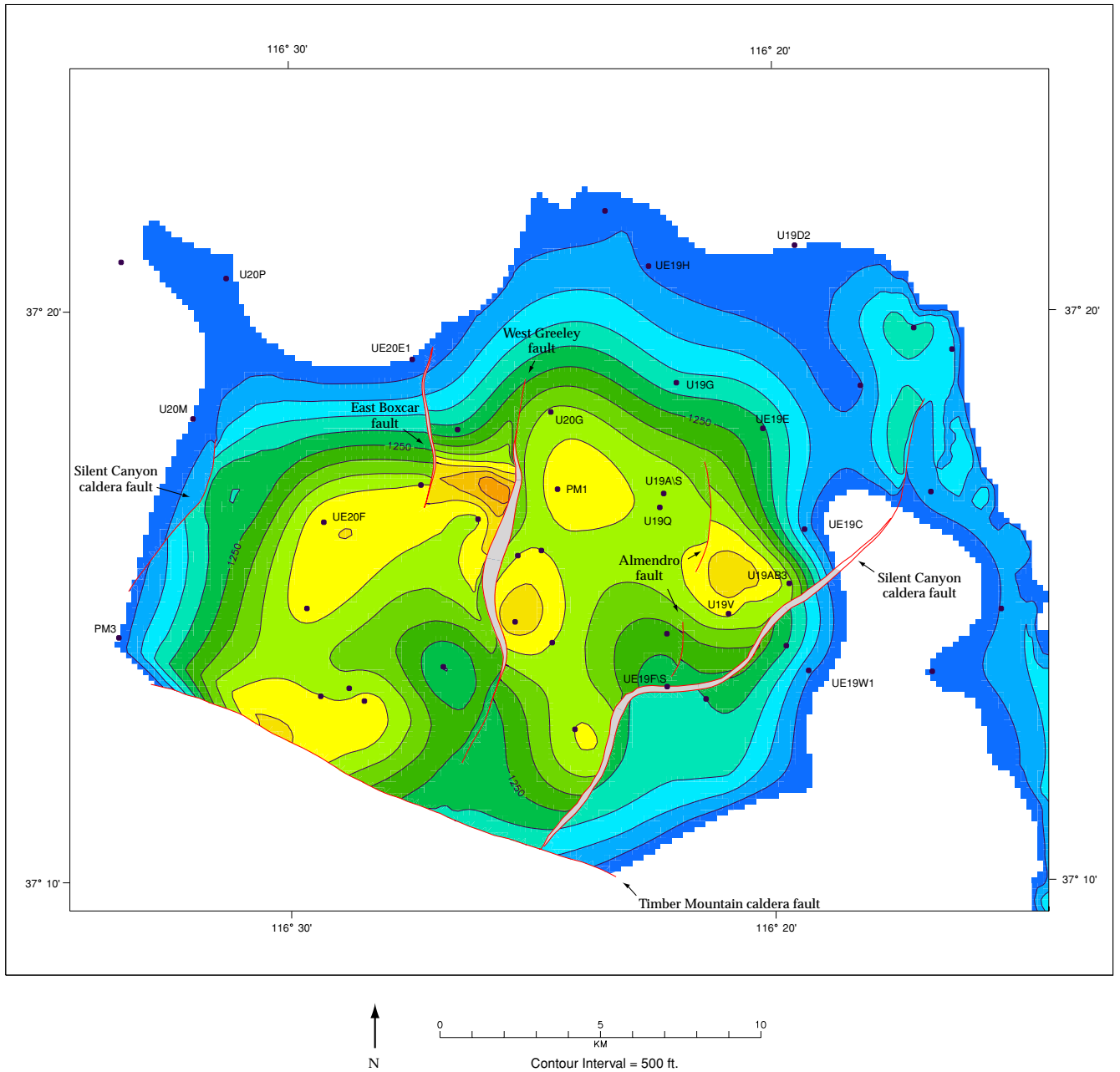
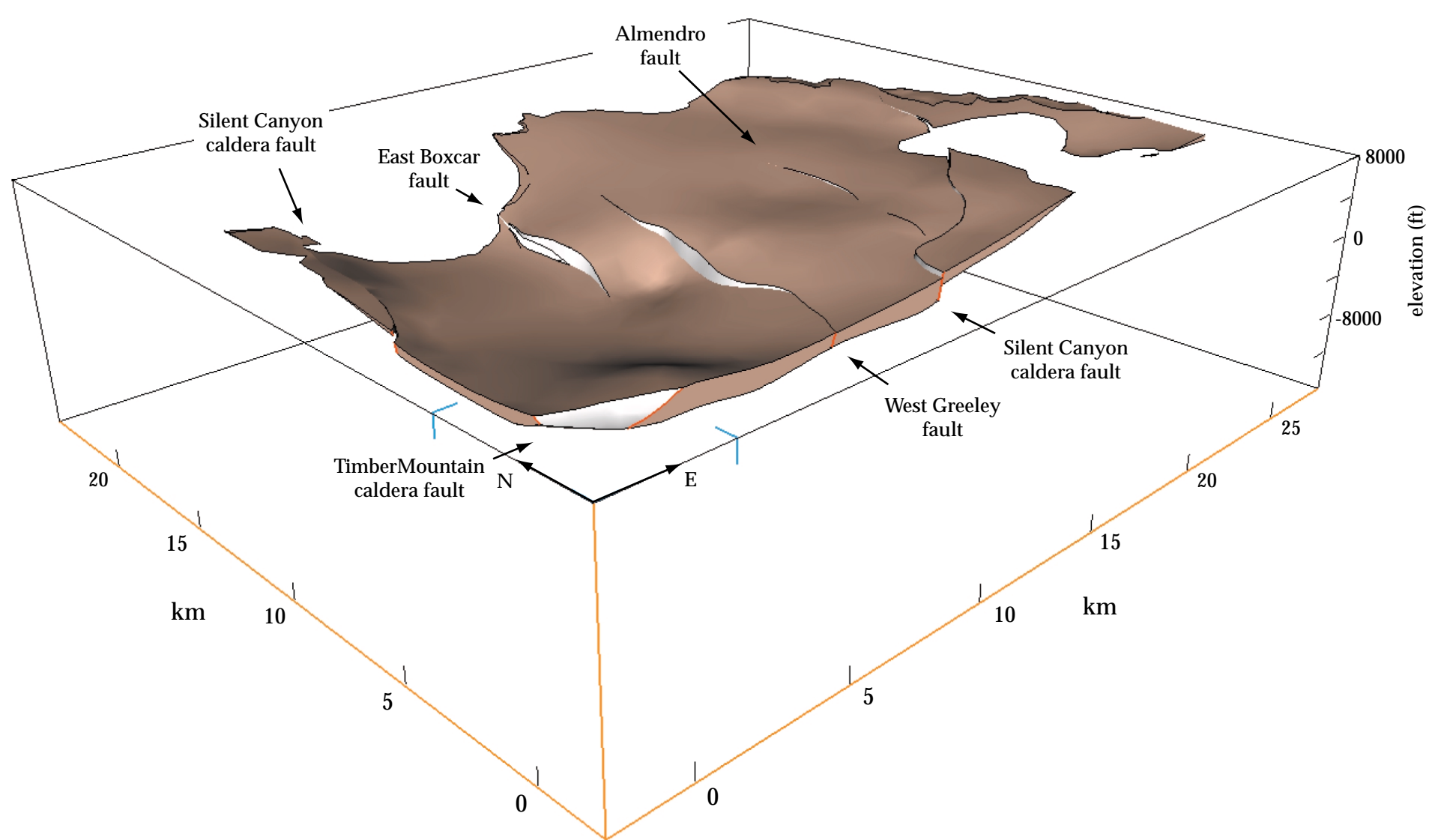


Figure 9a. Bullfrog Tuff confining unit. Distribution and thickness map (thickness in feet). Fault traces are grey where the orientation of the fault is not vertical and a thickness calculation is not possible. Drill holes that penetrate this unit or units stratigraphically beneath it are labelled by number; control points used to constrain the surface in EarthVision are dots. No thickness is shown south of the Timber Mountain caldera fault because of lack of drill hole control.

[Link to oversize version](#)



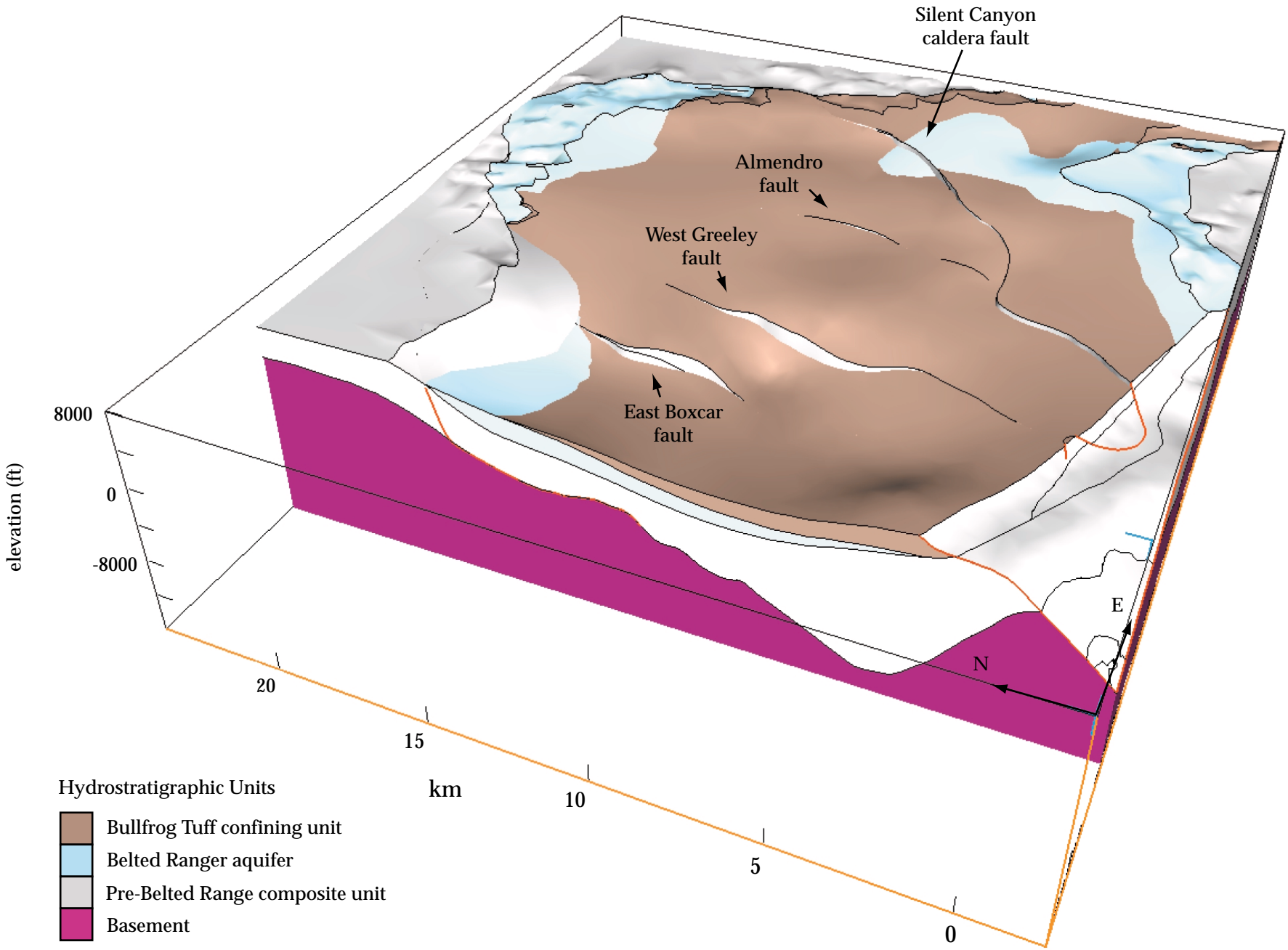
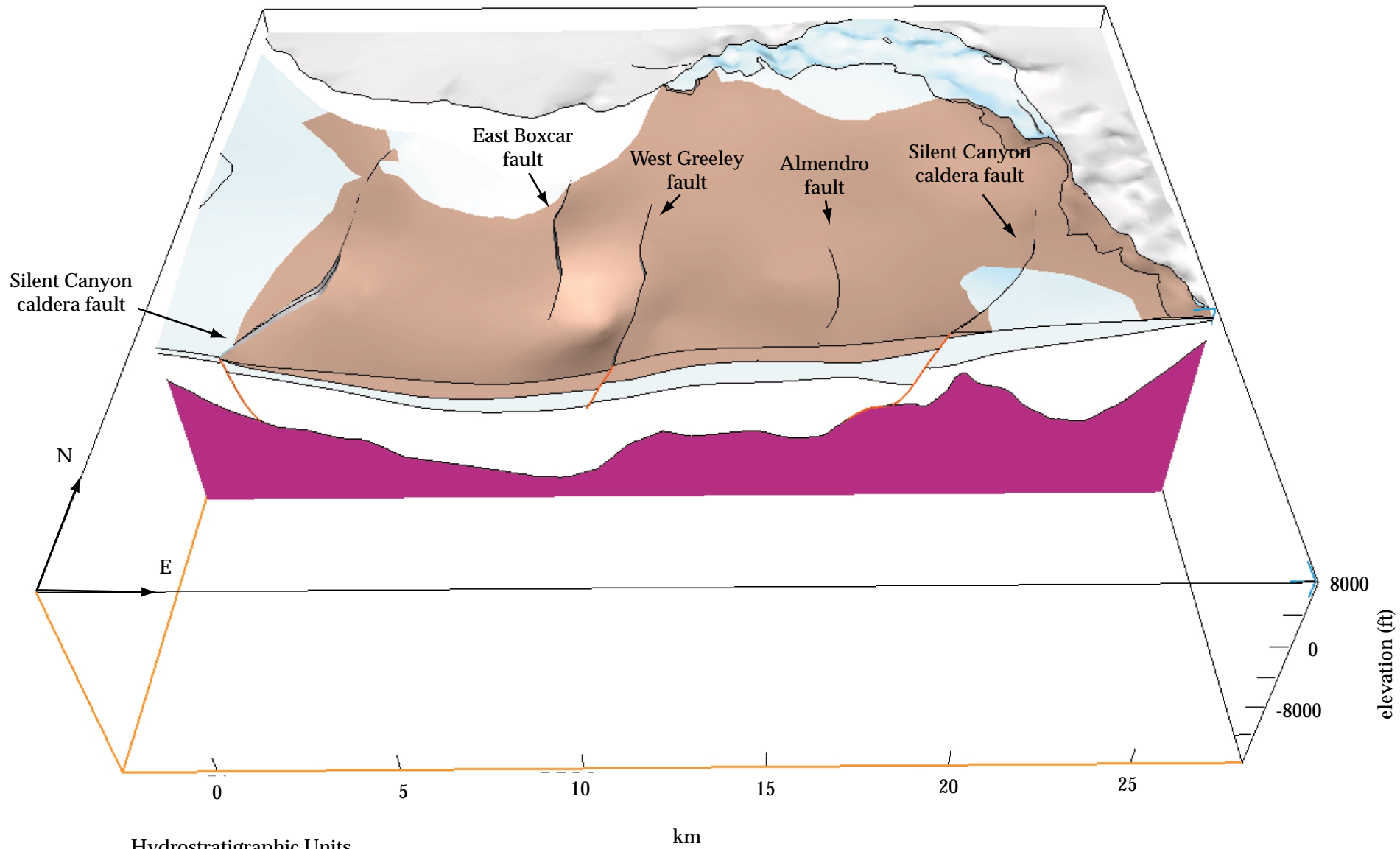


Figure 9c. Bullfrog Tuff confining unit. No vertical exaggeration. Three-dimensional view looking east, shown in place over lower units. Timber Mountain fault block is omitted because of lack of drill hole control.



thick and, in the southwestern two thirds of the caldera complex, is below the water table at depths where it should have a great effect on ground-water flow.

#### Belted Range aquifer

The Belted Range aquifer is composed of lava flows and tuffs of the Dead Horse Flat Formation underlain by the Grouse Canyon Tuff. Comendite lava flows of Split Ridge and Quartet Dome are considered to be precursor lavas to the Grouse Canyon Tuff but not caldera causing eruptions (Sawyer and Sargent, 1989; Sawyer and others, 1994). These units comprise the Belted Range Group (table 1). Lava flows of the Dead Horse Flat Formation and Grouse Canyon Tuff are the principal caldera-filling rocks of a caldera that developed in the NE half of the SCCC during and after eruption of the Grouse Canyon Tuff (Noble and others, 1968; Sawyer and others, 1994; Ferguson and others, 1994). The Belted Range aquifer underlies most of Pahute Mesa, and has been identified in drill holes across all of the SCCC (fig. 10). It is particularly thick (greater than 1,800 m (6,000 ft)), in the northeastern part of the caldera complex near the down-faulted eastern margin. The Grouse Canyon tuff and lava flows of the Belted Range Group thin at the caldera's margin and crop out as thin out-flow (extracaldera) units around and outside most of the caldera complex (fig. 10 a,b,c,d). Within the SCCC, the Belted Range aquifer is saturated; outside the caldera it is above the water table.

#### Pre-Belted Range composite unit

The lower half or more of the depression filling rocks of the SCCC beneath Pahute Mesa comprise the pre-Belted Range composite unit (fig. 11). The deepest drill-holes, and drill holes SE and W of the SCCC on Pahute Mesa have penetrated the upper part of this hydrostratigraphic unit but as much as 3,000 m (9,900 ft) of presumed volcanic rock exists between the deepest holes and the basement. These volcanic rocks are most likely lava flows and welded and nonwelded tuffs. Rocks in the Tertiary sequence below the Belted Range Group in areas adjacent to Pahute Mesa include the rhyolite

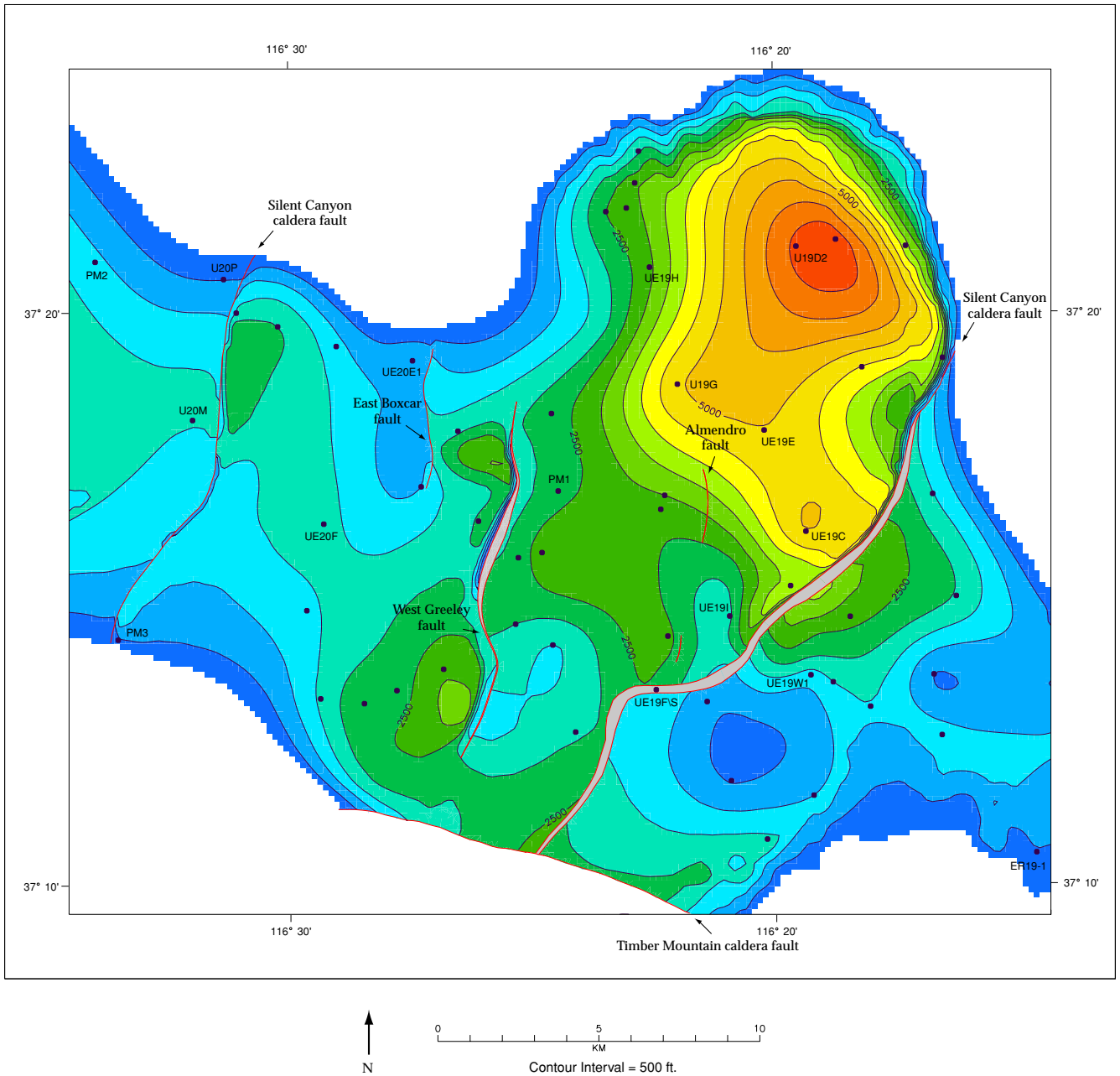


Figure 10a. Belted Range aquifer. Distribution and thickness map (thickness in feet). Fault traces are grey where the orientation of the fault is not vertical and a thickness calculation is not possible. Drill holes that penetrate this unit are labelled by number; control points used to constrain the surface in EarthVision are dots. No thickness is shown south of the Timber Mountain caldera fault because of lack of drill hole control.

[Link to oversize version](#)

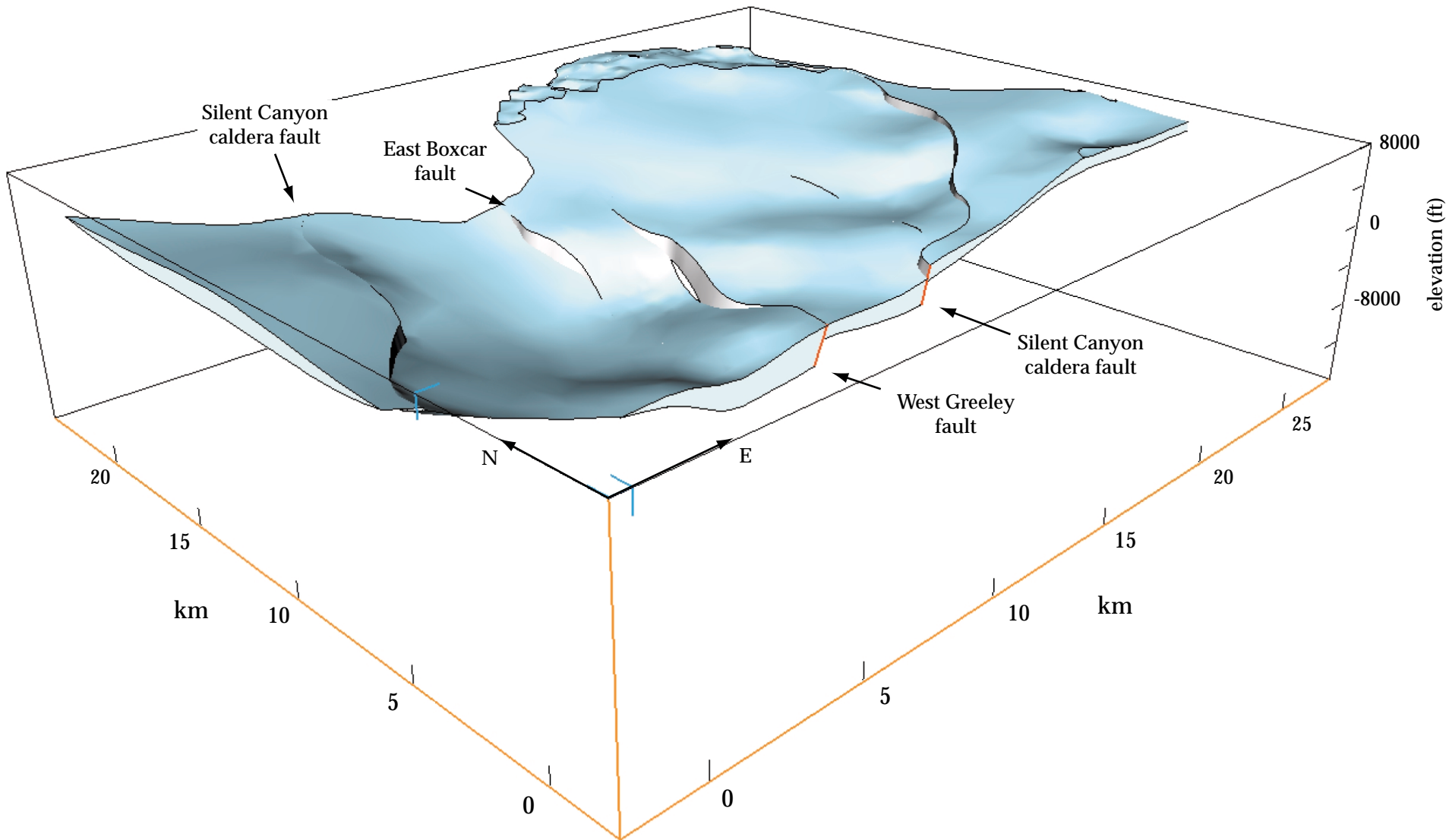


Figure 10b. Belted Range aquifer. No vertical exaggeration. Three-dimensional view looking NE. Note the trace and offset on the east and west parts of the Silent Canyon caldera margin and the East Boxcar and West Greeley north-south faults.

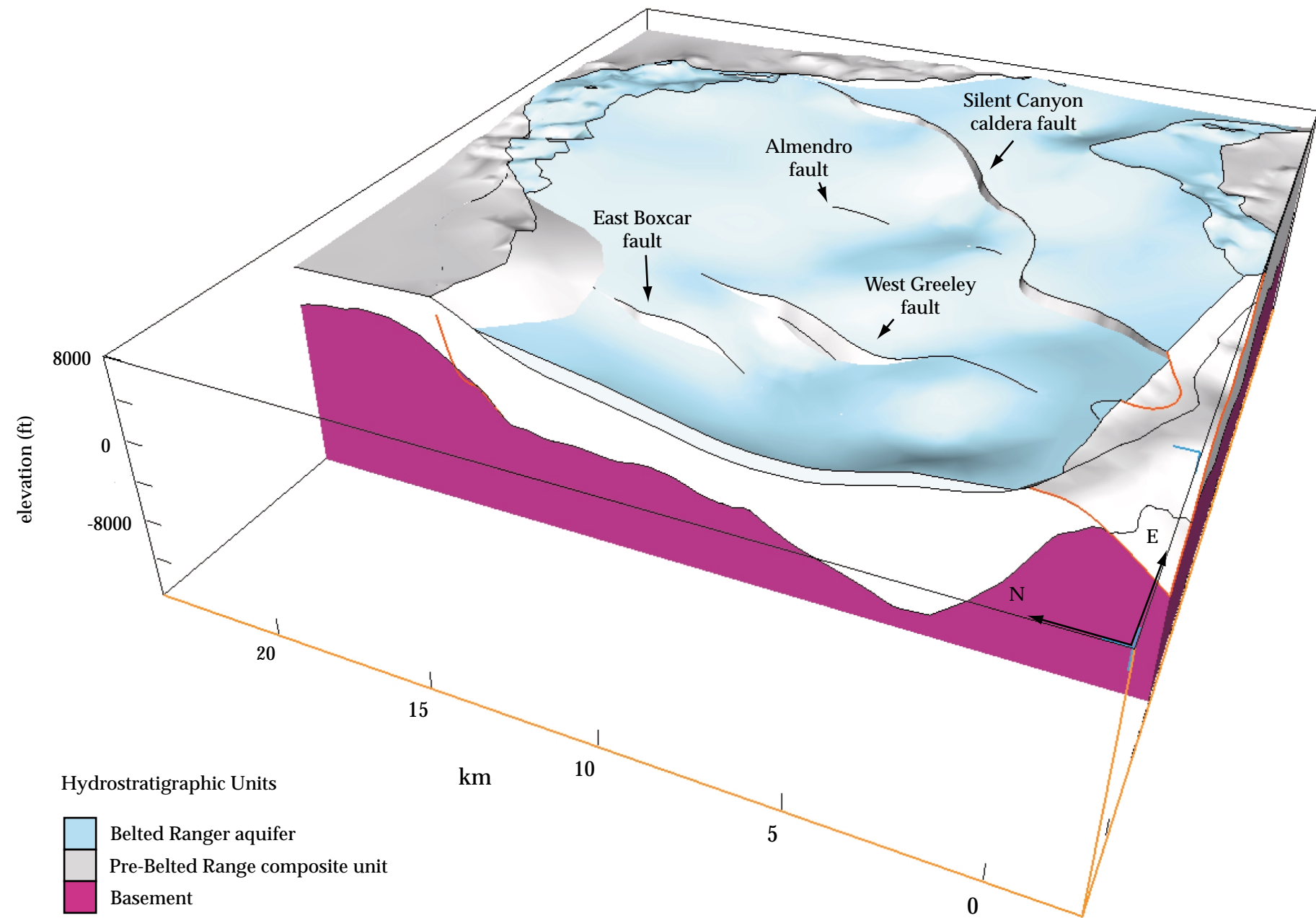
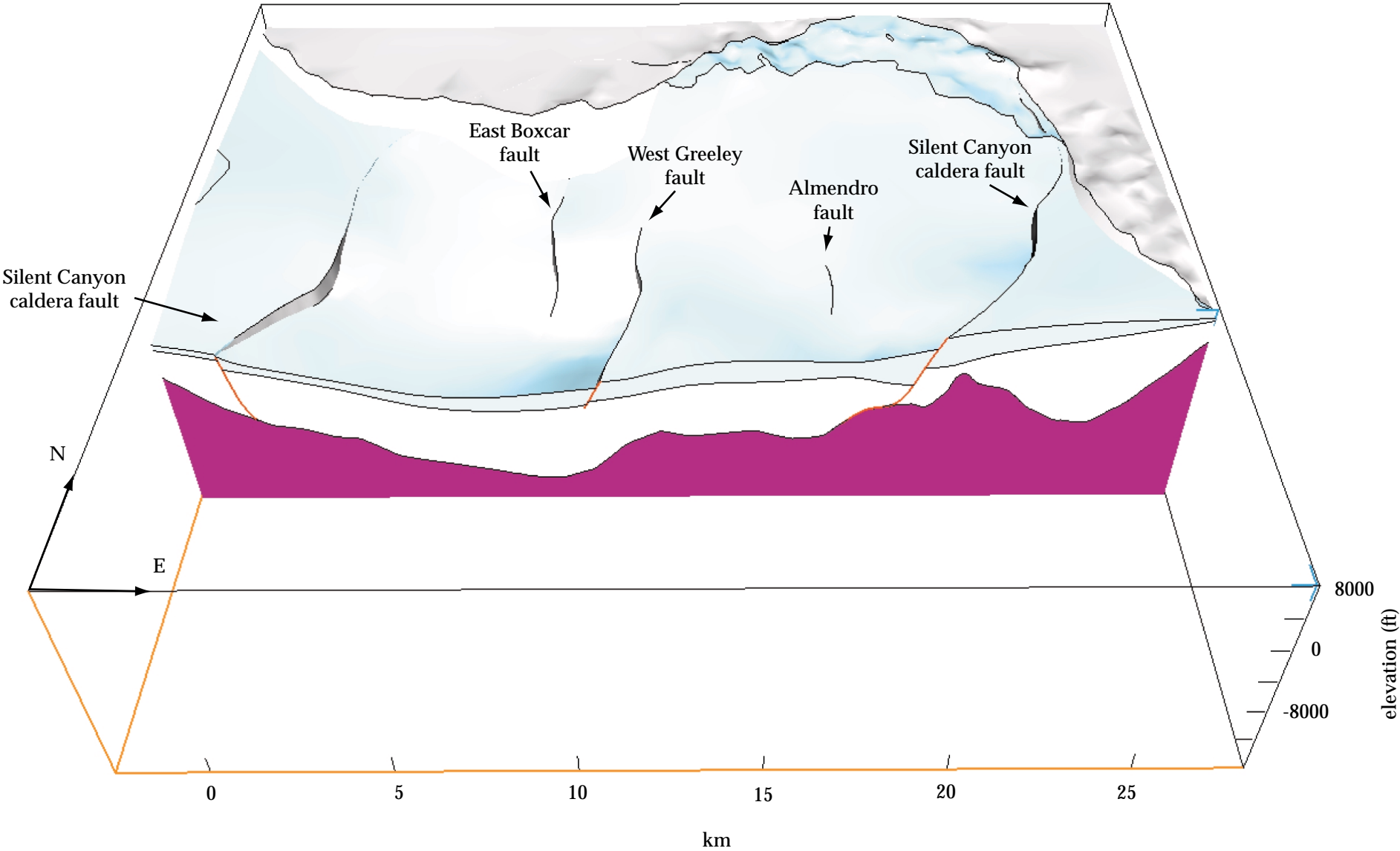


Figure 10c. Belted Range aquifer. No vertical exaggeration. Three-dimensional view looking east, shown in place over lower units. Timber Mountain fault block is omitted because of lack of drill hole control.



Hydrostratigraphic Units

- Belted Ranger aquifer
- Pre-Belted Range composite unit
- Basement

Figure 10d. Belted Range aquifer. No vertical exaggeration. Three-dimensional view looking north, shown in place over lower units.

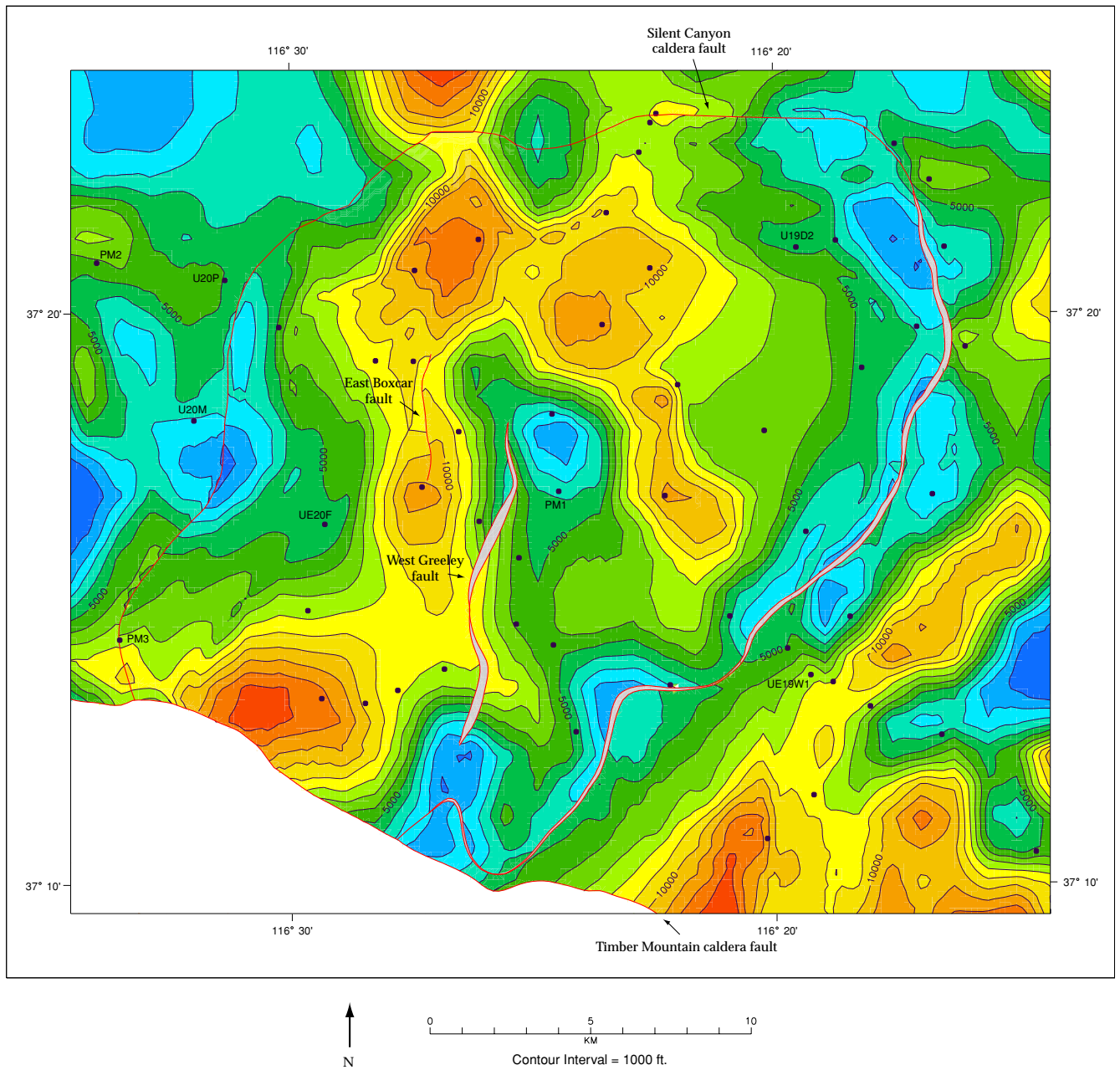


Figure 11a. Pre-Belted Range composite unit. Distribution and thickness map (thickness in feet). Fault traces are grey where the orientation of the fault is not vertical and a thickness calculation is not possible. Drill holes that penetrate this unit are labelled by number; control points used to constrain the surface in EarthVision are dots. No thickness is shown south of the Timber Mountain caldera fault because of lack of drill hole control.

[Link to oversize version](#)

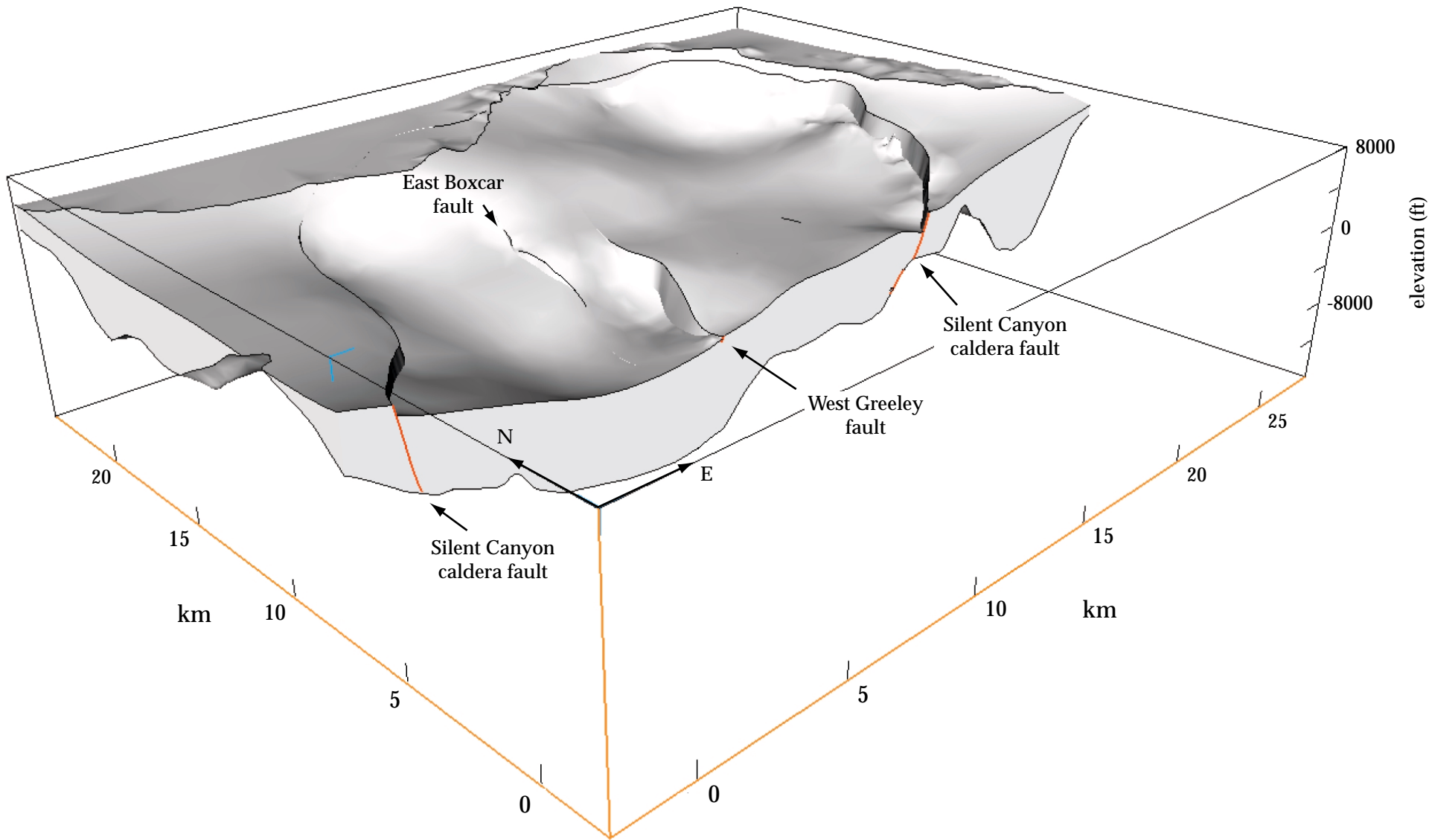


Figure 11b. Pre-Belted Range composite unit. No vertical exaggeration. Three-dimensional view looking NE. Note the trace and offset of the Silent Canyon caldera margin and the East Boxcar and West Greeley north-south faults.

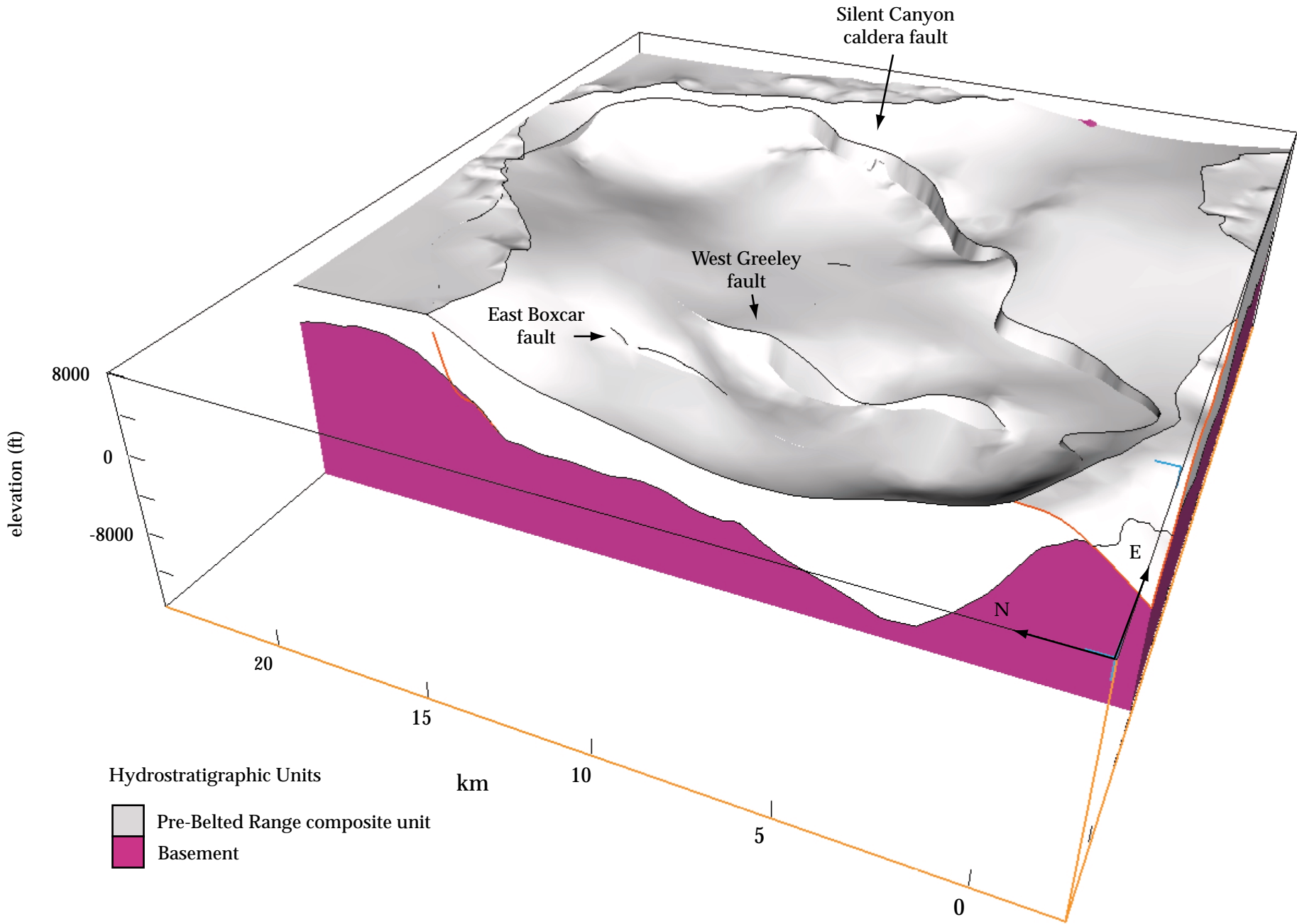
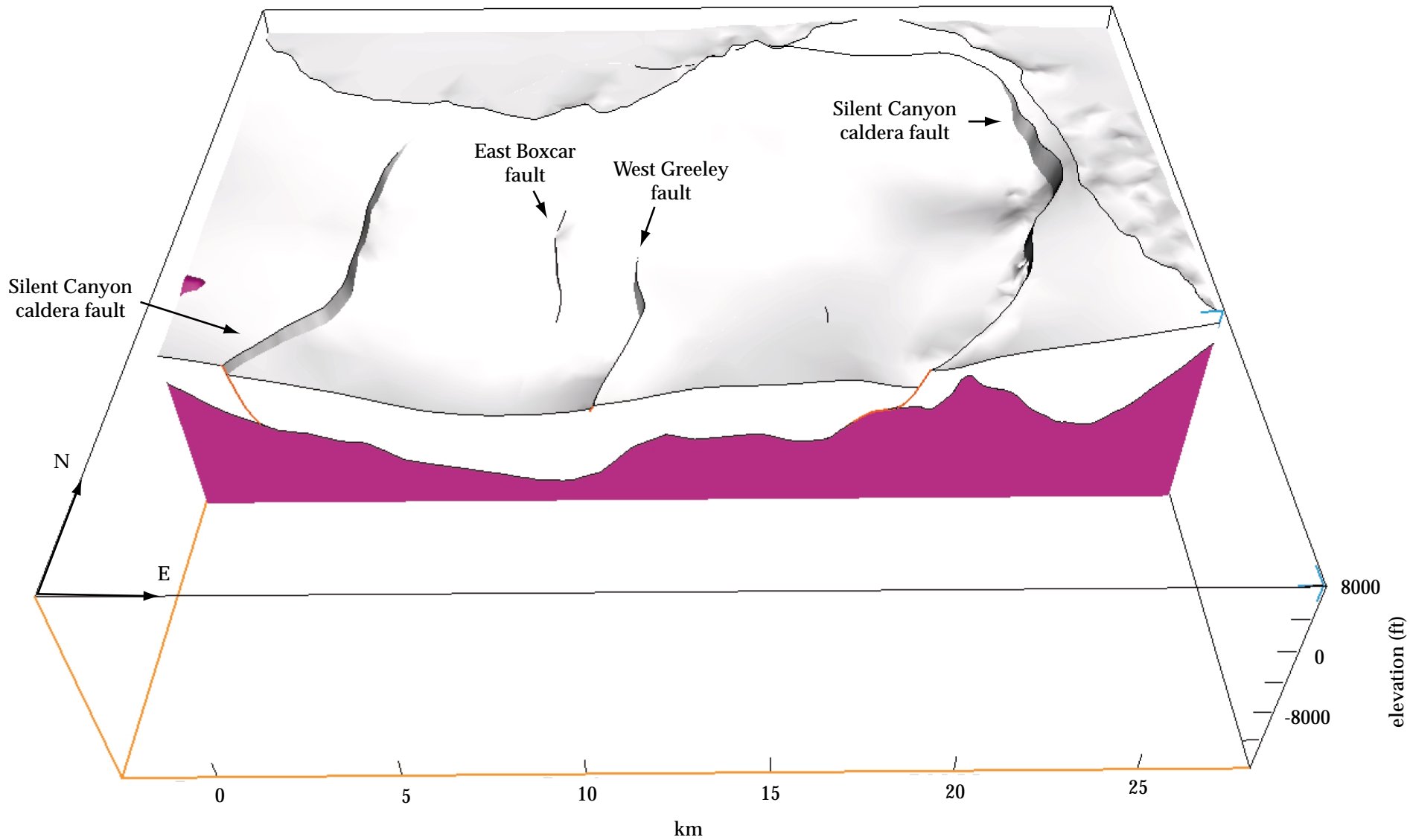


Figure 11c. Pre-Belted Range composite unit. No vertical exaggeration. Three-dimensional view looking east, shown in place over lower units. Timber Mountain fault block is omitted because of lack of drill hole control.



Hydrostratigraphic Units

- Pre-Belted Range composite unit
- Basement

Figure 11d. Pre-Belted Range composite unit. No vertical exaggeration. Three-dimensional view looking north, shown in place over lower units.

of Quartet Dome, the Lithic Ridge Tuff, the tuff of Tolicha Peak, the dacite of Mount Helen, the Tub Spring Tuff, the Redrock Valley Tuff, and other units (Table 1). The lava flows and welded tuffs in this sequence generally form fracture-flow aquifers. The nonwelded tuffs are almost always devitrified and zeolitized and are confining units. Rocks in the lower parts of the pre-Belted Range composite unit most likely act as a confining unit due to compaction and alteration of these rocks which are buried to great depths.

### Basement

Nowhere in Pahute Mesa on the NTS do basement rocks crop out or are they penetrated by any drill hole. Gravity modeling indicates that the basement is generally more than 1,200 m (4,000 ft), and in places as much as 6,000 m (19,800 ft), below the surface (*see* Basement gravity section). It is postulated here that the basement of Pahute Mesa is granitic rock of the upper part of the SCCC magma system that intruded slightly metamorphosed quartzite, siltstone, and limestone of Precambrian and Paleozoic age. In the pre-Tertiary rocks, carbonates frequently act as aquifers and siliceous rocks, including granitoids, are confining units. All of the basement rocks, however, are much faulted which create possible flow paths unless the faults are healed and thus impede flow. In general, the basement probably does not act as a barrier to ground-water flow although it is at such great depth beneath the SCCC that it is assumed to be below the principal zone of ground-water flow.

### STRUCTURE

The structural framework of Pahute Mesa is that of a buried multiple collapse caldera complex-- the Silent Canyon caldera complex (SCCC). The elements of the caldera complex are not visible at the surface, being concealed by hundreds of feet of nearly flat-lying welded tuff from sources south and west of Pahute Mesa. The only evidence of the buried calderas at the surface are inward dips of the Timber Mountain Tuff (Orkild and others, 1969) possibly caused by ramping against, and over, the topographic margin of the partially buried caldera complex. The youngest tuffs, the Trail Ridge, Pahute Mesa, and Rocket Wash Tuffs from the Black Mountain volcanic center to the

west of Pahute Mesa spread across the western edge of the completely buried caldera topographic rim.

The location and approximate geometry of the SCCC caldera margin can be determined only by indirect means, although the general area of subsidence is well documented by the many drill holes that penetrate caldera-filling rocks within the structural basin underlying Pahute Mesa. Gravity analyses (*see* Basement surface section) estimate the location of the edge, slope, and depth of the basin beneath the nearly horizontal upper welded tuffs. Extrapolation of this surface upward to the outer, or topographic, edge of the SCCC as shown by Wahl and others (1997) and Laczniaik and others (1996) defines the upper part of the caldera collapse structure. Contrary to the commonly held conceptual view of a caldera fault, and described here in the section “Caldera Concept”, the extrapolated upper part of the structure in this model of the SCCC is more steeply dipping than the deeper gravity-defined part of the surface. The reason for this departure from the conceptual caldera view is probably due to the imprecise location of the buried topographic rim and the simplification of effects of gravity inversion to smooth curves at depth. A caldera topographic margin is not shown because more empirical data is needed to build it into the model. The crenulated, steeply dipping, oval shaped surface of the basin is assumed to be the youngest ring fault at the margin of the caldera complex (fig.12a, b, c). Older caldera faults within the SCCC that are partially or completely destroyed are not detected by gravity contrasts in the low density rocks of the SCCC. The deeper gravity defined surface beneath the SCCC may be a series of steeply dipping step-like faults. Because of the great depth of this surface (>3,000 m; (10,000 ft)), the inverted gravity data will likely be unable to resolve the individual fault surfaces. As a result of this the caldera boundary surface is smooth and gently dipping. Boundaries of younger calderas within the SCCC are also not seen by gravity contrasts but geologic evidence from drill hole data, for the Area 20 caldera is compelling. Eruption of the Bullfrog Tuff is presumed to be responsible for this caldera (Sawyer and Sargent, 1989;

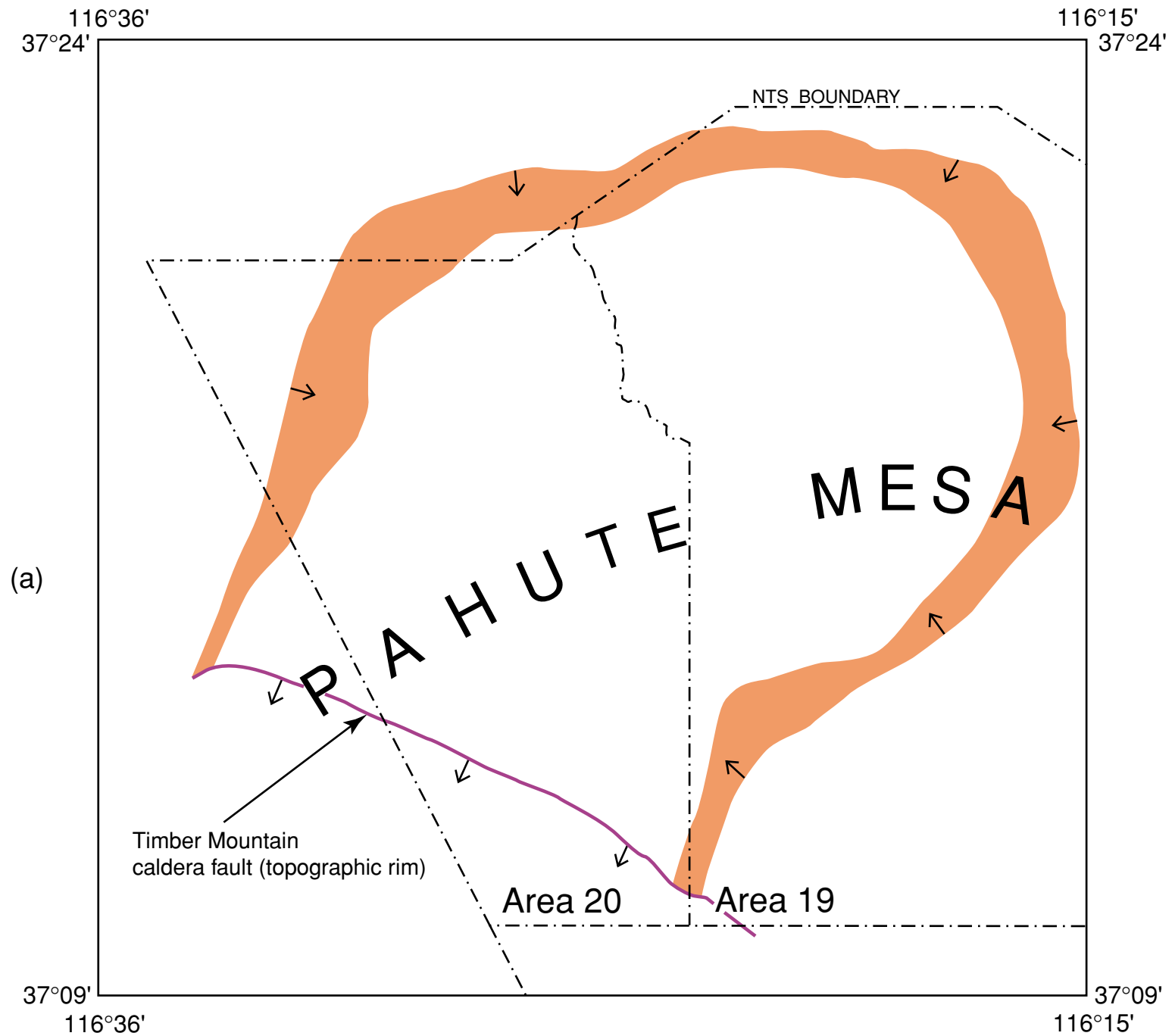


Figure 12a. The Silent Canyon caldera complex margin. (a) Plan view, with arrows showing dip direction of the buried ring fault. Inner edge is deeper than the outer edge, with a dip  $45^\circ$  or more in most places. (b) three-dimensional view of the Silent Canyon ring fault looking N (same as plan view) and (c) looking NE. The southwestern portion is cut off by the Timber Mountain caldera margin (not shown).

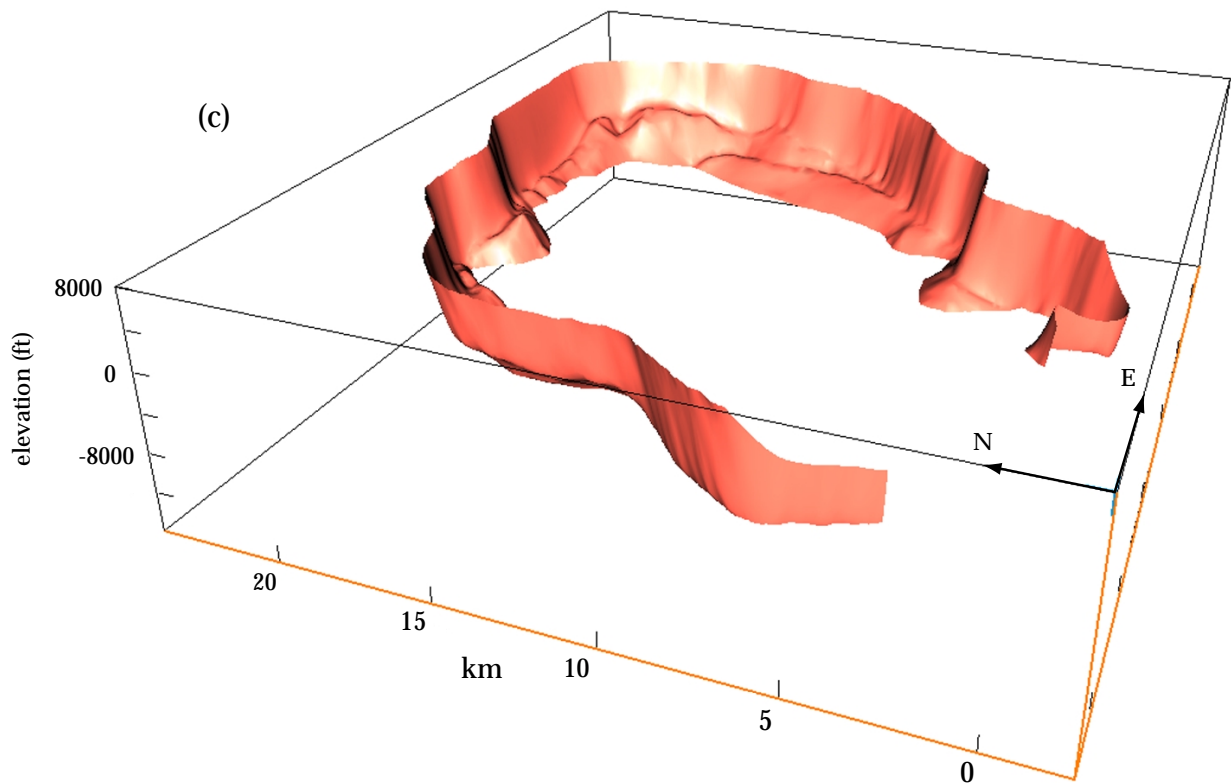
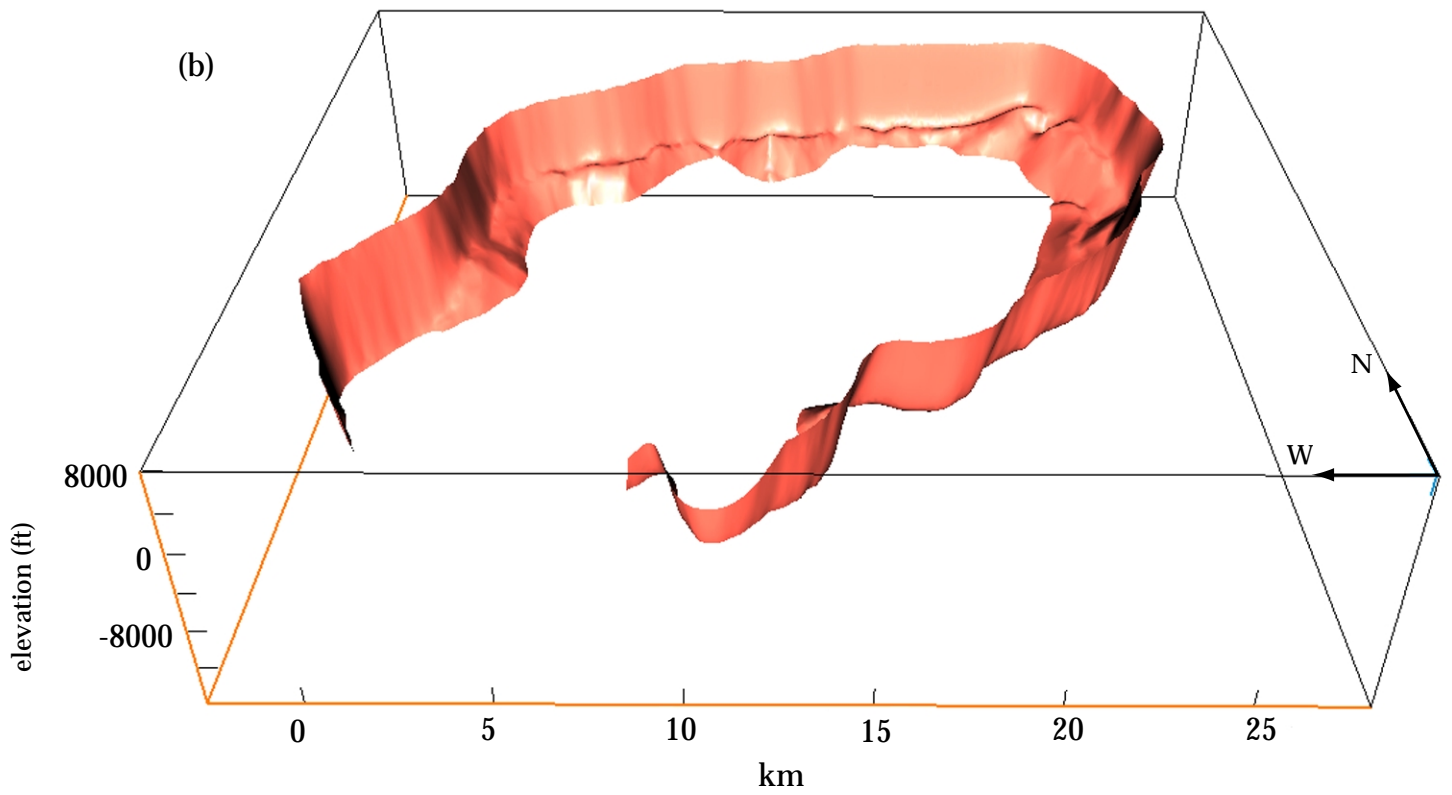


Figure 12 b, c. The Silent Canyon caldera fault surface from the "EarthVision" model. No vertical exaggeration. (b) View in the same orientation as figure 12a. (c) View looking northeast.

Sawyer and others, 1994) and the thick accumulation of this tuff (*see* Figure 9) outlines the general margin of the Area 20 caldera as envisioned by Sawyer and others (1994). Because our model bases the caldera margins on a density contrast the Area 20 caldera fault does not appear in our model.

A second, arcuate, south-dipping surface which is a segment of the Timber Mountain caldera complex caldera margin truncates the southwestern part of the SCCC (fig.13). The faults around the southern part of the SCCC and rocks within this caldera complex are down-dropped into the northern part of the younger Timber Mountain caldera complex. Lack of drill hole data makes geologic models for this area very speculative.

Faults younger than the SCCC cut the youngest post-caldera Tuffs of the Thirsty Canyon and Timber Mountain Groups at many places on Pahute Mesa. These faults are all north-striking, high-angle, normal faults; on most of them, the western side is down dropped. Few of them can be traced north or south of Pahute Mesa and those that can be, extend only a short distance. Vertical offset on the faults is small, generally less than a few hundred feet. The most important of these faults are shown on figure 14; only those with enough offset to be judged significant on the 1:48,000-scale geologic cross sections are used in this study -- they are highlighted in red on figure 14. Even the three faults considered most significant do not have much offset at the surface: the East Boxcar fault has 76 to 121 m (250 to 400 ft), the West Greeley has 76 to 152 m (250 to 500 ft) and the Almendro has 33 to 66 m (100 to 200 ft) (Orkild and others, 1969; Blankennagel and Weir, 1973). The episodic nature of the faults on Pahute Mesa, however, has been addressed by Warren and others (1985) who point out the differences in their offsets at depth. Drill hole data have been interpreted to show progressively greater offset at depth so that there is almost 600 m (1,980 ft) of displacement of the Calico Hills Formation to about 1,500 m (4,950 ft) below the surface. Ferguson and others (1994) suggested that the fault was active during emplacement of the Calico Hills Formation in the SCCC and acted as an ancillary fault to the circular caldera ring fault of the Area 20 caldera. The East Boxcar, West Greeley, and Almendro

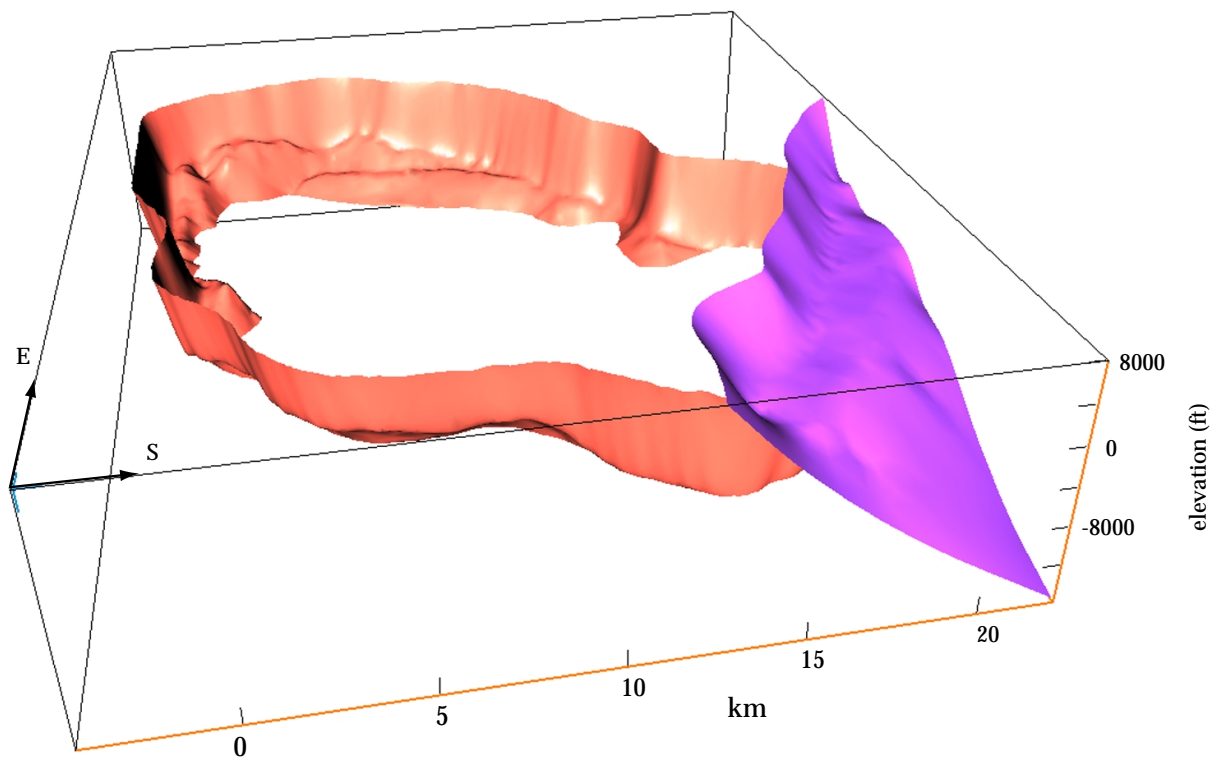
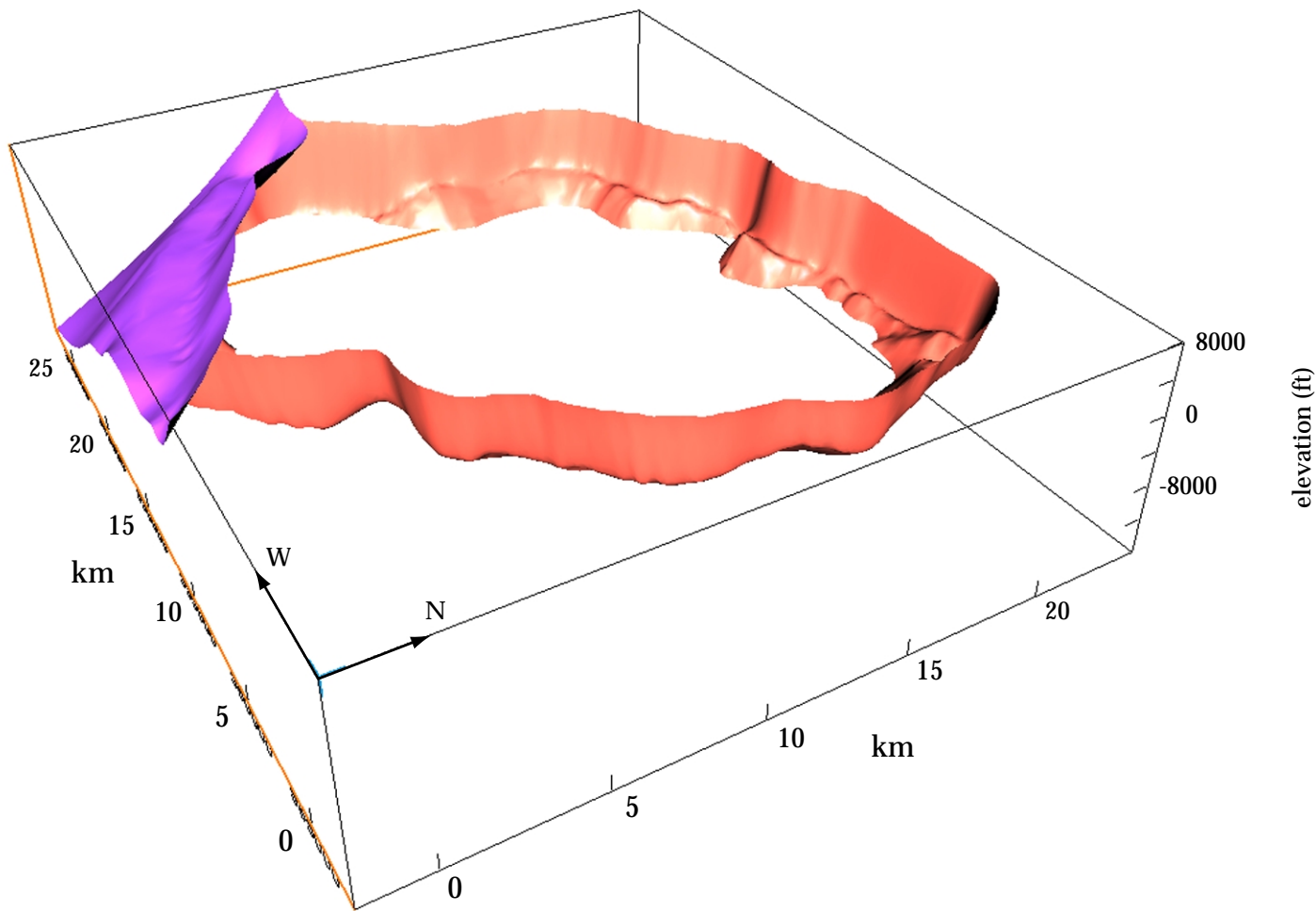


Figure 13. Two views of the north edge of the Timber Mountain caldera margin (purple) cutting off the Silent Canyon caldera margin (pink). The Timber Mountain caldera curves around to the south outside the limits of the block-diagram. No vertical exaggeration.

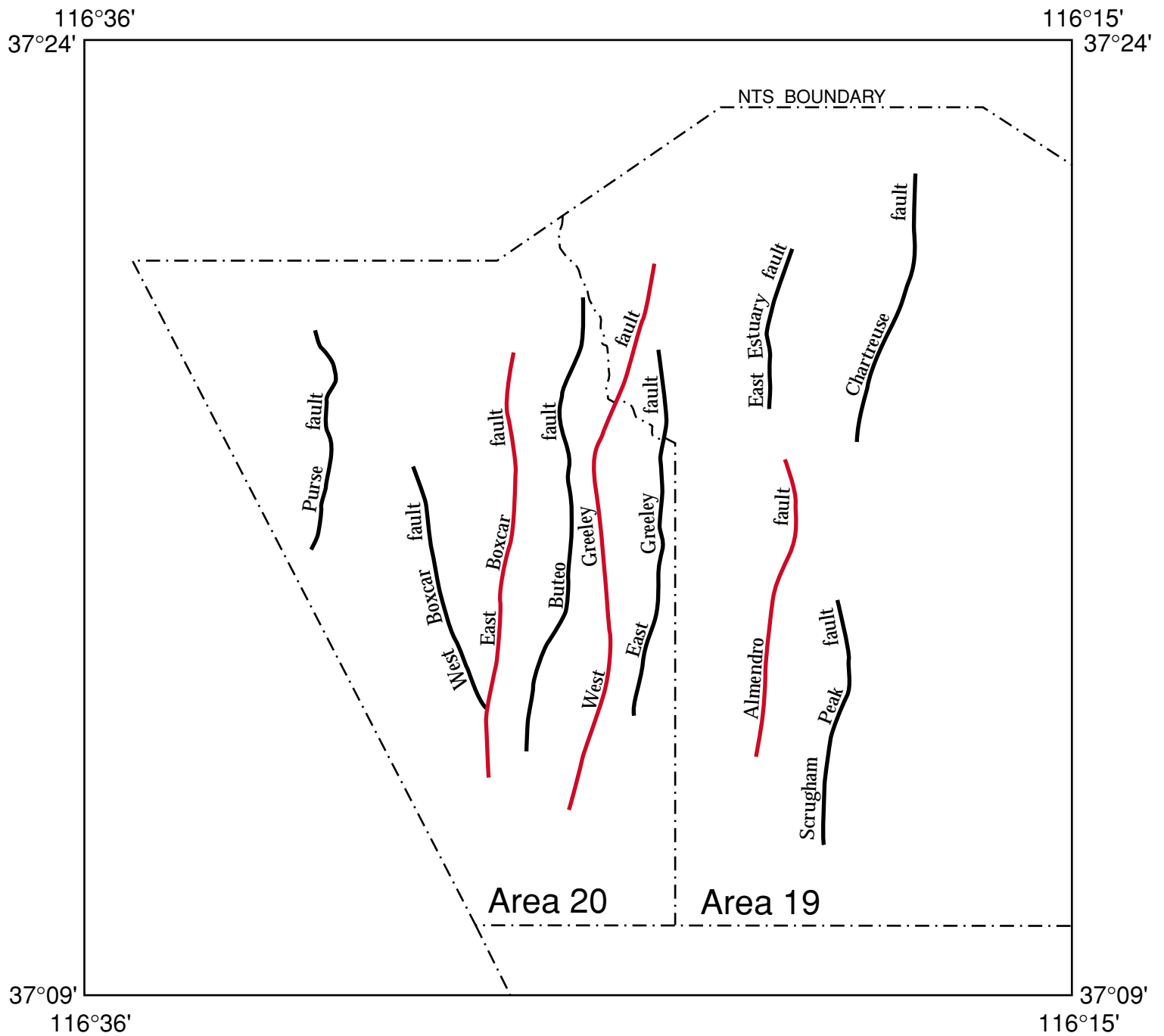


Figure 14. The major faults mapped at the surface of Pahute Mesa. These faults are mostly within the surface trace of the buried Silent Canyon caldera complex (see fig. 12a and 15). The three faults colored red offset units within the caldera complex enough to be significant at the scale of 1:48,000 used to compile and evaluate the data for this 3-dimensional model. The West Greeley fault has increasing offset with depth (see cross section A-A', figure 18).

faults all lie within the SCCC; their geometric relationship to the SCCC caldera and the north edge of the Timber Mountain caldera complex are shown in figure 15.

## BASEMENT SURFACE

The isostatic residual gravity field of the region shown in Figure 4a is based on about 4,000 gravity measurements (Mankinen and others, 1999). The overall distribution of gravity stations is roughly one station within  $0.7 \text{ km}^2$  on the average, although denser coverage exists within the area of the SCCC. Mankinen and others (1999) described the data reduction process to obtain the Bouguer gravity anomaly. The isostatic residual anomaly was calculated using a reduction density of  $2,670 \text{ kg/m}^3$ , crustal thickness of 30 km, and a mantle-crust density contrast of  $350 \text{ kg/m}^3$  (see Simpson and others, 1986). All data were gridded at a spacing of 1 km using a minimum curvature algorithm of Webring (1981).

To the first order, the isostatic residual gravity field reflects the pronounced contrast between dense basement rocks (about  $2,670 \text{ kg/m}^3$ ) and significantly less dense (generally  $< 2,500 \text{ kg/m}^3$ ) younger volcanic and sedimentary rocks. The prominent gravity lows (fig. 4a) over the SCCC and parts of the Timber Mountain caldera complex mostly delineate the thick, anomalously low-density volcanic caldera fill (Healey, 1968; Ferguson and others, 1994; Grauch and others, 1997; Hildenbrand and others, 1999). The gravity low over Pahute Mesa is one of the most prominent lows in western U.S., suggesting an unusually thick volcanic pile. In contrast granitic resurgent domes (density about  $2,670 \text{ kg/m}^3$ ) under Timber Mountain and Black Mountain appear to produce gravity highs (Kane and other, 1981; Grauch and others, 1997).

Using the gravity inversion method derived by Jachens and Moring (1990; modified to include drill-hole data), we separated the isostatic residual anomaly into a basin field and a basement field. The basin gravity field reflects variations in the thickness and density of low-density Tertiary volcanic and sedimentary rocks. The basement gravity field reflects changes in density related to lithologic variations within the denser pre-Tertiary rocks or dense Tertiary granitic intrusions. In the inversion process, the density of basement

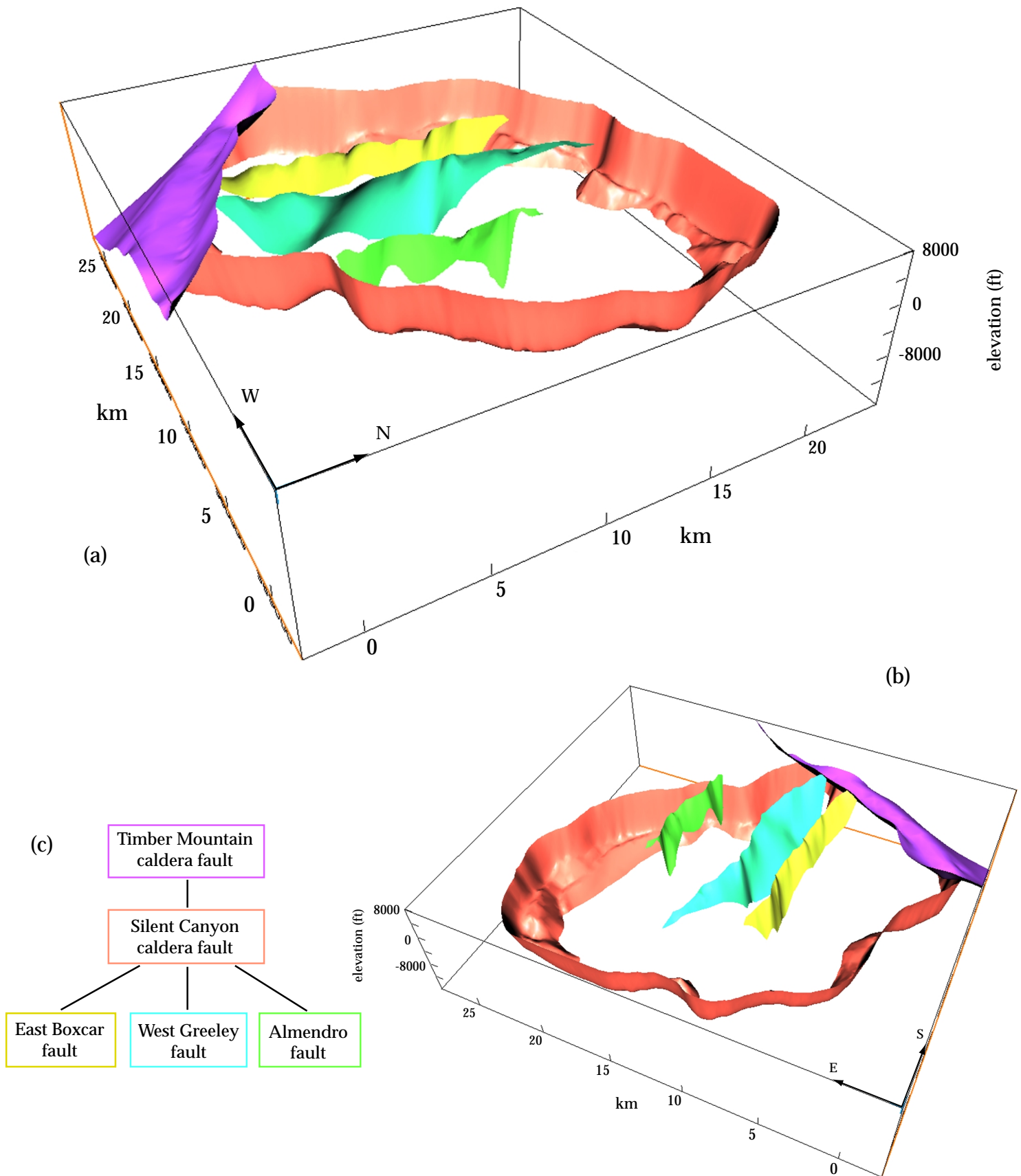


Figure 15. (a, b) Two views of the East Boxcar (yellow), West Greeley (blue), and Almendro (green) north-south faults within the Silent Canyon caldera complex (pink). Note the Timber Mountain caldera margin (purple) which cuts off the south edge of the SCCC. No vertical exaggeration. (c) Fault tree showing the hierarchy of faults in this model. Those faults higher up in the tree will take precedence over those lower in the tree where the faults intersect.

varies horizontally but the density of basin-filling deposits is fixed using a representative density versus depth relationship. Knowledge of the thickness of low density rocks (outside the SCCC) and of basement rock types and densities based on drill hole information constrains the calculations. Refer to Hildenbrand and others (1999) for details on the generation and constraints of the basin thickness data shown in figure 4b.

In general, basement is shallower outside the caldera along the western and southern parts of the study area. Basement descends to great depths beneath the SCCC. What are most likely the resurgent granitic domes of the Black Mountain caldera and the Timber Mountain caldera complex are clearly expressed as elliptically shaped basement highs.

#### Density-depth functions

The accuracy of the thickness calculation is dependent on the assumed density-depth relation of the Tertiary rocks and the initial density assigned to basement rocks. The Tertiary rocks are almost entirely of volcanic origin (although thin alluvial deposits are found throughout the study area). Complicating this task of selecting representative densities at a particular depth is the significant variation in density related to the degree of welding and alteration of the ash-flow tuffs, to structure (e.g., landslides and shallow, dense volcanic domes), and to water saturation. Because density generally increases with depth due to compaction, a layered density model is assumed for the Cenozoic deposits, although the lenticular nature of the volcanic rocks is acknowledged.

Based on deep-borehole gravimeter studies and borehole density logs from moderately deep and deep wells in the region of the SWNVF, Hildenbrand and others (1999) used a density-depth relation of the Cenozoic basin fill and basement shown as model A (table 2) to derive the basement depths in figure 4b. Although this relation may be a reasonable approximation for the large region shown in figure 4, it may lead to significant errors in more local areas. For example, anomalously low-density tuff bodies are observed beneath Pahute Mesa. Borehole gravimeter measurements in the SCCC (Ferguson

and others, 1994; Warren, personal communication, 1999) indicate densities of  $2,100 \text{ kg/m}^3$  extending in many areas to depths of over 1,000 m (3,300 ft). In such situations calculated basement depths in figure 4b will be overestimated. Thus for the present study a different density-depth relation for the SCCC area was necessary. Several models were considered and are shown in table 2.

Table 2. Density-depth functions used to determine the thickness of basin-filling deposits and calculated depths near and at drill hole Ue20f.

<u>Depth Range</u>	<u>Density (kg/m<sup>3</sup>) for 5 models</u>				
	A	B	C	D	E
0.0–0.2 km	1,900	1,900	1,900	1,900	1,900
0.2–0.6 km	2,100	2,100	2,100	2,100	2,100
0.6–1.2 km	2,300	2,100	2,100	2,100	2,100
1.2–1.5 km	2,450	2,300	2,100	2,100	2,100
1.5–2.0 km	2,450	2,300	2,100	2,100	2,300
>2.0 km	2,450	2,450	2,450	2,300	2,450
Max. Depth (km)	8.9	6.6	5.4	3.8	6.2
Ue20f depth (km)	6.8	4.5	3.3	2.7	4.3

In table 2, for all five models densities are the same above 600 m (1,980 ft) but vary considerably below 600 m. A careful analysis of deep drill hole data outside the SCCC (Hildenbrand and others, 1999) and of a large drill hole data base of density values from Warren (1999, personal communication) for the SCCC area leads us to the same density-depth relationship to depths of 600 m (1,980 ft) for all models. Below 600 m the basin fill within the SCCC is likely greater than or equal to 2,100 kg/m<sup>3</sup>, although less dense than the rocks outside the caldera complex (assumed to be represented by model A). Models B through E are considered representative of the possible range of general density distributions within the SCCC. To understand the sensitivity of the basement depths to changes in the depth-density function, maximum depth to basement just east (about 3.2 km or 2 mi) of drill hole Ue20f (figure 16) and basement

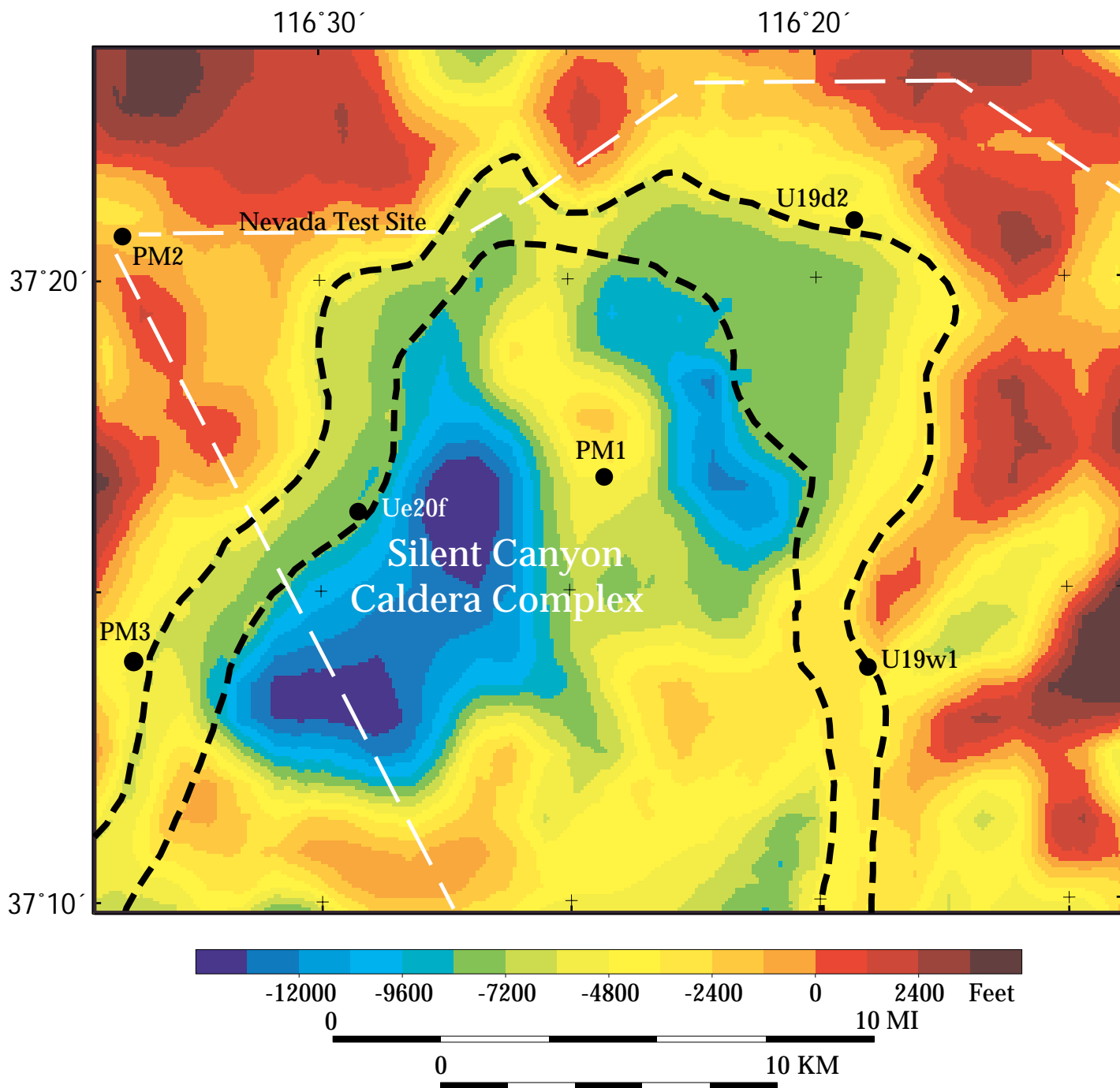


Figure 16. Basement surface beneath the region of the Silent Canyon caldera complex based on the inversion of gravity data. Inside the inner dashed black line, a density-depth relation is used with densities lighter than those in the density-depth relation in the region outside the outer dashed line. Basement elevations in the region between the dashed lines were derived by interpolation using a minimum curvature algorithm. The Nevada Test Site boundary and eight drill holes (black circles) provide points of reference.

depth at Ue20f were determined for all models and are shown in table 2. At a depth of about 4.2 km (13,743 ft) Ue20f bottomed in volcanic rocks.

General comments on the depth results shown in table 2 are (1) basement depths are sensitive to the densities assumed below 0.6 km where our knowledge is limited, (2) models B and E provide reasonable basement depths at Ue20f, which bottomed in old volcanic rock at 4.2 km and (3) a viable density-depth function can only be derived intuitively by our knowledge of rock types (and thus their densities) inside and outside the caldera that are expected to be present at depth within the SCCC.

Our knowledge of rock densities at depth ( $> 2$  km) is based on limited data from deep drill holes (e.g., Hildenbrand and others, 1999; Warren, 1999, personal communication). Based on these data and due to expected high pressures and temperatures at depth, one would not expect substantial volumes of low density volcanic rocks ( $< 2450 \text{ kg/m}^3$ ) at depths greater than 2 km. A density-depth function depicting volcanic rock of density of about  $2100 \text{ kg/m}^3$  extending to depths of 2 km is also unlikely (simply because such a large volume of these unusually low density rocks has not been observed in any drill hole in southern Nevada). Thus models C and D are considered unrealistic. Moreover, models C and D lead to basement depths at Ue20f that are much shallower than the known depth of volcanic rocks. Both models B and E lead to similar, reasonable solutions and possess densities that are defensible based on drill hole density data. For our study we chose models A and E to represent the density distributions outside and within the SCCC, respectively.

### Basin geometry

The basement surface in the region of the SCCC (figure 16) was derived using the two density-depth models (models A and E, table 2). To successfully merge the two depth data it was necessary to define a zone dividing regions outside and inside the caldera complexes where no depth values were assigned (a buffer region between the dashed lines in figure 16). In this zone depth values were calculated using a minimum curvature

algorithm that utilized the depths based on the low-density model E inside the pair of dashed lines and depth values from the high-density model A outside these lines.

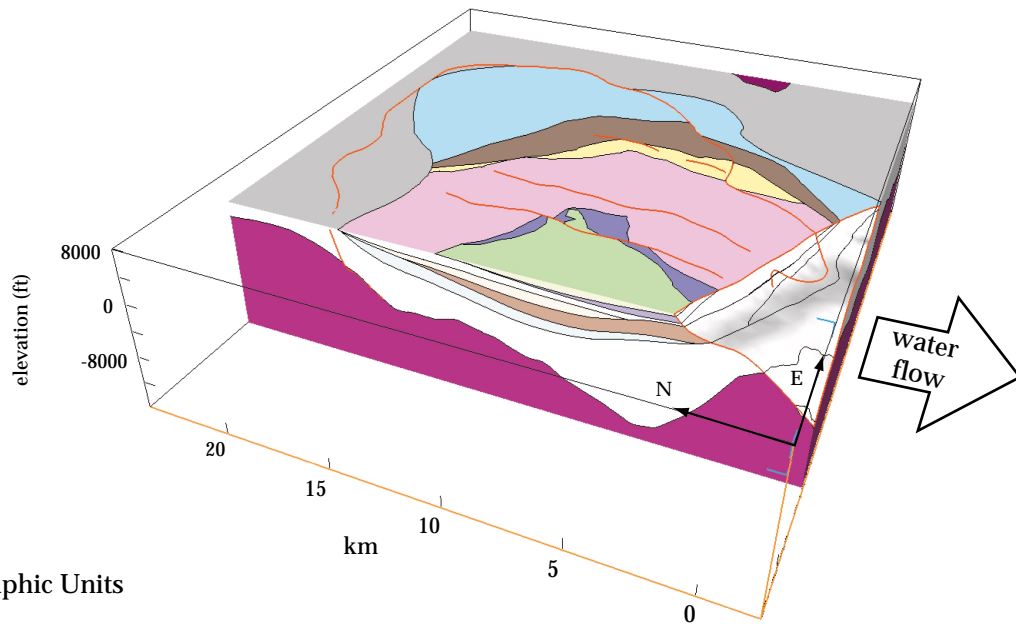
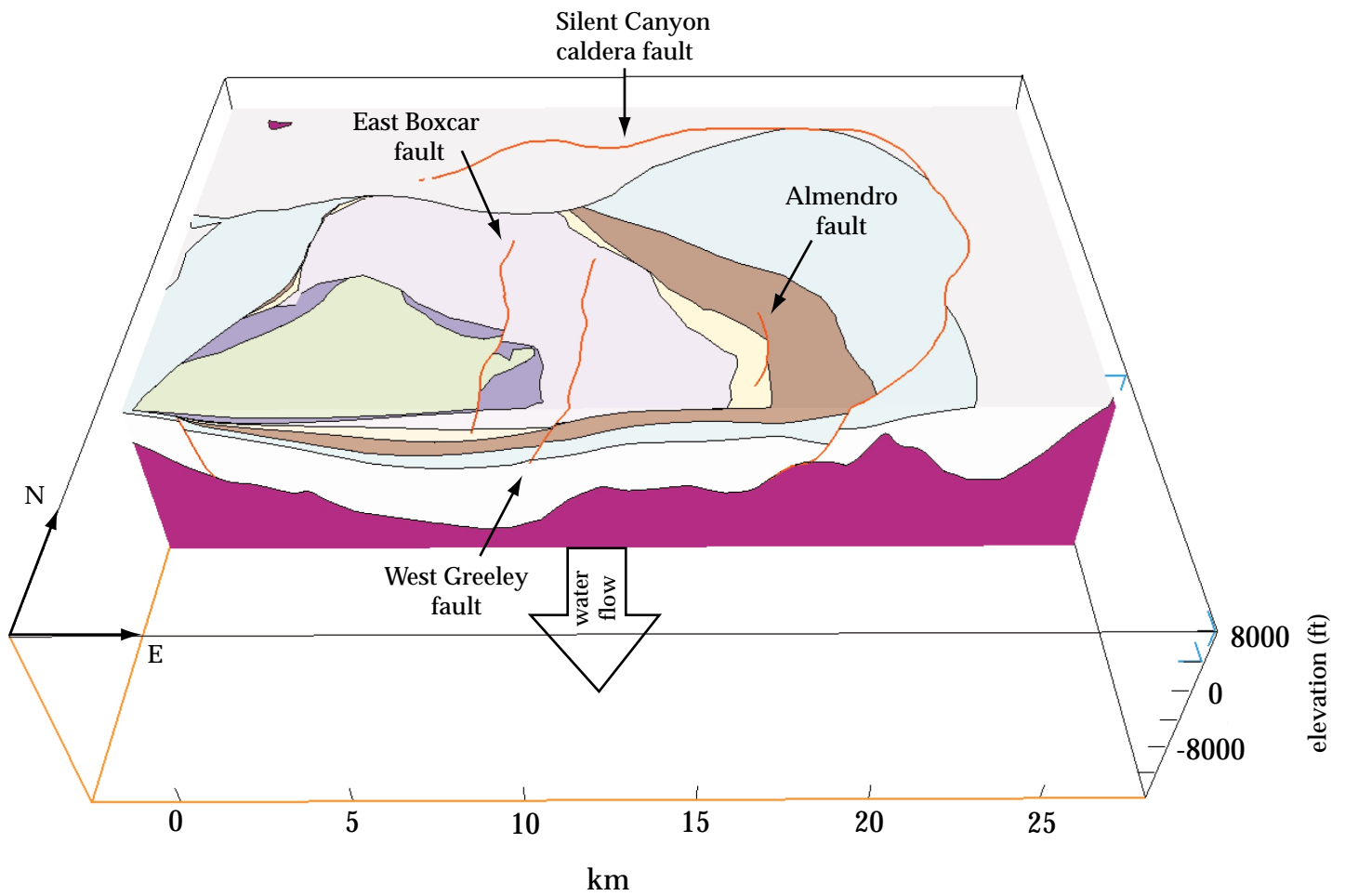
The resulting basement surface in figure 16 indicates that the estimated average thickness of the basin fill is about 4.5 km (14,850 ft.) and that the maximum thickness may exceed 6 km (19,800 ft.). A north-north-west-striking gravity high and resulting basement ridge cuts the SCCC and lies beneath mapped surface faults with small displacements. Because the density data of Warren (1999, personal communication) do not suggest a shallow dense zone, the source of this gravity high probably lies at or near the basement surface. The source of the NNW-striking gravity high is uncertain although it is subparallel to the surface trace of the West Greeley fault and may be related in some way to that fault. The associated basement ridge may be caused by granitic intrusions related to a resurgent dome at depth or it may be related to a pre-Tertiary structural high. Another basement ridge occurs at the southern edge of Pahute Mesa (the SW edge of figure 16) and is probably within the structural margin of the SCCC.

### THREE-DIMENSIONAL MODEL

The Silent Canyon caldera complex is modeled in three-dimensions using the "EarthVision"(Dynamic Graphics Inc.) geological computer program. EarthVision produces a three-dimensional model of the geology of a defined area using structural and stratigraphic data. The fault data and cross-cutting hierarchy defines a fault tree or framework in which the stratigraphic units fit (fig. 15). The faults and stratigraphic units are modeled using a minimum curvature function based on Briggs (1974) controlled by drill hole depths. The units are offset the appropriate amount in the established fault framework. After a structural model has been developed, data can be added that describe the properties of the stratified units, and surfaces can be created that model the properties inside of each stratigraphic unit. The Pahute Mesa subsurface

model was created using the Universal Transverse Mercator coordinate system with x and y units in meters and z units in feet. The scale of 1:48,000 was selected for the map and cross section evaluation because it produced maps of a manageable size with enough detail to model ground-water flow paths beneath Pahute Mesa. No vertical exaggeration was used in the resulting block diagrams and cross sections. The fault data were collected from gravity inversion calculations (*see* Basement Surface section), geologic map surface traces, and geologic data from drill holes with inferred geology between drill holes. Data for the stratigraphic units were compiled from drill hole data (52 sites were used) and the gravity measurements for the basement surface. The surface terrain was produced from the 30-m digital elevation model for Pahute Mesa. The EarthVision minimum curvature function (called the "minimum tension") was used for modeling the faults and stratigraphic units in this model, because the density of data points is appropriate.

The surfaces produced in the computer model are only as good as the quality and quantity of the data that control them. Surfaces defined by many drill hole depth intercepts will produce a mathematically sound model, which can be checked for geologic validity. The model can be manipulated in many ways to give perspective views or can be used to create a variety of products such as cross sections, isopach maps, and block diagrams (*see* figs. 7, 8, 9, 10, 11, 17, 18, 19, 20, and 21). The computer-generated, three-dimensional model was checked for geologic validity by comparing cross sections made from it (fig. 18 b,c,d) with conventionally drawn cross sections. This model is limited to the three-dimensional geologic structure and hydrostratigraphy of Pahute Mesa and does not include stratigraphic unit property data. Block diagrams (figs. 19, 20, and 21) cut along the same vertical planes as the cross sections shown in figure 18 b, c, and d give a three-dimensional aspect which



Hydrostratigraphic Units

- Timber Mountain composite unit
- Topopah Spring tuff aquifer
- Calico Hills composite unit
- Crater Flat composite unit
- Bullfrog Tuff confining unit
- Belted Ranger aquifer
- Pre-Belted Range composite unit
- Basement

Figure 17. Two views of the Silent Canyon caldera complex with the upper 2000 feet of rock removed down to the water table level. This shows the hydrostratigraphic units that the south flowing water would encounter. Timber Mountain fault block is omitted because of lack of drill hole control. No vertical exaggeration.

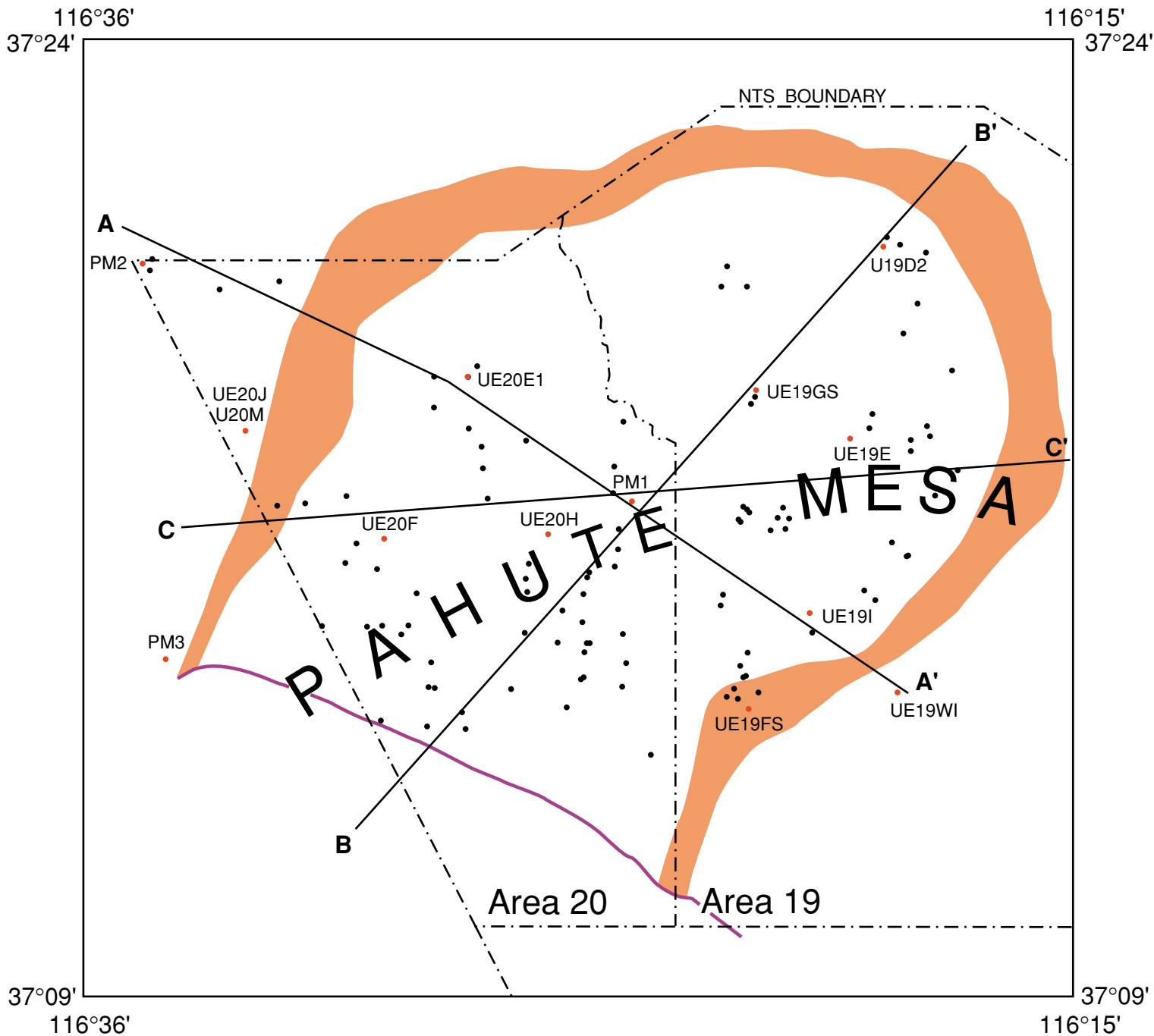
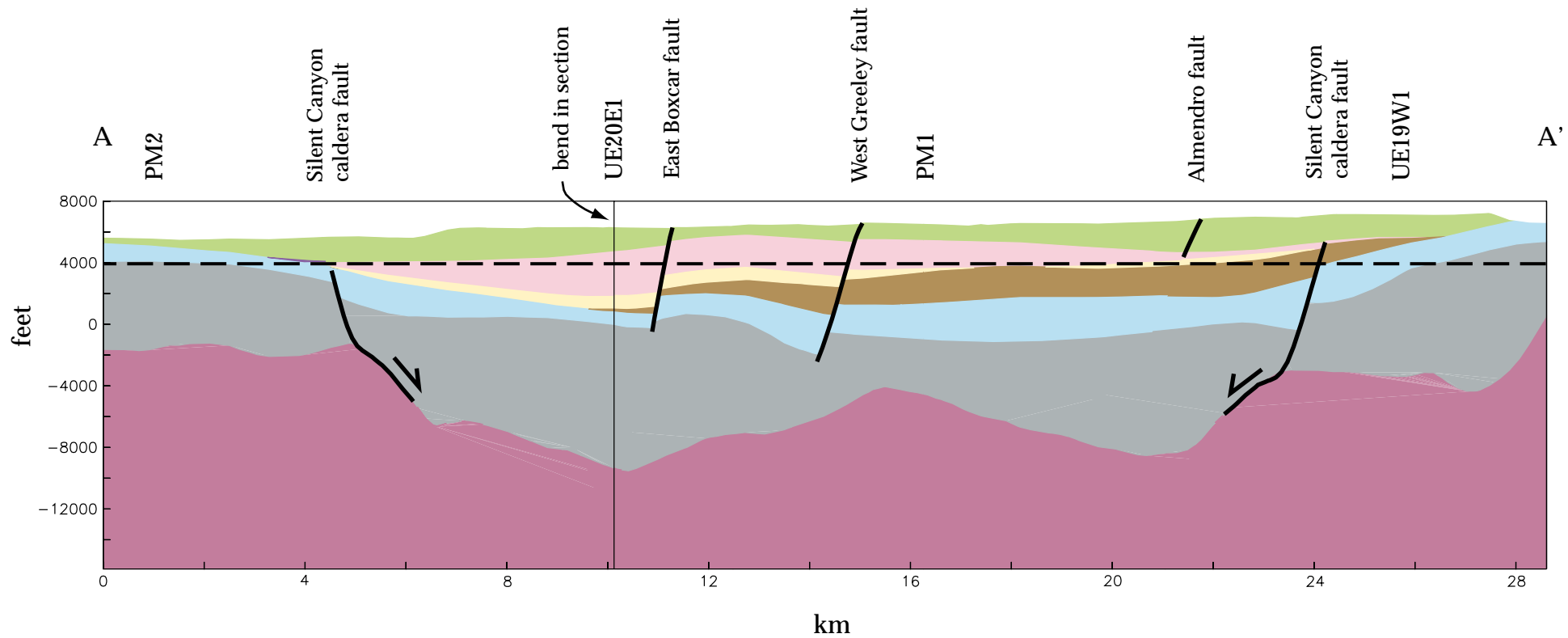


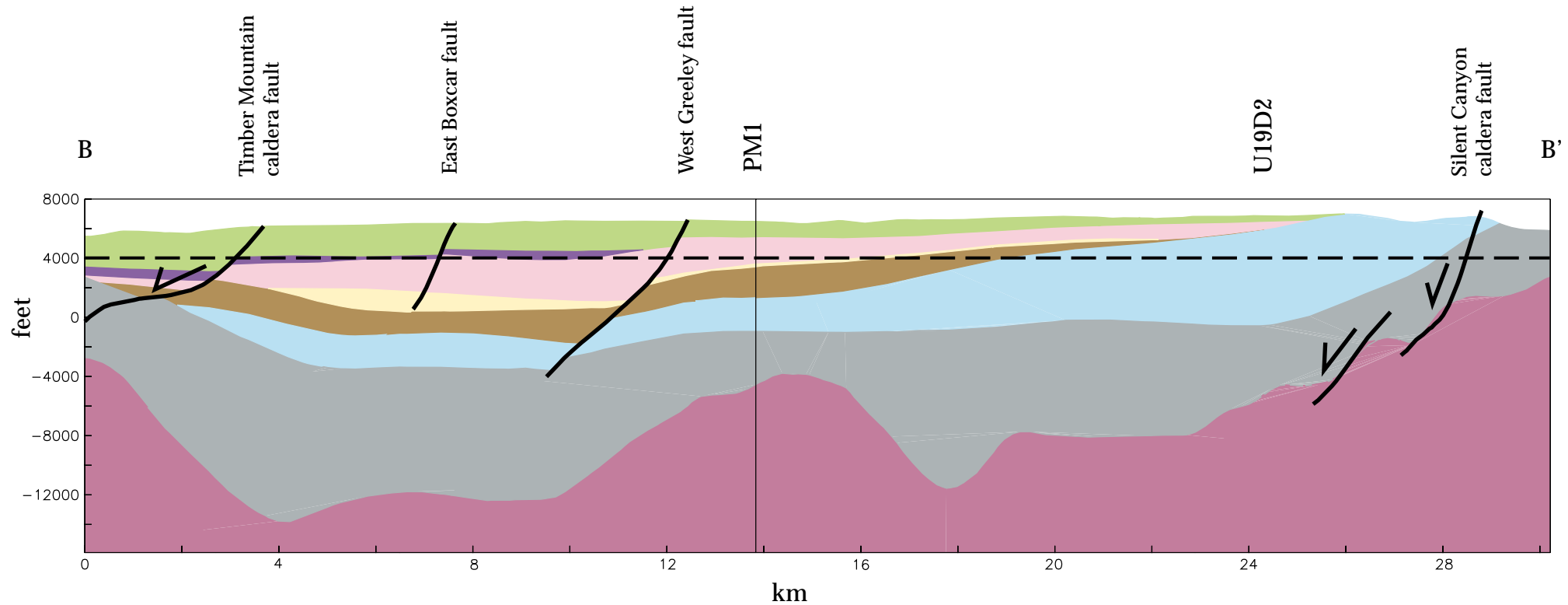
Figure 18a. Cross sections across the buried Silent Canyon caldera complex, drawn from "EarthVision" 3-dimensional model. Black dots are wells, red dots are the deepest wells and are identified by letter and number. Pink ribbon is the buried Silent Canyon caldera complex fault, purple line is the north edge of the Timber Mountain caldera fault.



Hydrostratigraphic Units

- |   |                                |   |                                 |
|---|--------------------------------|---|---------------------------------|
|    | Timber Mountain composite unit |    | Bullfrog Tuff confining unit    |
|    | Topopah Spring tuff aquifer    |    | Belted Ranger aquifer           |
|   | Calico Hills composite unit    |   | Pre-Belted Range composite unit |
|  | Crater Flat composite unit     |  | Basement                        |

Figure 18b. Profile A-A' as shown in figure 18a. Dotted line is the approximate elevation of the water table. No vertical exaggeration.



Hydrostratigraphic Units

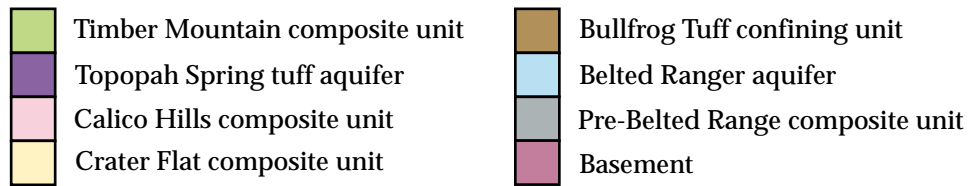
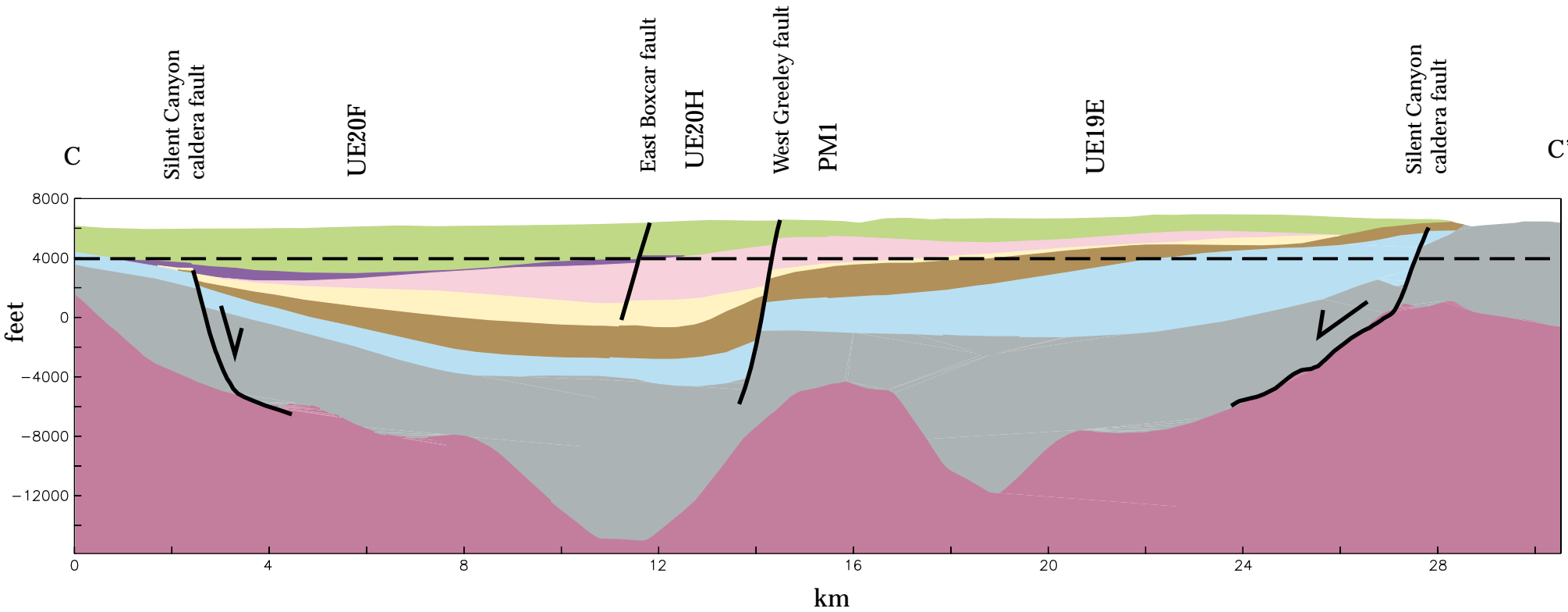


Figure 18c. Profile B-B' as shown in figure 18a. Dotted line is the approximate elevation of the water table. No vertical exaggeration. The Silent Canyon caldera fault at the northeast end of this section is interpreted as two smaller faults. Splitting of the Silent Canyon caldera fault at this small of a resolution was impossible in the 3 dimensional model because of lack of data coverage.



Hydrostratigraphic Units

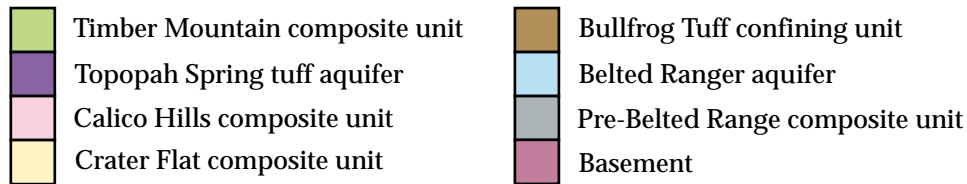
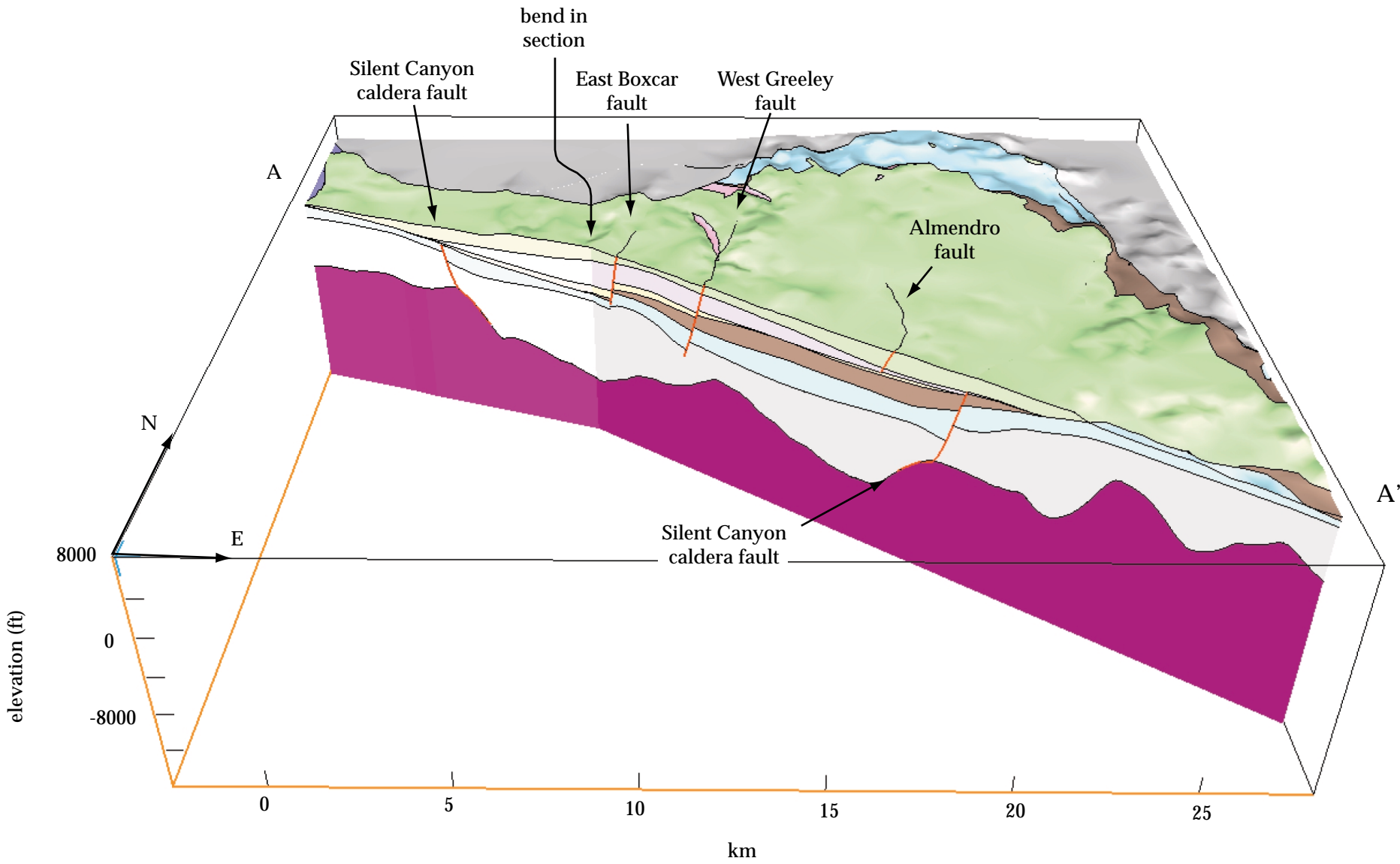


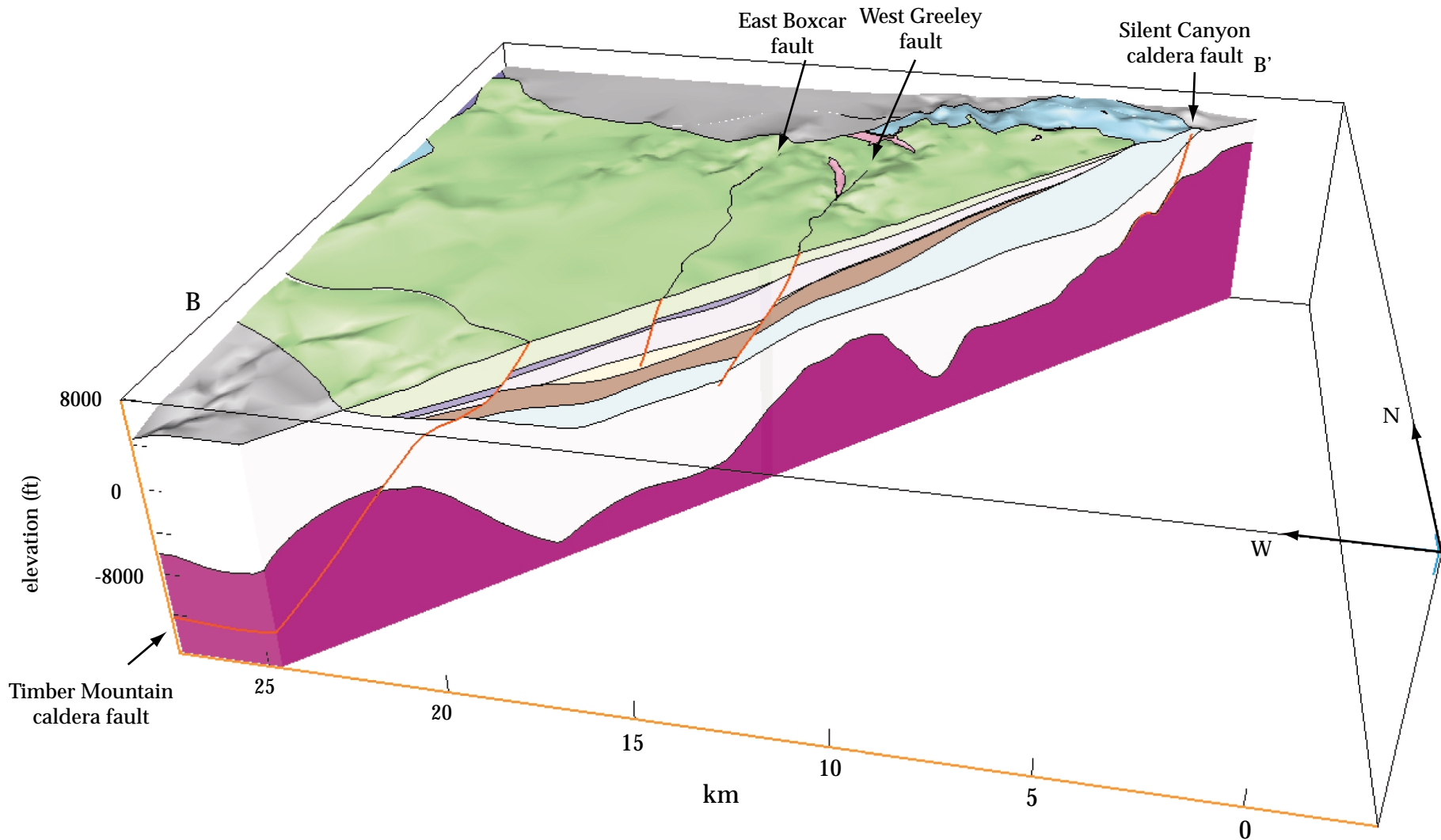
Figure 18d. Profile C-C' as shown in figure 18a. Dotted line is the approximate elevation of the water table. No vertical exaggeration.



Hydrostratigraphic Units

- |  |   |
|--|---|
|  Timber Mountain composite unit |  Bullfrog Tuff confining unit    |
|  Topopah Spring tuff aquifer    |  Belted Ranger aquifer           |
|  Calico Hills composite unit    |  Pre-Belted Range composite unit |
|  Crater Flat composite unit     |  Basement                        |

Figure 19. Three dimensional diagram of Pahute Mesa sliced along section A-A' in figure 18a, the same section as figure 18b. No vertical exaggeration.



#### Hydrostratigraphic Units

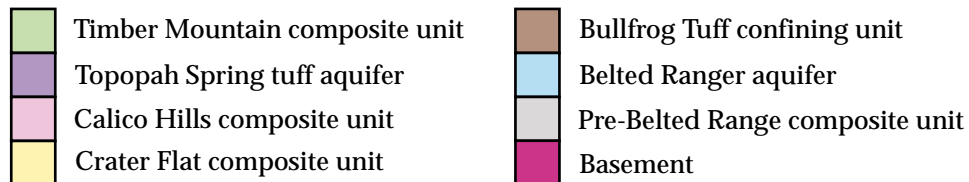
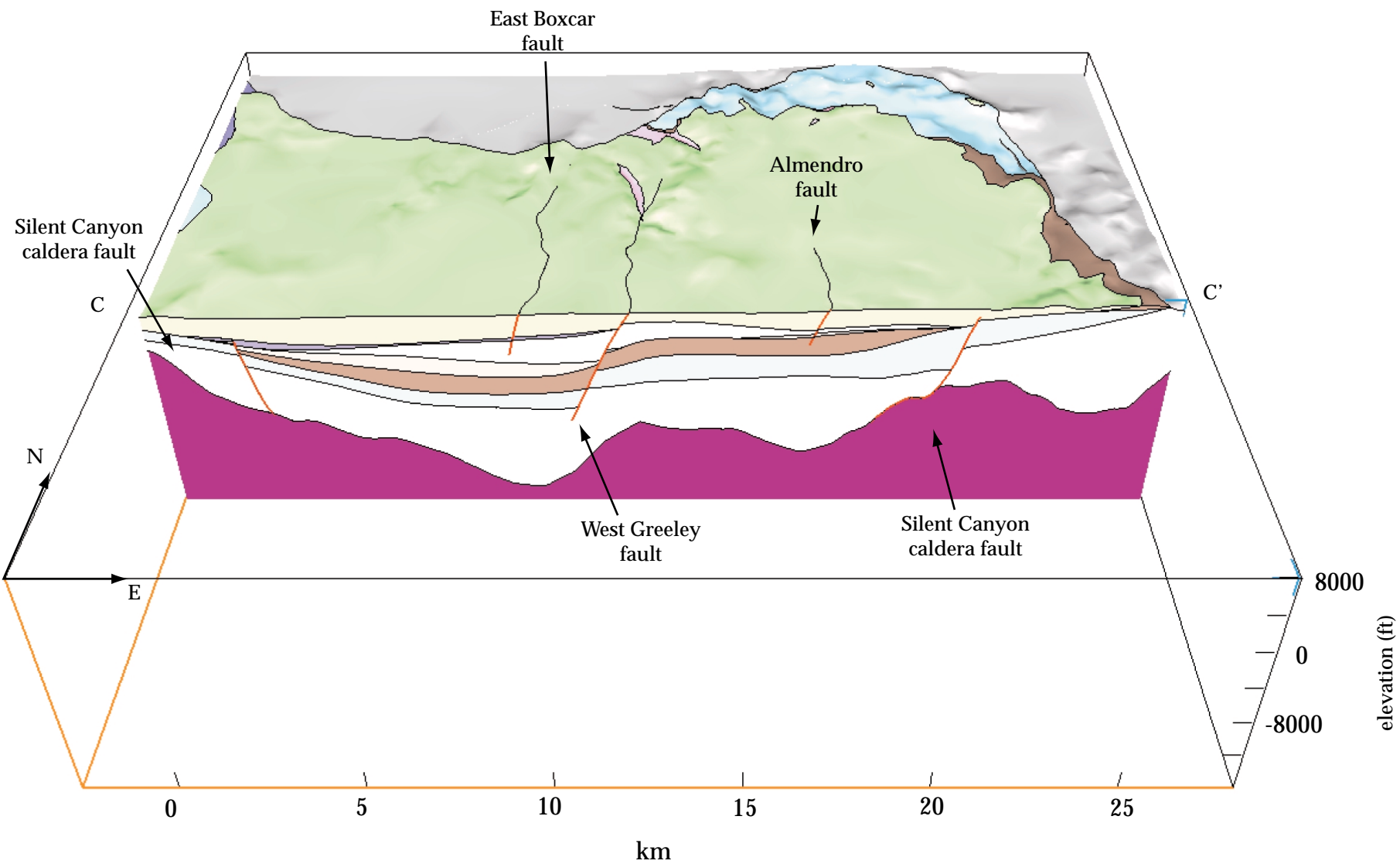


Figure 20. Three-dimensional diagram of Pahute Mesa sliced along section B-B' in figure 18a, the same section as figure 18c. No vertical exaggeration.



Hydrostratigraphic Units

<ul style="list-style-type: none"> <li><span style="display: inline-block; width: 20px; height: 15px; background-color: #90EE90; border: 1px solid black; margin-right: 5px;"></span> Timber Mountain composite unit</li> <li><span style="display: inline-block; width: 20px; height: 15px; background-color: #9370DB; border: 1px solid black; margin-right: 5px;"></span> Topopah Spring tuff aquifer</li> <li><span style="display: inline-block; width: 20px; height: 15px; background-color: #F080F0; border: 1px solid black; margin-right: 5px;"></span> Calico Hills composite unit</li> <li><span style="display: inline-block; width: 20px; height: 15px; background-color: #FFFF00; border: 1px solid black; margin-right: 5px;"></span> Crater Flat composite unit</li> </ul>	<ul style="list-style-type: none"> <li><span style="display: inline-block; width: 20px; height: 15px; background-color: #A0522D; border: 1px solid black; margin-right: 5px;"></span> Bullfrog Tuff confining unit</li> <li><span style="display: inline-block; width: 20px; height: 15px; background-color: #ADD8E6; border: 1px solid black; margin-right: 5px;"></span> Belted Ranger aquifer</li> <li><span style="display: inline-block; width: 20px; height: 15px; background-color: #D3D3D3; border: 1px solid black; margin-right: 5px;"></span> Pre-Belted Range composite unit</li> <li><span style="display: inline-block; width: 20px; height: 15px; background-color: #800080; border: 1px solid black; margin-right: 5px;"></span> Basement</li> </ul>
--	--

Figure 21. Three-dimensional diagram of Pahute Mesa sliced along section C-C' in figure 18a, the same section as figure 18d. No vertical exaggeration.

allows better understanding of the geologic relationships of the SCCC. The block diagrams are especially useful in visualizing structural and stratigraphic relationships. Figure 17 illustrates the visual impact, and usefulness for ground-water flow analysis, of a three-dimensional model of Pahute Mesa viewed at the water table surface. From these diagrams one can see that ground-water at the top of the water table will flow above the Bullfrog Tuff confining unit through the Crater Flat composite unit, the Calico Hills composite unit, the Topopah Spring tuff aquifer, and the bottom of the Timber Mountain composite unit in the western part of the SCCC. It will flow beneath the Bullfrog Tuff confining unit through the Belted Range aquifer in the eastern part of the SCCC. Other depth slices and other view angles can be used to visualize the components of the ground-water system from almost any imaginable perspective.

#### ACKNOWLEDGEMENTS

This investigation was performed as part of an interagency effort between the USGS and DOE under Interagency Agreement DE-AI08-96NV11967.

#### REFERENCES

- Blankennagel, R.K. and Weir, J.E., Jr., 1973, Geohydrology of the eastern part of Pahute Mesa, Nevada Test Site, Nye County, Nevada: U.S. Geological Survey Professional Paper 712-B, 35 p.
- Borg, I.Y., Stone, R., Levy, H.B., and Ramspott, L.D., 1976, Information pertinent to the migration of radionuclides in groundwater at the Nevada Test Site, Part 1, Review and analysis of existing information: Lawrence Livermore National Laboratory Report UCRL-52078 Part 1, 216 p.

- Briggs, I.C., 1974, Machine contouring using minimum curvature; Geophysics, v. 39, no. 1, p. 39-48.
- Byers, F.M., Jr., Orkild, P.P., Carr, W.J. and Quinlivan, W.D., 1968, Timber Mountain Tuff, southern Nevada, and its relation to caldera subsidence, *in* Eckel, E.B., ed., Nevada Test Site: Geological Society of America Memoir 110, p. 87-97.
- Byers, F.M., Carr, W. J., Christiansen, R. L., Lipman, P.W., Orkild, P.P., and Quinlivan, W.D., 1976a, Geologic map of the Timber Mountain area, Nye County, Nevada: U.S. Geological Survey Miscellaneous Investigations Series Map I-891, scale 1:48,000.
- Byers, F. M., Carr, W. J., Orkild, P.P., Quinlivan, W. D., and Sargent, K. A., 1976b, Volcanic suites and related calderas of Timber Mountain-Oasis Valley caldera complex, southern Nevada: U.S. Geological Survey Professional Paper 919, 70p.
- Carr, M.D., Sawyer, D.A., Nimz, Kathryn, Maldonado, Florian, and Swadley, W.C., 1996, Digital bedrock geologic map database of the Beatty 30x60-minute quadrangle, Nevada and California: U.S. Geological Survey Open-File Report 96-291, scale 1:100,000.
- Christiansen, R.L., and Noble, D.C., 1965, Black Mountain volcanism in southern Nevada: *in* Abstracts for 1964: Geological Society of America Special Paper 82, p. 246.
- Christiansen, R.L., Lipman, P.W., Carr, W.J., Byers, F.M., Orkild, P.P., and Sargent, K.A., 1977, The Timber Mountain-Oasis Valley caldera complex of southern Nevada: Geological Society of America Bulletin, v. 88, p. 943-959.
- Drellack, S.L., Jr., and Prothro, L.B., 1997, Descriptive narrative for the hydrogeologic model of western and central Pahute Mesa Corrective

- Action Units: Interim Documentation Report for the UGTA Project, submitted in support of the FY 1997 Pahute Mesa hydrogeologic modeling effort, Bechtel Nevada, Las Vegas, NV. 90 p.
- Ferguson, J.F., Cogbill, A.H., and Warren, R.G., 1994, A geophysical-geological transect of the Silent Canyon caldera complex, Pahute Mesa, Nevada: *Journal of Geophysical Research*, v. 99, no. B3, p. 4323-4339.
- Grauch, V.J.S., Sawyer, D.A., Fridrich, C.J., and Hudson, M.R., 1997, Geophysical interpretations west of and within the northwestern part of the Nevada Test Site: U.S. Geological Survey Open-File Report 97-476, 45 p.
- Healey, D.L., 1968, Application of gravity data to geologic problems at Nevada Test Site, *in* Eckel, E.B., ed., Nevada Test Site: Geological Society of America Memoir 110, p. 65-74.
- Healey, D.L., Harres, R.N., Ponce, D.A., and Oliver, H.W., 1987, Complete Bouguer gravity map of the Nevada Test Site and vicinity Nevada: U.S. Geological Survey Open-File Report 87-506.
- Hildenbrand, T.G., Langenheim, V.E., Mankinen, E.A., and McKee, E.H., 1999, Inversion of gravity data to define the pre-Tertiary surface and regional structures possibly influencing ground-water flow in the Pahute Mesa-Oasis Valley region, Nye County, Nevada: U.S. Geological Survey Open-File Report 99-49, 27 p.
- Jachens, R.C., and Moring, B.C., 1990, Maps of the thickness of Cenozoic deposits and the isostatic residual gravity over basement for Nevada: U.S. Geological Survey Open-File Report 90-404, 15 p.
- Kane, M.F., Webring, M.W., and Bhattacharyya, B.K., 1981, A preliminary analysis of gravity and aeromagnetic surveys of the Timber Mountain area, southern Nevada: U.S. Geological Survey Open-File Report 81-189, 40 p.

- Laczniak, R.J., Cole, J.C., Sawyer, D.A., and Trudeau, D.A., 1996, Summary of hydrogeologic controls on ground-water flow at the Nevada Test Site, Nye County, Nevada: U.S. Geological Survey Water-Resources Investigations Report 96-4109, 59 p.
- Lipman, P.W., 1976a, Geologic map of the Lake City caldera area, western San Juan Mountains southwestern Colorado: U.S. Geological Survey Miscellaneous Investigations Series Map I-962, scale 1:48,000.
- \_\_\_\_\_ 1976b, Caldera collapse breccias in the western San Juan Mountains, Colorado: Geological Society of America Bulletin, v. 87, p.1397-1410.
- \_\_\_\_\_ 1984, The roots of ash-flow calderas in North America-- Windows into the tops of granitic batholiths: Journal of Geophysical Research, v. 89, p. 8801-8841.
- \_\_\_\_\_ 1997, Subsidence of ash-flow calderas-- Relation to caldera size and magma chamber geometry: Bulletin Volcanologique, v. 59, p. 198-218.
- Mankinen, E.A., Hildenbrand, T.G. Dixon, G.L., McKee, E.H., Fridrich, C.J., and Laczniak, R.J., 1999, Gravity and magnetic study of the Pahute Mesa and Oasis Valley region, Nye County, Nevada: U.S. Geological Survey Open-File Report 99-303 57 p.
- McCafferty, A.E., and Grauch, V.J.S., 1997, Aeromagnetic and gravity anomaly maps of the southwestern Nevada volcanic field, Nevada and California: U.S. Geological Survey Geophysical Investigations Map GP 1015, scale 1:250,000.
- Minor, S.A., Sawyer, D.A., Wahl, R.R., Frizzell, V.F., Jr., Schilling, S.P., Warren, R.G., Orkild, P.P., Coe, J.S., Hudson, M.R., Fleck, R.J., Lanphere, M.A., Swadley, W.C., and Cole, J.C., 1993, Preliminary geologic map of the Pahute Mesa 30'x60' quadrangle, Nevada: U.S. Geological Survey Open-File Report 93-299, 39 p., scale 1:100,000.

- Noble, D.C., Sargent, K.A., Mehnert, H.H., Eckel, E.B., and Byers, F.M., Jr., 1968, Silent Canyon volcanic center, Nye County, Nevada, *in* Ekren, E.B., ed., Nevada Test Site: Geological Society of America Memoir 110, p. 65-74.
- Noble, D.C., and Christiansen, R.L., 1974, Black Mountain volcanic center, *in* Guidebook to the geology of four Tertiary volcanic centers in central Nevada: Nevada Bureau of Mines and Geology Report 19, p. 27-34.
- Orkild, P.P., Byers, F.M., Jr., Hoover, D.L., and Sargent, K.A., 1968, Subsurface geology of Silent Canyon caldera, Nevada Test Site and vicinity, Nye County, Nevada, *in* Eckel, E.B., ed., Nevada Test Site: Geological Society of America Memoir 110, p. 77-86.
- Orkild, P.P., Sargent, K.A., and Snyder, R.P., 1969, Geologic map of Pahute Mesa, Nevada Test Site and vicinity, Nye County, Nevada: U.S. Geological Survey Miscellaneous Geologic Investigations Map I-567, scale 1:48,000.
- Sawyer, D.A., and Sargent, K.A., 1989, Petrologic evolution of divergent peralkaline magmas from the Silent Canyon caldera complex, southwestern Nevada volcanic field: *Journal of Geophysical Research*, v.94, no. B5, p. 6021-6040.
- Sawyer, D.A., Fleck, R.J., Lanphere, M.A., Warren, R.G., Broxton, D.E., and Hudson, M.R., 1994, Episodic caldera volcanism in the Miocene southwestern Nevada volcanic field-- Revised stratigraphic framework,  $^{39}\text{Ar}/^{40}\text{Ar}$  geochronology, and implications for magmatism and extension: *Geological Society of America Bulletin*, v. 106, p. 1304-1318.
- Sawyer, D.A., Wahl R.R., Cole, C.C., Minor, S.A., Lacznik, R.J., Warren, R.G., Engle, C.M., and Vega, R.G., 1995, Preliminary digital geologic map of the Nevada Test Site, Nevada: U.S. Geological Survey Open-File Report 95-0567.

- Schenkel, C.J., Hildenbrand, T.J., and Dixon, G.L., 1999, Magnetotelluric study of the Pahute Mesa and Oasis Valley region, Nye County, Nevada: U.S. Geological Survey Open-File Report, 99-355, 46p.
- Simpson, R.W., Jachens, R.C., Blakeley, R.J., and Saltis, R.W., 1986, A new isostatic residual gravity of the conterminous United States, with a discussion of the isostatic residual anomalies: *Journal of Geophysical Research*, v. 91, p. 8348-8372.
- Slate, J.L., Fridrich, C.J., Berry, M.E., Rowley, P.D., Morgan, K.S., Workman, J.B., Young, O.D., Williams, V.S., Swadley, W.C., Lundstrom, S.C., Cole, J.C., Warren, R.G., Menges, C.M., Grunwald, D.J., Yount, J.C., and Jayko, A.S., 1999, Digital geologic map of the Nevada Test Site and vicinity, Nye, Lincoln, and Clark Counties, Nevada, and Inyo County, California: U.S. Geological Survey Open-File Report 99-450, scale 1:100,000.
- Smith, R.L., 1960, Ash flows: *Geological Society of America Bulletin*, v. 71, p.795-842.
- Smith, R.L., and Bailey, R.A., 1968, Resurgent cauldrons, *in* Coats, R.R., Hay, R.L., and Anderson, C.A., eds., *Studies in volcanology-- A memoir in honor of Howel Williams: Geological Society of America Memoir 116*, p. 613-662.
- Smith, R.L., Bailey, R.A., and Ross, C.S., 1970, Geologic map of the Jemez Mountains, New Mexico: U.S. Geological Survey Miscellaneous Geologic Investigations Map I-571, scale 1:125,000.
- Snyder, D.B., and Carr, W.J., 1984, Interpretation of gravity data in a complex volcano-tectonic setting, southwestern Nevada: *Journal of Geophysical Research*, v.89, p. 10193-10206.
- Steven, T.A., and Lipman, P.W., 1976, Calderas of the Marysvale volcanic field, southwestern Colorado: U.S. Geological Survey Professional Paper 958, 35 p.

- Wahl, R.R., Sawyer, D.A., Minor, S.A., Carr, M.D., Cole, J.C., Swadley, W.C., Laczniak, R.J., Warren, R.G., Green, K.S., and Engle, C.M., 1997, Digital geologic map database of the Nevada Test Site area, Nevada: U.S. Geological Survey Open-File Report 97-140, CD-ROM, scale 1:100,000.
- Warren, R.G., 1985, Beyers, F.M., Jr., and Orkild, P. P., 1985, Post- Silent Canyon caldera structural setting for Pahute Mesa, in Proceedings of the Third Symposium on Containment of Underground Nuclear Explosions, vol. 2, *CONF-850953*, pp. 3-30, Lawrence Livermore National Laboratory, Livermore, California.
- Warren, R.G., 1994, Structural elements and hydrogeologic units of the southwestern Nevada volcanic field; *attachment* to Los Alamos National Laboratory letter to Ed Price, GeoTrans, Las Vegas, NV: 19 p., 4 figures, Structural Block Model Map, 2 Cross Sections, May 1994.
- Warren, R.G., Sawyer, D.A., Byers, F.M., Jr., and Cole, G.L., 1999, A petrographic/geochemical database and structural framework for the southwestern Nevada volcanic field. Available from the National Geophysical Data Center at <http://qeeg.ngdc.gov/seg/geochem/swnvf> or at <ftp://ftp.ngdc.noaa.gov/Solid-Earth/Geochem/SWNVF>.
- Webring, Michael, 1981s, MINC—A gridding program based on minimum curvature: U.S. Geological Survey Open-File Report 81-1224, 43 p.
- Williams, Howel, 1941, Calderas and their origin: University of California Publication, Department of Geological Sciences, v. 25, p. 239-346.
- Winograd, I.J., and Thordarson, William, 1975, Hydrogeologic and hydrochemical framework, south-central Great Basin, Nevada-California, with special reference to the Nevada Test Site: U.S. Geological Survey Professional Paper 712-C, 126 p.